ASSESSING THE STRENGTH AND BEARING CAPACITY OF TAILINGS FOR OIL SANDS RECLAMATION

by

Abigail Louisa Paul

A thesis submitted in partial fulfillment of the requirements for the degree of

Master of Science

in

Geoenvironmental Engineering

Department of Civil and Environmental Engineering
University of Alberta

Abstract

Reclamation of oil sands mines in northern Alberta presents a significant challenge for mine operators, particularly the reclamation of tailings deposits that are produced by the mine waste stream. A proposed approach to reclaiming tailings deposits as upland or wetland landforms is capping which involves placing material such as tailings sand or petroleum coke on the tailings surface. Critically, the underlying tailings deposit must have sufficient strength, density, and bearing capacity to support the cap as well as the equipment and personnel required to place it. Otherwise, equipment can “punch through” the cap into the underlying tailings, posing a significant hazard for the equipment and operator.

Clay minerals play a significant role in the challenging geoenvironmental behaviour of oil sands tailings, and therefore must be considered in the design and implementation of capped deposits. A well-established method for quantifying clay behaviour in geotechnical engineering is the Atterberg limits, which define the water contents for which clay will exhibit plastic behaviour. Atterberg limits can also be used to develop correlations between the liquidity index and remoulded undrained shear strength. Atterberg limits are currently used to characterize oil sands tailings, however, there are unique challenges to applying existing measurement methods to these materials compared to natural soils. There is also no relationship between remoulded strength and liquidity index for strong, dense tailings that are being targeted as capped deposits, though relationships exist for natural soils and fluid, low-density tailings. Current practice to evaluate deposits is to predict bearing capacity from peak undrained shear strength and apply an appropriate factor of safety.

A laboratory testing program and a review of existing published data was undertaken to investigate the Atterberg limits, strength, and bearing capacity of oil sands tailings. A series of Atterberg limits tests in which material properties, preparation method, and test procedure were varied were completed. It was determined that these factors influenced the measured Atterberg limits, though it was challenging to determine the effect of individual factors compared to the quantified variability of the tests. Air-drying the tailings from above the liquid limit to the plastic limit at low temperatures is proposed as a standard preparation method as this preserves the properties of the as-received tailings and is straightforward to perform. Atterberg limits and strength measurements determined in the test program were also used to determine a mathematical correlation between the remoulded strength and liquidity index of high-density tailings. Model footing tests at the benchtop scale demonstrated that existing methods of predicting bearing capacity from peak strength are appropriate. The sensitivity ratio was used to apply the proposed correlation between remoulded strength and liquidity index to the model footing results and propose a new method for predicting bearing capacity from index properties. The results of this research program support the idea that index properties such as Atterberg limits can provide a cost-effective method for long-term monitoring and the preliminary design of capped deposits.

Preface

This thesis is an original work completed under the supervision of Dr. Nicholas Beier. I was responsible for the preparation of the thesis manuscript and interpreting results. Dr. Beier was responsible for editing and technical review.

All laboratory testing was performed at the University of Alberta with the exception of material characterization tests and sample preparation (Dean Stark and cold extraction methods). Material characterization tests were performed by Bureau Veritas Laboratories and the Northern Alberta Institute of Technology as noted in the text. Sample preparation methods were also performed by Bureau Veritas Laboratories and solids were shipped back to the University of Alberta for further testing.

The remainder of the laboratory test program was completed by me with the much appreciated support of several individuals. Caroline Alexon assisted with many of the laboratory tests. Kate Harrison performed Atterberg limits and fall cone tests on EPK Kaolin. Tony Zheng developed the model footing test procedure and will be providing further details on this method in forthcoming publications. Dr. Heather Kaminsky provided significant guidance on the direction of the laboratory test program, in particular on investigating Atterberg limits and oil sands clays.

Portions of Chapter 2 will be published in the forthcoming proceedings of the 77th Canadian Geotechnical conference as:

Paul, A. and Beier, N. 2024. A review of Atterberg limits and remoulded strength relationships of oil sands tailings. *In* Proceedings of the 77th Canadian Geotechnical Conference. Canadian Geotechnical Society, Montreal, Quebec, Canada.

Acknowledgements

Many times over the past three years, I said to my husband, “I hope that I will wake up one day and my thesis will suddenly be done.” This was unfortunately not the case. It is to the credit of everyone who has supported me in this degree that I was able to dedicate the time, effort, and motivation to finally complete it.

First, thank you to my supervisor Dr. Nicholas Beier for hiring me as a co-op student in 2020 and continuing to let me overstay my welcome. Your generous feedback and patience were invaluable to this project, and I’m looking forward to the next one. Thank you as well to Dr. Albert Liu and Dr. Ward Wilson for serving as examiners, and to Dr. Micheal Hendry for chairing my defense. I am incredibly fortunate to have had the support of the team at the UAlberta Geotechnical Centre during my degree. Thanks especially to Jen Stogowski, Vivian Giang, Lucas Duerksen, David Barsi, and Dr. Louis Kabwe. I also had the great privilege of sharing the lab with Tony Zheng, Peter Kaheshi, Yunhai Zhang, Mahmoud Ahmed, and Dr. Yawu Liang – thank you all for being so generous with your knowledge and not for complaining about my road trip playlist on the way to conferences. To Caroline Alexon, thanks for helping me stay on track and for being a great friend over this past year (and I hope for a lot longer). Kate Harrison also spent her WISEST program messing around with clay and helping me troubleshoot my lab procedures.

It was a treat to work with the Centre for Oil Sands Sustainability team at NAIT for portions of this project. Thanks especially to Dr. Heather Kaminsky for helping the test program take shape and to Niamh Donoghue for training me on Atterberg limits.

I am incredibly grateful to my family and friends, who I’m sure do not want to hear me mention clay ever again. Thank you to my parents Doug and Laurie (who told me “school was my job” one too many times growing up), and my brother Eric (who will never be getting his old bike back) for your unconditional love and support. I love you all, and I will continue crashing your plans to see more of you. My favourite in-laws Scott and Tricia kept me motivated with words of encouragement, sparkling water, and guinea pigs. Thanks as well to my brother-in-law Alex for helping me prioritize what’s really important: skiing and mountain biking. I’ve also been lucky to have a wonderful, supportive group of friends around me as I completed this thesis. To my old friends, new friends, undergrad

friends, high school friends, biking friends, junior high friends, grad school friends, TTRPG friends – thank you, and sorry for all the “fun facts” about tailings.

I gratefully acknowledge the financial support given to this research, in particular the NSERC/COSIA Industrial Research Chair in Oil Sands Tailings Geotechnique (IRCPJ 460863 – 18). I am also appreciative of the scholarships I received to support this degree including the Alberta Graduate Excellence Scholarship, Alexander Graham Bell Canada Graduate Scholarship (NSERC CGS-M), Earle Klohn Graduate Scholarship, Dennis Becker Canadian Foundation for Geotechnique MSc. Student Award, Golder Associates Mine Closure Scholarship, Government of Alberta Women in STEM Scholarship, University of Alberta Graduate Recruitment Scholarship, Walter H. Johns Graduate Fellowship, and Westmoreland Coal Company Graduate Scholarship.

Lastly, to my husband, Evan. This never would have happened without you, not just because you convinced me to go to grad school in the first place, but also because you believe in me more than I ever possibly could. Thank you for picking me.

Land Acknowledgment

It is with gratitude that I acknowledge that this work was completed in Treaty 6 territory the traditional territory of many Indigenous peoples including the Cree, Blackfoot, Métis, Nakota Sioux, Iroquois, Dene, Ojibway/Saulteaux/Anishinaabe, and Inuit, and in Métis Nation of Alberta Region 4. The samples used in this study were sourced from Treaty 8 territory, traditional lands of the Dene and Cree, and Métis Nation of Alberta Region 1.

Table of contents

List of Figures

List of Tables

List of symbols and acronyms

CE	Sample has been treated by cold extraction method
DS	Sample has been treated by Dean Stark method
e	Void ratio
FT	Fluid tailings
G_s	Specific gravity
I_P	Plasticity index
MFT	Mature fine tailings
q_{ult}	Bearing capacity
S	Saturation ratio
SAR	Sodium Absorption Ratio
SFR	Sand to fines ratio
S_t	Sensitivity ratio
Su	Undrained shear strength
Su_r	Remoulded undrained shear strength
TSF	Tailings storage facility
w	Water content
w_L	Liquid limit
w_P	Plastic limit
wt%	Percent by mass

1 Introduction

1.1 Background

Oil sands tailings are the waste product of oil sands mining in Northern Alberta. Tailings consist of mineral particles (sand, silt, and clay), water, bitumen, and other chemical constituents (Alberta Government 2015). Initially, tailings have a fluid consistency and are deposited by pipeline in either above-ground structures or mined-out pits referred to as tailings storage facilities (TSFs). Segregation occurs upon deposition and coarse particles and approximately half of the fine particles form a beach along the perimeter of the facility (BGC Engineering Inc. 2010). The remaining fine particles and other constituents flow with the water to form a pond at the centre of the facility with an initial solids content of 6-10 wt% (Chalaturnyk et al. 2002). Over time, the fine tailings solids will settle and consolidate to a denser, stronger material in the TSF (solids content >30 wt%). However, further strength gain through consolidation may take over a century, and a number of techniques are employed in the oil sands region to further improve the engineering properties of tailings (Chalaturnyk et al. 2002, BGC Engineering Inc. 2010, COSIA 2012). Tailings that must be managed include both new and previously deposited tailings, often referred to as legacy tailings (AER 2023). New tailings are treated prior to deposition in TSFs and legacy tailings are re-handled and re-deposited in order to apply treatment methods.

The engineering behaviour of oil sands tailings presents a significant challenge for oil sands mine reclamation. Once mining has ceased, oil sands mines, including tailings deposits, are required to be reclaimed to a self-sustaining boreal forest ecosystem (AER 2017). A proposed approach to the reclamation of tailings deposits is capping in which material such as sand or petroleum coke is placed on the tailings surface in order to reclaim the deposit as an upland or wetland landform (COSIA 2022). This cap serves several functions including separating the tailings from the ecosystem, improving the engineering properties of the deposit, and providing a stable platform from which further reclamation work can occur. Critically, the underlying tailings deposit must be able to safety support both the cap and the equipment and personnel required to place it. Otherwise, equipment can “punch through” the cap and become mired or even completely

buried in the soft tailings below, which is a significant hazard for the operator and equipment.

Clay minerals play a significant role in the challenging engineering behaviour of oil sands tailings, and therefore must also be considered in the design and implementation of capped deposits. Atterberg limits are a relatively straightforward and well-established method for evaluating clay behaviour in geotechnical engineering and are currently used to characterize tailings. However, tailings present unique challenges to the measurement of Atterberg limits compared to natural soils (e.g. Gidley and Moore, 2013). Nonetheless, index tests provide a cost-effective approach for long term monitoring of tailings deposits (Sobkowicz and Morgenstern 2009).

Atterberg limits can be used to develop correlations between the water content (normalized as the liquidity index, I_L) with remoulded undrained shear strength (Su_r) to predict the strength of a deposit. Previous work has focused on the application of existing relationships (e.g. Locat and Demers, 1988) for natural soils to tailings (Beier et al. 2013). Existing relationships developed for tailings (e.g. Banas, 1991) were also developed for fluid, low solids content tailings, which do not have sufficient strength or density to support a cap. There is therefore a need for a relationship relating the Su_r and I_L of dense, high-solids content tailings if index properties are to be used for the long-term monitoring of capped deposits.

Strength, density, and bearing capacity (q_{ult}) are key design parameters for capped tailings deposits (COSIA 2022). Current practice is to predict bearing capacity from peak undrained shear strength (Su), which is linked to the Su_r by the sensitivity ratio (S_t). By developing a relationship between Su_r and I_L, it is possible to develop a prediction for q_{ult} from index properties.

1.2 Objectives

The objectives of this research program are as follows:

1. Investigate the effect of material properties, preparation method, and test procedure on the Atterberg limits of oil sands tailings through a laboratory test program and a review of existing published data.

2. Develop a mathematical correlation between Su_r and I_L for oil sands tailings between the liquid limit (w_L) and plastic limit (w_P) using laboratory test data and compare this to the relationship developed by Locat and Demers (1988).
3. Evaluate predictions of q_{ult} from Su at the benchtop scale and compare laboratory results to predictions of q_{ult} from S_t and Su_r (using the relationship developed in objective 2).

1.3 Organization of thesis

This thesis is organized into 5 chapters:

- Chapter 2 is a literature review which provides a detailed background of relevant information to support the research program.
- Chapter 3 describes the laboratory test program, including materials and methods.
- Chapter 4 presents the results of the laboratory test program and includes a discussion of findings.
- Chapter 5 details the conclusions of this research as well as recommendations for future research.

2 Literature review

2.1 Oil sands mining and tailings production

2.1.1 Overview

The fourth-largest proven oil reserves in the world are oil sands deposits located in Northern Alberta (Government of Alberta 2023). These reserves are reported to be 158.9 billion barrels. Of the over 140 000 km^2 of surface area underlain by oil sands deposits, only 4 800 km^2 or approximately 3.4% are able to be surface mined. These deposits are in the Athabasca oil sands area (Figure 2.1). In surface mining, the oil sands ore is removed from the ground using haul trucks and excavators (AER 2020a). The bitumen is then removed from the oil sands and can be upgraded to produce synthetic crude oil. The waste product of the bitumen extraction process is known as oil sands tailings.

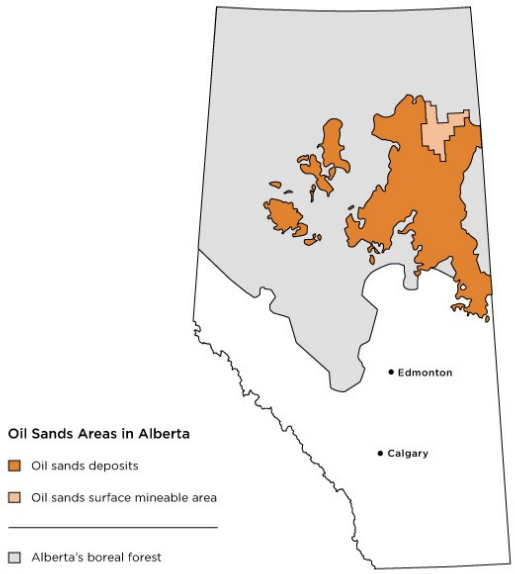

Figure 2.1. Map of oil sands areas in Alberta (AER 2020b)

2.1.2 Athabasca oil sands geology and minerology

Oil sands in Alberta were deposited in the Cretaceous age, or around 110 million years ago (Mossop 1980). In the Athabasca oil sands area, most oil sands are in the McMurray geological formation. Oil sands are a matrix of coarse- and fine-grained mineral matter with bitumen in the pore spaces. Chalaturnyk et al. (2002) states that the composition of oil sands in the McMurray formation is 84-86 wt% (percent by mass) mineral grains, 3-6

wt% water, and 0-19 wt% bitumen. Mineral grains are primarily quartz, silt, and clay. Clay occurs in discontinuous bands 1-15 cm thick with a minerology of 40-70 wt% kaolinite, 28-45 wt% illite, and 1-15 wt% montmorillonite.

2.1.3 Bitumen extraction

Oil sands mineral grains are hydrophilic, meaning that each grain is surrounded by a thin film of water and is not directly in contact with the bitumen (Mossop 1980, Masliyah et al. 2004). Clays are present in the film of water surrounding the coarser grains. A conceptual depiction of oil sands constituents is presented in Figure 2.2. This ore structure allows the bitumen to be extracted using the hot water extraction process.

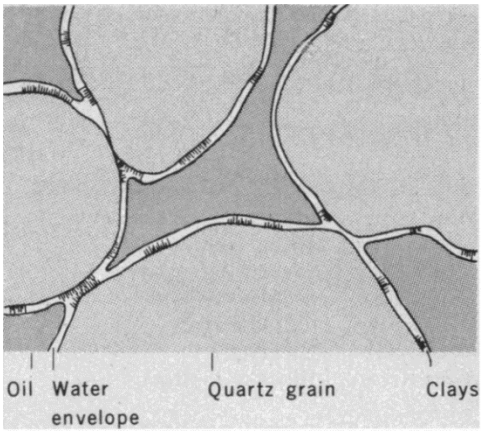

Figure 2.2. Schematic representation of oil sands constituents (Mossop 1980)

The extraction process used to separate and collect the bitumen from oil sands ore first consists of mixing crushed oil sands ore with hot water and caustic agents. (Clark and Pasternack 1932, Mossop 1980, Chalaturnyk et al. 2002, Masliyah et al. 2004). This creates a slurry mixture of mineral grains and bitumen. The coarse grains then settle to the bottom of the slurry and the bitumen floats to the top to be collected (Masliyah et al. 2004). The fine clay particles remain suspended and will eventually become the primary component of the tailings stream. The hot water extraction process results in a bitumen recovery of over 90% (Chalaturnyk et al. 2002). A caustic agent (typically NaOH) is also added in the hot water extraction process to separate the bitumen from the mineral grains and water, which ultimately results in the disintegration of the oil sands ore structure and allows the bitumen to be extracted. Addition of a caustic agent raises the pH, which

promotes the emulsification of water in bitumen, and causes the clays to swell and disperse in the pore fluid (Clark and Pasternack 1932, Chalaturnyk et al. 2002).

2.1.4 Tailings production and disposal

The tailings stream produced by the hot water extraction process is not a consistent product, and the specific composition varies depending on the composition of the ore and on the operating conditions within the extraction plant (BGC Engineering Inc. 2010). The composition is generally considered to be around 55 wt% solids, which can be further subdivided into 82 wt% sand, 17 wt% fine particles smaller than 44 μm, and 1 wt% bitumen (Chalaturnyk et al. 2002). In oil sands geotechnique, it is common practice to define “fines” as particles smaller than 44 μm (BGC Engineering Inc. 2010).

The tailings stream is hydraulically transported through a pipeline to a tailings storage facility (TSF) where it is deposited at the crest of an embankment (BGC Engineering Inc. 2010). Upon deposition, the tailings undergo segregation of the fine and coarse fraction in which the larger sand-sized particles and approximately half of the fines are deposited near the end of the pipeline. The remaining fine particles flow with the water to a pond at the centre of TSF. These tailings are referred to as fluid tailings (FT) and have an initial solids content of 6-10 wt%. The tailings are referred to as mature fine tailings (MFT) once they have achieved a solids content >30 wt% through settling and consolidation (Chalaturnyk et al. 2002). The transformation of FT to MFT typically takes a few years, however, subsequent densification of MFT to a solid state able to support the loads required for reclamation may take more than a century (Chalaturnyk et al. 2002, BGC Engineering Inc. 2010, COSIA 2012). This is in part due to the role of clays in oil sands tailings behaviour.

2.1.5 Influence of clays on oil sands tailings behaviour

Clay minerals are characterized by their small particle size (usually considered to be less than 2 μm), plasticity when mixed with water, planar shape, and negative surface charge (Mitchell and Soga 2005). Clay minerals consist of layers of different structural units (Figure 2.3, Figure 2.4) arranged into sheets. These sheets are then arranged in different combinations to form the different types of clay minerals (Figure 2.5).

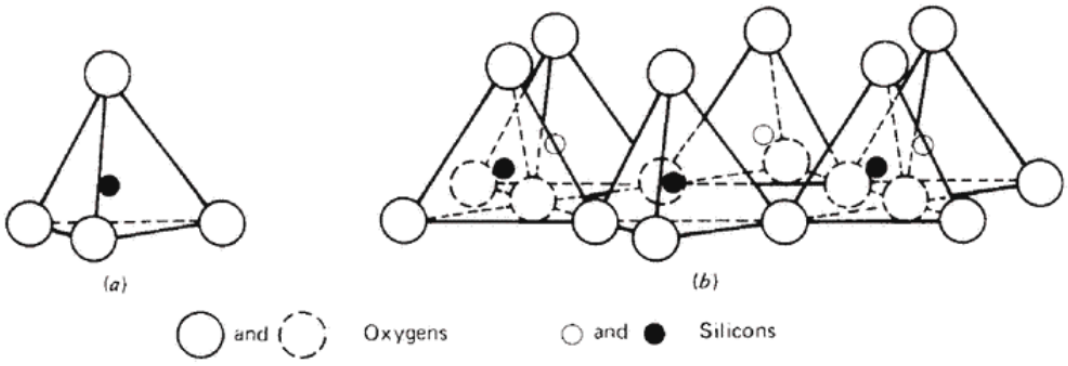

Figure 2.3. Silicon tetrahedron and sheet structure (Mitchell and Soga 2005)

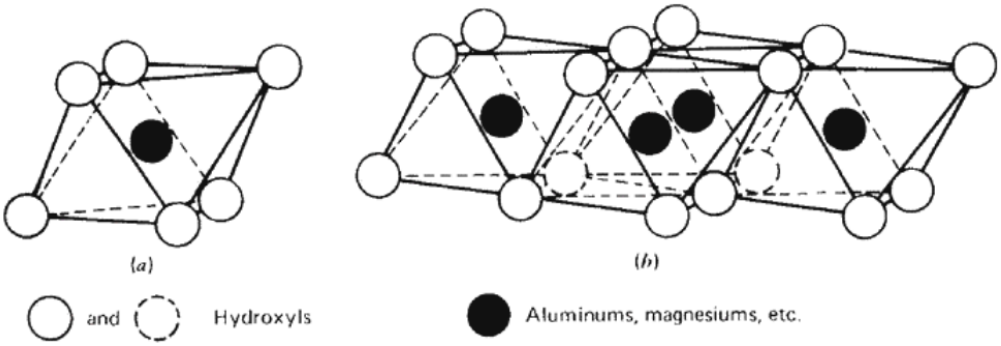

Figure 2.4. Octahedral unit and sheet structure (Mitchell and Soga 2005)

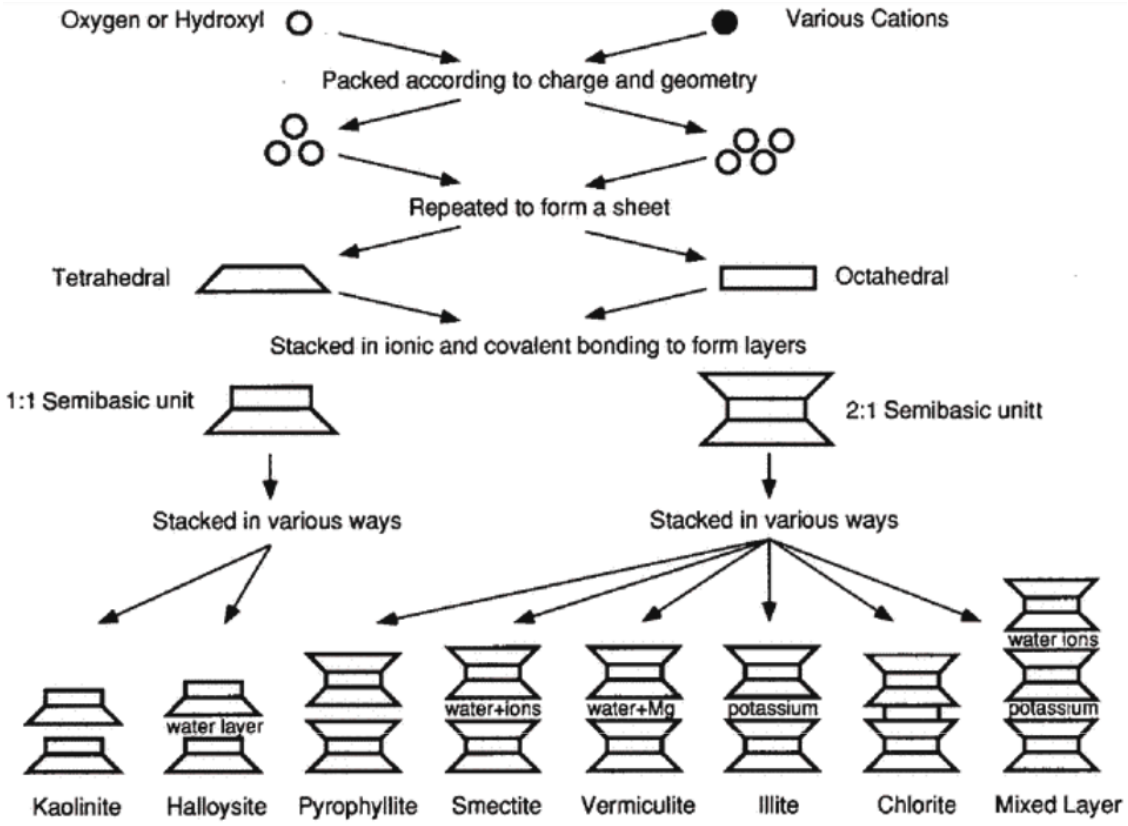

Figure 2.5. Schematic formation of clay mineral types (Mitchell and Soga 2005)

Within the crystal structure, it is possible for a different cation to occupy the central position of the tetrahedron or octahedron (e.g. Si^{4+}replaced with Al^{3+} in a silicon tetrahedron) (Mitchell and Soga 2005). This is referred to as isomorphous substitution and is the cause of the negative surface charge in most clays. The negative surface charge results in a system of clay-water-ion interactions in which changes in pore water chemistry influence geotechnical behaviour.

Of the clays present in oil sands tailings, montmorillonite has the strongest influence on overall behaviour (Chalaturnyk et al. 2002). Montmorillonite is a mineral in the smectite group and is characterized by a high degree of isomorphous substitution (Mitchell and Soga 2005). As a result, montmorillonite has a strong attraction to cations to balance out the negative charge. Montmorillonite also swells significantly in the presence of water. Conversely, kaolinite is notable within the clay minerals because occurrences of isomorphous substitution are theorized to be few to none. Interactions between kaolinite,

water, and ions are the result of pH-dependent “edge” charges perpendicular to the long direction of the sheet.

Interactions between clay, water, and ions in the hot water extraction process ultimately influence the overall geotechnical behaviour oil sands tailings. The high concentration of Na^+ from the addition of NaOH as a caustic agent causes the clay particles to become highly dispersed (Chalaturnyk et al. 2002, Mitchell and Soga 2005, Miller et al. 2009, 2010). As a result, oil sands tailings have poor geotechnical characteristics upon deposition and consolidate and increase in strength very slowly.

2.2 Oil sands tailings reclamation

2.2.1 Regulatory framework

The overall direction on oil sands tailings reclamation is set by the Government of Alberta through the *Tailings Management Framework for the Mineable Athabasca Oil Sands* (TMF) (Alberta Government 2015). The goal of the TMF is to decrease the risk created by the accumulation of large volumes of tailings on the landscape by setting project-specific limits on tailings production. These limits are intended to encourage progressive reclamation of the tailings during the mining operations. The TMF ultimately requires that all tailings are ready to reclaim within 10 years of the end of bitumen mining.

These volume limits are enacted and enforced by the Alberta Energy Regulator (AER) in Directive 085: Fluid Tailings Management for Oil Sands Mining Projects (AER 2017). Each project must operate within an approved tailings volume profile over the life of the mine. This profile is intended to capture both the increase in tailings volumes on-site during the initial stages of production as well as the decrease in volume as tailings are progressively reclaimed. An example of an approved tailings volume profile is shown in Figure 2.6.

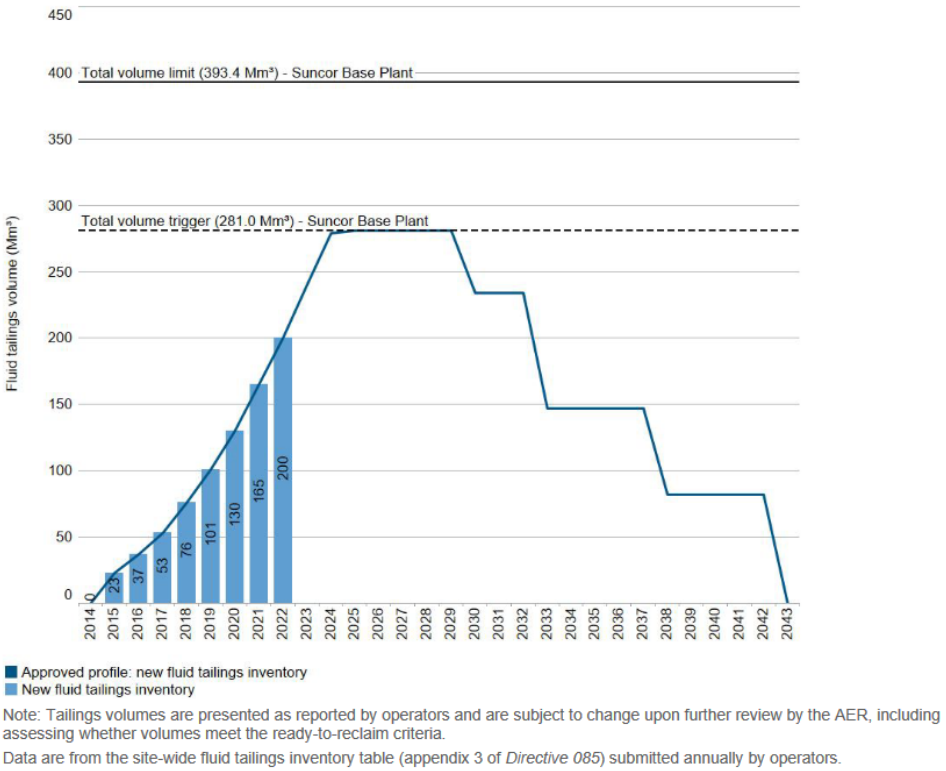

Figure 2.6. Approved new fluid tailings profile for Suncor Base Plant (AER 2023)

Tailings are removed from the profile once classified as “Ready to Reclaim” (RTR) (AER 2017). To be classified as RTR, the tailings must be processed, meet deposit-specific geotechnical and geoenvironmental performance criteria, and placed in their final position in what will become the reclaimed landscape. Examples of processing methods currently in use by operators to improve the geotechnical performance of tailings are presented in Table 2.1. These methods may be applied to both new tailings prior to deposition and previously deposited tailings (referred to as legacy tailings), which are removed from TSFs, treated, and re-deposited (AER 2023). Reclamation of untreated fluid tailings as an upland, terrestrial landform is not feasible. All tailings must be classified as RTR within ten years of the end of bitumen mining. *Directive 085* species that the ultimate objective of oil sands reclamation is to reclaim mining areas (including tailings deposits) to “a self-sustaining boreal forest ecosystem that is (1) integrated with the surrounding area and (2) consistent with the values and objectives identified in local, subregional, and regional plans” (AER 2017).

Table 2.1. Tailings treatment methods

Tailings treatment	Description[†]
Untreated FT	A fluid mixture of water and fines that has not undergone any further treatment.
MFT	FT that has increased in density through self-weight consolidation in a TSF.
Flocculated tailings	Flocculant is added to form chemical bonds between particles, causing them to agglomerate and settle faster.
Coagulated tailings	Coagulant is added to modify surface charge and promote agglomeration.
Flocculated and coagulated tailings	Coagulant is added in addition to flocculant.
Thickened tailings	Flocculant is added in a process vessel (thickener) to promote settling of suspended particles.
Centrifuged tailings	A portion of the fluid phase is separated from the solid phase by spinning in a centrifuge.
Cyclone overflow	A hydrocyclone is used to separate the tailings into underflow (high density, low fines) and overflow (low density high fines)
In-line thickened tailings	Flocculants and coagulants are mixed into cyclone overflow during pipeline transport.
Filtered tailings	Mechanical dewatering by applied pressure or vacuum.

[†] Descriptions summarized from BGC Engineering Inc. (2010)

2.2.2 Capping

After the tailings have been treated, the TSF must eventually be capped, which refers to the placement of material on top of the tailings surface. If a deposit is to be reclaimed as an upland or wetland landform, materials that can be used for a cap include tailings sand, petroleum coke, and other mine waste such as excess soil materials excavated during surface mining (COSIA 2022). Research on water capping tailings (i.e. end pit lakes) is ongoing (e.g. CEMA, 2012). Multiple oil sands mines are targeting terrestrial tailings deposits with wetlands as a reclamation strategy (AER 2023). Above the cap is the reclamation cover (including growth material and vegetation) that allows the deposit to function as part of the boreal forest ecosystem. A comprehensive summary of capping oil sands tailings deposits, including case histories, is presented in COSIA (2022).

Capping is a critical step in reclaiming the mine site and supports multiple closure objectives (COSIA 2022). The cap design selected is informed by the target end land use, capping material available, and the methods to be used to place that material. Methods for capping tailings are summarized in Figure 2.7. Key functions of the cap include:

- Physically, chemically, and biologically separating the tailings from the ecosystem.
- Water management, including directing surface drainage across the landform and managing water quantity and quality (e.g. tailings pore fluid released through consolidation).
- Enhancing geotechnical stability by increasing the strength and density of the underlying tailings.
- Providing a trafficable surface to safely the support equipment (e.g. trucks and bulldozers) placing the reclamation cover and end land uses (e.g. vehicles, foot traffic, and wildlife).
- Storing waste materials such as tailings sand, petroleum coke, and overburden.
- Support the reclamation ecosystem (e.g. by providing topographic diversity for wildlife habitat).

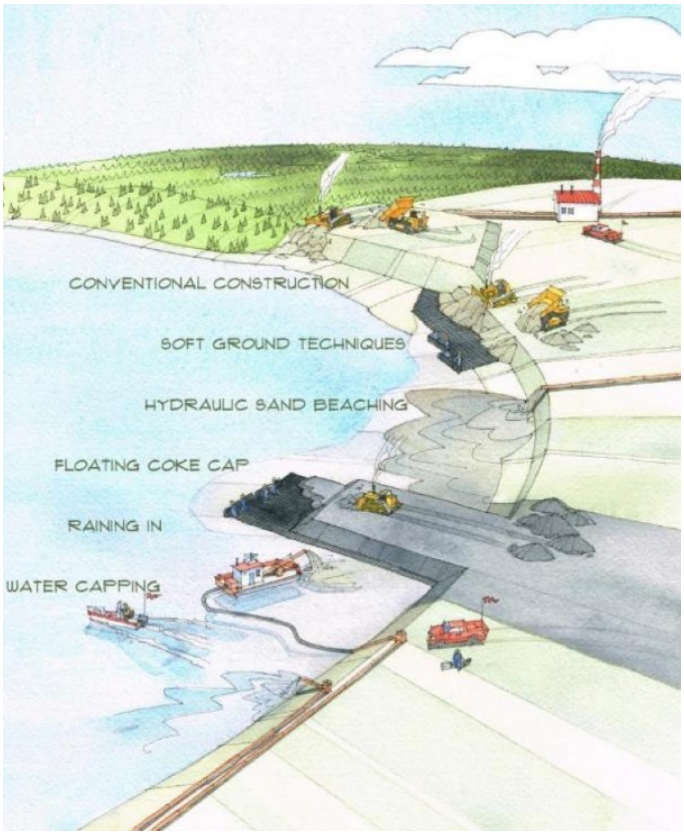

Figure 2.7. Methods for capping oil sands tailings deposits (COSIA 2022)

A combination of hydraulic and mechanical methods is typically used for tailings deposits targeting closure as a terrestrial landform (COSIA 2022). A first “blanket layer” is deposited to create a trafficable surface from which to place additional capping material. From this blanket layer, additional capping material is deliberately placed to provide topographic relief, which controls surface water drainage across the landform and supports diverse wildlife habitats (Jakubick and McKenna 2001, COSIA 2022).

The expected amount of post-reclamation settlement is a key cap design parameter (COSIA 2022). McKenna et al. (2016) plotted approximate ranges of different capping techniques by density (solids content) and peak undrained shear strength (*Su*) in Figure 2.8. Soft, high fines content tailings can settle tens of meters over hundreds of years, significantly impacting surface drainage and overall performance of the landform (COSIA 2022). Additionally, shear strength, consolidation, and hydraulic conductivity govern the bearing capacity and settlement of tailings beneath a cap as well as the ability of the cap to prevent the migration of contaminants from the tailings deposit to the surrounding

ecosystem (Williams 2015). Water caps or floating coke caps may be most appropriate for deposits with high post-reclamation settlement (COSIA 2022). Coke is considered to be an ideal capping material due to its high strength and low density, which allows it to float on top of the tailings (Pollock et al. 2010). In contrast, the density of sand is higher than oil sands tailings, meaning that it is possible for inversion of the materials to occur where the sand sinks into the tailings deposit (Fredlund et al. 2018).

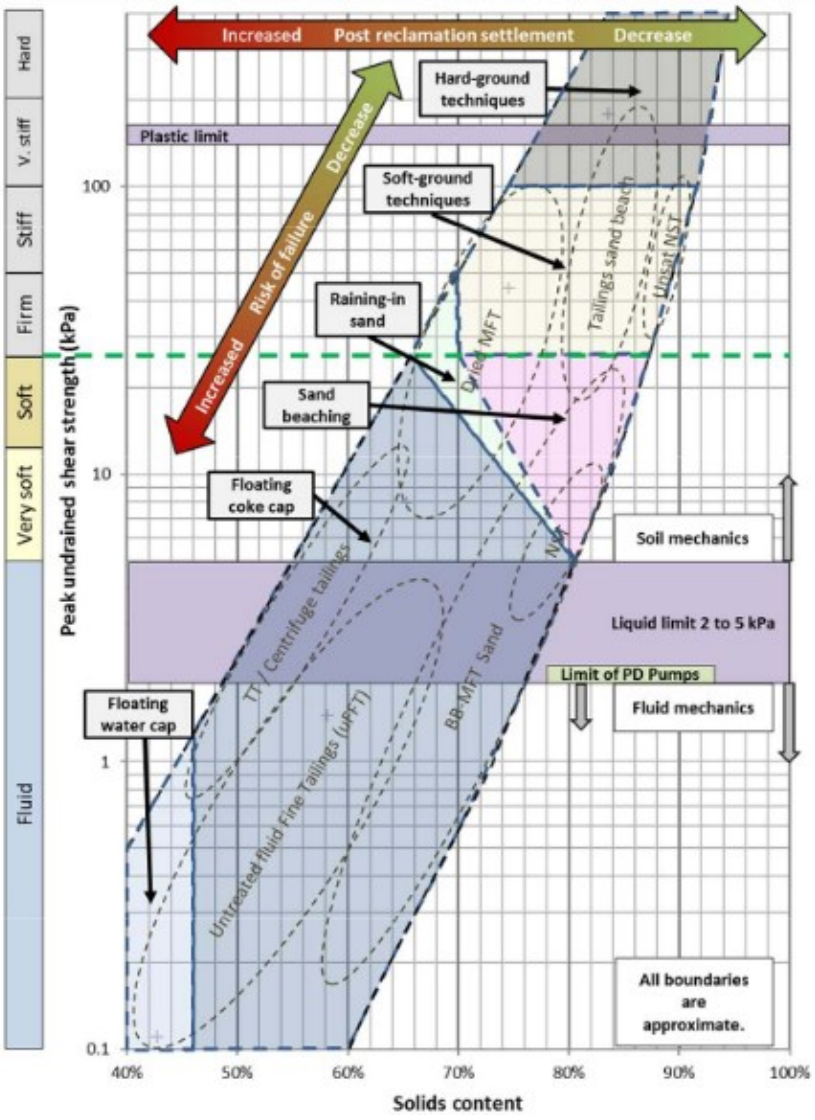

Figure 2.8. Applicability of capping technologies for approximate ranges of oil sands fine tailings shear strength and solids contents (McKenna et al. 2016)

Research on capping tailings deposits is ongoing, though are a number of successful case histories (COSIA 2022). In particular, the construction of a floating coke cap over MFT by Suncor is documented in detail by Pollock et al. (2010), Wells et al. (2010), and Abusaid and Pollock (2011). In a review of case histories, COSIA (2022) identified particular challenges to capping oil sands tailings as:

- Achieving the geotechnical stability needed to support the cap and reclamation cover, as well as the equipment required to place it (trafficability).
- Accounting for the design constraints created by the existing deposit, including tailings heterogeneity (from the depositional history over the life of the facility) and dyke geometry.
- Differential settlement of the consolidating tailings.
- Managing the effects of upward seepage of tailings pore water from consolidation on both surface water quality and quantity.
- Erosion of cap materials by wind and surface water.
- Spillway design.

For there to be a cap and reclamation cover, equipment must first be able to safely place this material, meaning that concerns about trafficability must be resolved to achieve closure goals. Equipment operating on the blanket layer can “punch through” and become mired in the soft tailings below, posing a significant hazard to the operator (COSIA 2022). Key design parameters for trafficability include strength, density, and bearing capacity (Pollock et al. 2010, COSIA 2022).

2.3 Atterberg limits of oil sands tailings

The influence of clays on the geotechnical behaviour of oil sands tailings is the source of many reclamation challenges such as slow strength gain and consolidation. To understand the engineering behaviour of oil sands tailings, it is therefore necessary to understand the behaviour of clays. A common method for quantifying the behaviour of clays is through Atterberg limits, which are water contents that define the limits of plastic behaviour. Atterberg limits were first defined by Albert Atterberg in the early 20th century (Atterberg 1911), though Casagrande and Terzaghi are credited with first applying the Atterberg limits to geotechnical engineering practice (Terzaghi 1925, Casagrande 1932).

The Atterberg limits of a soil are the geotechnical water contents (defined as the ratio of the mass of water to the mass of solids) that correspond to specific transitions in behaviour. Geotechnical solids content (defined as the ratio of the mass of solids to the total mass) can also be used to define Atterberg limits. The Atterberg limits are the plastic limit (w_P) and liquid limit (w_L) (Figure 2.9). The liquidity index (I_L) is the water content of the soil relative to w_P (I_L = 0) and w_L (I_L = 1). The plasticity index (I_p) is the difference between w_L and w_P and defines the range of water contents at which the soil behaves plastically rather than as a liquid or a brittle solid. A clayey soil will exhibit liquid-like behaviour at water contents above w_L and brittle behaviour at water contents below w_P. It has also been reported that most soils will begin to desaturate as the water content approaches w_P (Fredlund et al. 2012)

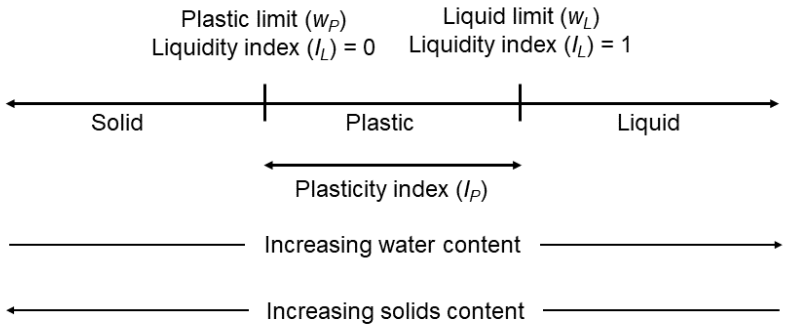

Figure 2.9. Atterberg limits definitions

The significance of Atterberg limits to oil sands tailings is that relationships can be developed between the Atterberg limits and the mechanical properties of a soil, such as the compression index and remoulded undrained shear strength (Su_r) (Wroth and Wood 1978). Sobkowicz and Morgenstern (2010) suggest that index tests such as Atterberg limits and field measurements of solids content could be a cost-effective approach to monitor the long-term performance of tailings deposits as a complement to in-situ tests (e.g. CPT, shear vane, etc.).

2.3.1 Methods for determining the Atterberg limits

Standard methods have been developed for determining the Atterberg limits. There are two methods that may be used to determine w_L. In North America, the Casagrande cup

(Figure 2.10) is typically used. Standards that describe this method include ASTM D4318-17 and CAN/BNQ 2501-090 (ASTM 2017, BNQ 2019). Alternatively, a fall cone penetrometer (Figure 2.11) may be used as described in CAN/BNQ 2501-02 and BS 1377(BNQ 2019, BSI 2022). w_P is typically determined by rolling the soil to a thread of a specified diameter (3.2 mm). A small metal rod of 3.2-mm diameter is often used to compare the thread to the target diameter (Figure 2.10). All tests are performed using only the fine fraction of material passing the No. 40 (425 μm) sieve. Common methods and equipment are summarized in Table 2.2. There have been several studies that have compared the use of the Casagrande apparatus and fall cone methods for determining the liquid limit. Claveau-Mallet et al. (2010) compared the methods for a Quebec saline clay and found that the methods produced similar results.

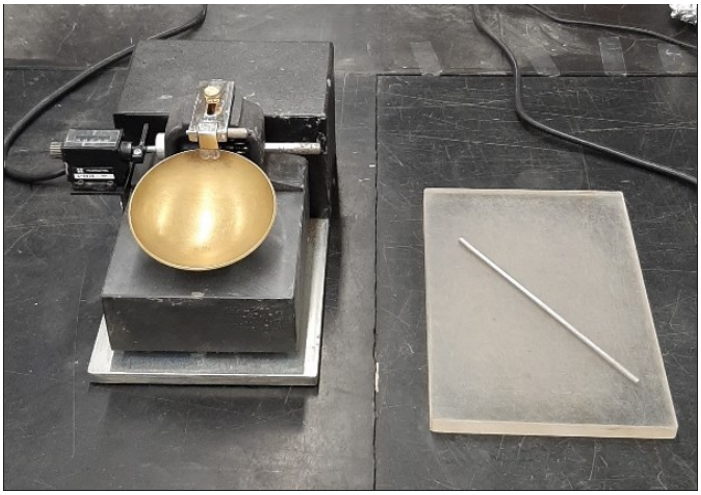

Figure 2.10. Casagrande cup (left) and 3.2-mm diameter rod (right)

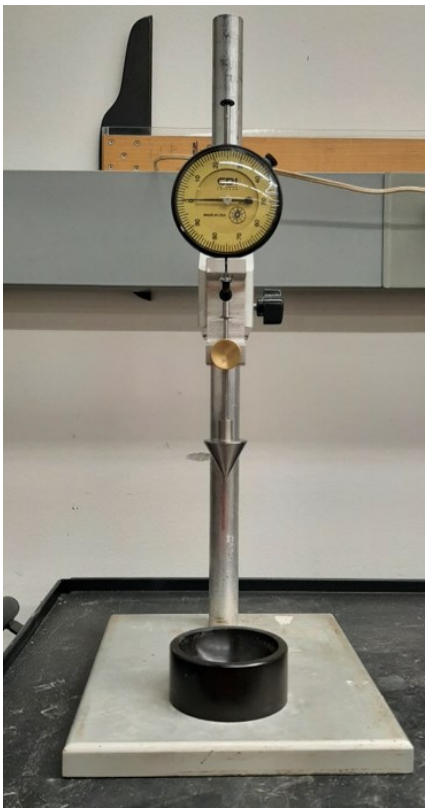

Figure 2.11. Fall cone penetrometer

Table 2.2. Summary of test methods (ASTM 2017, BNQ 2019)

Measurement	Method	Summary
w_L	Casagrande cup	w_L is the water content at which 25 drops of the Casagrande cup are needed to close a gap in the soil created by a standard grooving tool.
w_L	Fall cone penetrometer	w_L is the water content at which a 30˚cone (80g) penetrates 20 mm into the soil.
w_P	Thread rolling	w_P is the water content at which a thread of soil crumbles at a diameter of 3.2 mm.

2.3.2 Factors that influence the measurement of Atterberg limits

The Atterberg limits of a particular soil or clay mineral type are not a constant but rather exist as a range of values. Factors that influence the Atterberg limits of a particular soil are complex and include both the properties of the soil and the test method:

- Clay content: A soil with a higher clay content will have a higher w_L and w_P (Seed et al. 1964).
- Clay mineralogy: The structure and composition of a clay mineral influences its interaction with the pore fluid, which in turn affects the Atterberg limits. In particular, clay minerals with a larger specific surface areas (g/m^2) have a higher w_L (e.g. montmorillonite) (Mitchell and Soga 2005).
- Operator: The measured w_L and w_P vary depending on the experience of the operator (Liu and Thornburn 1964). The error is most significant for the w_P.
- Pore fluid chemistry: Reducing the concentration of salts reduces w_L, though the significance of this effect depends on the clay mineralogy (Skempton and Northey 1952). The type of water used for testing (e.g. deionized vs. tap) and how the sample was prepared (e.g. water content increased by addition of water vs. decreased by drying) therefore impacts results. An increase in the concentration of monovalent cations (e.g. Na^+) decreases w_L (Mitchell and Soga 2005). As the cation valence increases (e.g. increasing concentration of Ca^{2+}), w_L of expansive clays (e.g. montmorillonite) increases and w_L of non-expansive clays (e.g kaolinite) decreases.
- Oven drying: Basma et al. (1994) reported that oven-drying at high temperatures (110˚C) removes both free water in pore spaces as well as some bound water held in the lattice of the clay minerals. Compared to clays dried at room temperature and a low oven (60˚C), the clays dried at 110˚C had a lower fraction of clay-sized particles and w_L decreased. This was attributed to particle aggregation caused by higher ionic concentrations surrounding the particle as the water is removed. As clays move closer together to form larger particles, the surface area available for interaction with water is decreased, leading to a decrease in w_L. Drying temperature did not result in a significant effect on the measured w_P.

Like natural clays, the Atterberg limits of tailings are also influenced by factors including clay content, clay minerology, and pore fluid chemistry (Scott et al. 1985, Jeeravipoolvarn et al. 2008, Wells and Kaminsky 2015). Tailings also contain bitumen and additives (e.g. polymer flocculants) which influence their engineering behaviour, including their Atterberg limits. Factors that influence the Atterberg limits of oil sands tailings include:

- Bitumen content: Atterberg limits tests on tailings are usually performed including the bitumen, however, the role bitumen plays in tailings behaviour is not definitively understood. Scott et al. (1985, 2013) report that higher bitumen content results in a higher w_L and a higher I_P. Similarly, Gidley and Moore (2013) observed that the w_L and I_P for MFT from which bitumen was removed by the Dean Stark method decreased, and note that further study is needed to understand this mechanism.
- Clay content and fines content: Higher clay content results in a higher w_L and w_P (Sorta 2015). Similarly, a higher fines content results in a higher w_L and w_P. In oil sands tailings geotechnique, the fines content is defined as the fraction of material smaller than 44 μm. This fraction includes clay-sized particles (< 2 μm) and some silt sized particles. Jeeravipoolvarn et al. (2008) observed that it was possible to use the fines content rather than the clay content to compare the Atterberg limits.
- Sand content: Some tailings streams are mixed with sand to improve their engineering properties (e.g. thickened tailings). In some cases, the Atterberg limits of oil sands tailing are determined without removing sand-sized particles to better capture their behaviour. A higher sand content results in a lower w_L and I_p (Jeeravipoolvarn 2010, Kabwe et al. 2019, 2021).
- Process additives: Additives such as polymer flocculants increase w_L of tailings by absorbing water (Kabwe et al. 2013). There is also a relationship between the optimum dose of flocculant and the Atterberg limits of the tailings as they are both related to the quantity of the clay and clay-ion interactions (Anstey and Guang 2017). The effects of polymer flocculants on Atterberg limits have also been discussed by Jeeravipoolvarn (2010), Bajwa (2015), Wilson et al. (2018), and Kabwe et al. (2021). Tate et al. (2017) and Miller et al. (2010) studied the effects of coagulants.

- Clay minerology and origin: The dominant clay minerals in oil sands tailings are typically reported as kaolinite and illite, though small quantities of interstratified smectite strongly influence the overall behaviour (Chalaturnyk et al. 2002, Kaminsky et al. 2006). Different depositional histories of the parent oil sands (e.g. estuarine vs. marine) can also impact the properties and therefore the Atterberg limits (Jeeravipoolvarn 2010).
- Extraction process: Additives (e.g. NaOH) are used in the extraction process to enhance bitumen recovery from oil sands. Miller et al. (2010) evaluated the impact of caustic (NaOH) and non-caustic (H_2SO_4) extraction processes on the properties of tailings and observed that tailings with a higher concentration of Na^+ had a lower w_L.
- Thixotropy: Oil sands tailings are a highly thixotropic material, meaning that they experience rapid strength gain following remoulding. Since Atterberg limits tests are performed on remoulded samples, tests on oil sands tailings must be performed immediately after remoulding. Allowing tailings to experience thixotropic strength gain leads to a larger measured w_L (Miller et al. 2010).

The number of factors that are captured in the Atterberg limits illustrates their complexity despite the relatively simple procedures used to measure them. The composition and properties of tailings vary between and within mine sites, as well as within the same facility. Atterberg limits are most effective when comparing tests from the same mine (Wells and Kaminsky 2015). Additional tests (e.g. pore fluid chemistry, bitumen content, fines content, methylene blue index, etc.) are also necessary to characterize the material.

The effect of test methodology on the measured Atterberg limits of MFT was previously studied by Gidley and Moore (2013). The preparation methods used were wet and dry, and the type of water used in the test (deionized [DI] or process water) was varied. Tests were also performed on 2 types of flocculated MFT and MFT from which bitumen was removed using the Dean Stark method. Results are presented in Figure 2.12. It was concluded that the test methodology significantly impacts the results, and that a standardized method should be developed for oil sands tailings.

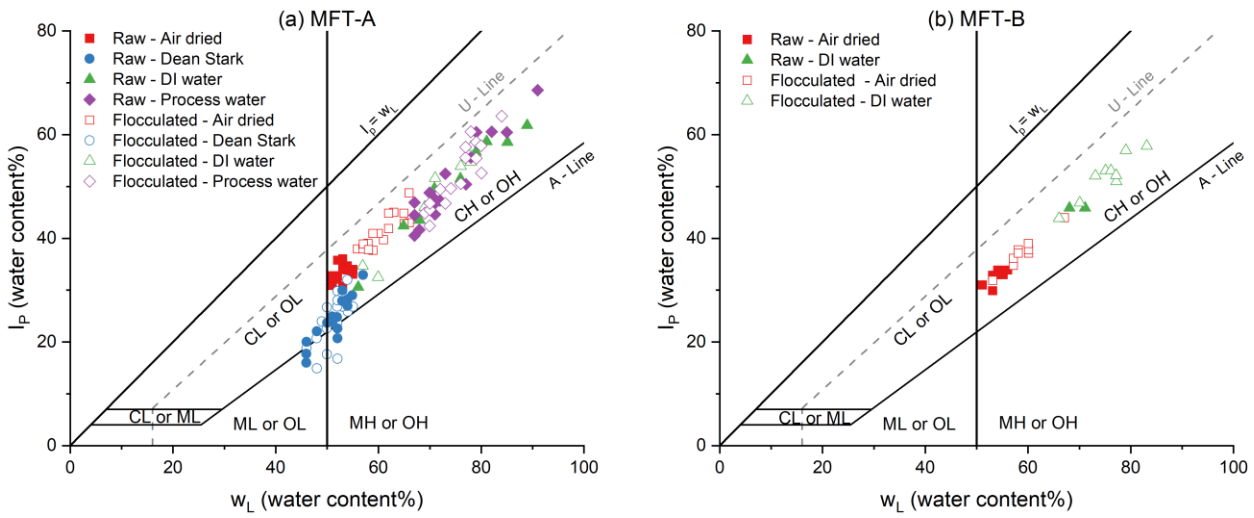

Figure 2.12. Plasticity chart - MFT using different methods and amendments (data from Gidley and Moore, 2013)

Average values for each measurement are presented in Table 2.3. Rewetting the sample with deionized water or process water increased both w_L and w_P compared to air-drying the sample to the consistency limit, and there was little difference between the effect of deionized water or process water. However, it is not reported whether the rewetted samples were oven dried prior to the test. The effect of Dean Stark extraction (bitumen is removed and the sample is oven-dried) appears to be an increase in w_P and a decrease in w_L.

Table 2.3. Average values of Atterberg limits from Gidley and Moore (2013)

MFT		Average w_L (%)				Average w_P (%)			
		Air-dried	DI Water	Process water	Dean Stark	Air-dried	DI Water	Process water	Dean Stark
A	Raw	52.8	74.4	74.3	51.2	19.4	24.1	23.3	26.8
	Flocc.	60.9	69.8	75.5	51.2	19.5	22.5	23.2	27.0
B	Raw	54.0	69.6			21.3	23.7		
	Flocc.	57.1	70.1			21.7	23.4		

2.3.3 Challenges in determining the Atterberg limits of oil sands tailings

While many factors that influence tailings behaviour can be captured with Atterberg limits, it is difficult to achieve reliable and accurate results. Existing methods and equipment were developed for natural soils, and deviations from standards are often required. Unlike natural clays, oil sands tailings typically exist in a fluid state above w_L and must be dewatered prior to testing. This can be accomplished by air-drying at low temperatures or consolidation where the water is pushed out of the tailings using an applied load. The tailings may be either “dried down” (i.e. the first data point is above w_L and subsequent data points have progressively lower water contents) or “wetted up” (i.e. the first data point is below the w_L and water is added such that the data points have progressively higher water contents. If the tailings are “wetted up,” the water chemistry (i.e. deionized water, pore water, etc.) will have implications for the measured values.

The presence of bitumen also complicates the application of existing standards (COSIA 2014a). It is preferred to perform Atterberg limits tests on tailings including the bitumen fraction to best represent field conditions. Standard methods also require that Atterberg limits tests are performed on the fraction passing the No. 40 (425 µm) sieve (ASTM 2017). However, it is impractical to remove the coarser material using a sieve without also removing a significant fraction of bitumen. Further, Yao (2016) reported difficulties in capturing the bitumen fraction for Atterberg limits testing because it adhered to container walls.

2.3.4 Published Atterberg limits of oil sands tailings

A plasticity chart was prepared using publicly available Atterberg limits data (Figure 2.13). The majority of tailings can be classified as either lean clay (CL) or fat clay (CH). All data is presented as geotechnical water content. Data points have been sorted by tailings processing method. The range of properties and number of data points for each type of tailings is presented in Appendix A along with data sources.

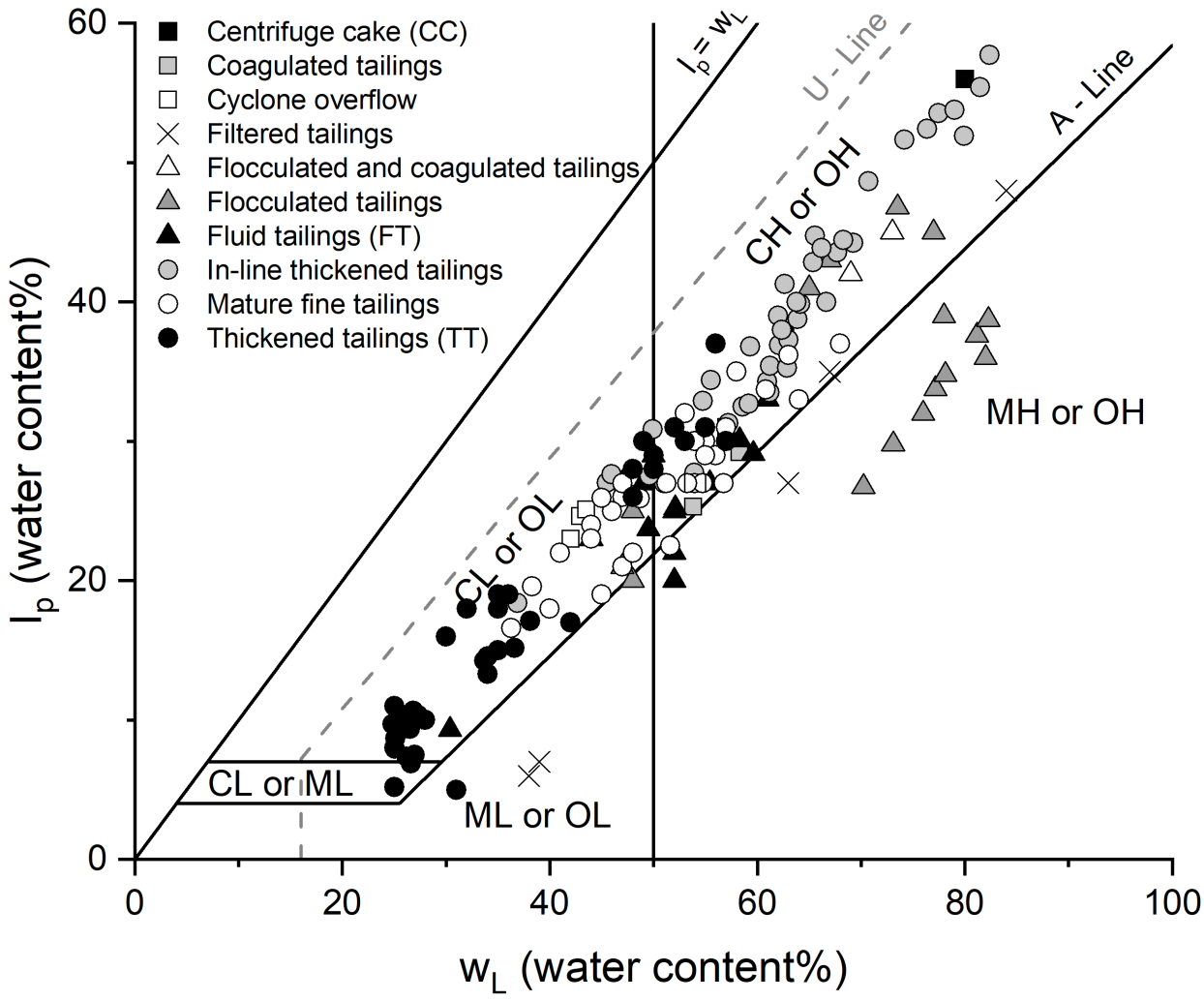

Figure 2.13. Atterberg limits of oil sands tailings from literature

Differences in reporting methods of bitumen content and fines content prevented the comparison of Atterberg limits based on these factors. Bitumen content may be reported as the percentage of bitumen relative to the total mass, mass of fines, or mass of solids. It is often not reported which definition is being used. Similarly, fines content may be reported as the percentage of fines relative to the total mass or solids mass.

The procedures and equipment used by different to determine the Atterberg limits were also noted. The overall findings include:

- Equipment: Most authors report using ASTM D4318 (Casagrande apparatus) or do not report their methods. Wijermars (2011), Bajwa (2015), Elias (2019), and

Salam (2020) report using the fall cone penetrometer to determine w_L. Salam (2020) also estimated w_P from w_L using the model proposed by Feng (2001) that considers cone penetration depth and water content.

- Dewatering method: Air-drying was the most commonly used method to dewater the tailings among authors who reported their procedures. Banas (1991), Jeeravipoolvarn et al. (2008), Miller et al. (2010), Innocent-Bernard (2013), Kabwe et al. (2013), and Yao (2016) allowed water to evaporate at room temperature. Banas (1991) reported using a fume hood to increase the rate of dewatering at room temperature. A centrifuge was used by Banas (1991) and Tang (1997). A low oven (26˚C) was also used by Tang (1997). Only Sorta (2014) reported using loading and self-weight consolidation to dewater the tailings, which preserves the fines content, pore fluid chemistry, and bitumen content of the sample. However, the consolidation of tailings is very slow and a sample can take multiple weeks to prepare (Miller et al. 2010, Sorta 2015). Wijermars (2011) oven-dried and ground the tailings prior to testing, though this is not recommended as high temperatures impact the minerology and composition.
- Test water: Banas (1991) and Innocent-Bernard (2013) reported using distilled water to determine w_L. No other authors reported whether the tailings were diluted to determine w_L.
- Thixotropy: Jeeravipoolvarn (2005), Miller et al. (2010), and Sorta (2014) note the importance of thixotropy and specify that w_L was determined immediately after remoulding.

2.4 Relationship between Atterberg limits and strength

The Atterberg limits describe a change in behaviour from semi-solid to plastic to liquid behaviour as the water content increases. This change in behaviour is also observed as a change in strength and may be represented as a mathematical relationship between the remoulded undrained shear strength (Su_r) and water content. Atterberg limits can then be used to convert the water content to I_L and express Su_r as a function of I_L. Su_r is distinguished from the peak undrained shear strength Su, which is the strength prior to remoulding or the undisturbed strength. The ratio between the peak and remoulded strengths is referred to as sensitivity (S_t). The specific value of S_t is unique for a given soil

under a particular set of conditions and is influenced by the influenced by the soil fabric and chemistry, as well as by thixotropic strength gain over time following remolding (Mitchell and Soga 2005).

The relationship between Su_r and I_L has been widely accepted in geotechnical engineering practice for several decades. Wroth and Wood (1978) note that this relationship provides a straightforward method to estimate a lower bound of strength, though it does not replace a detailed sampling and site investigation program. Shimobe and Spagnoli (2020) identified over 20 relationships between Su_r and I_L for natural soils. Individual relationships were developed using different soils and methods for measuring Su_r (including fall cone penetrometers, shear vanes, and viscometers). Many relationships are based on assumptions of strength at w_L and w_P. A common assumption is that Su_r at the w_L is 1.7 kPa (based on the work of Wroth and Wood, 1978) and that Su_r at w_P is 100 times that at the w_L (~ 170 kPa) (e.g. Sharma and Bora 2003, Mitchell and Soga 2005). Sharma and Bora (2003) demonstrated the general validity of these assumptions by performing fall cone penetrometer tests on a variety of inorganic soils.

2.4.1 Remoulded strength – liquidity index relationships for oil sands tailings

Relationships developed for natural soils have previously been used to understand the behaviour of oil sands tailings. Banas (1991) observed that the relationship between Su_r and w_L of MFT was similar to those that had previously developed for natural soils. Beier et al. (2013) found that deposits of MFT behaved similarly to natural clay slurries based on a comparison of Su_r and w_L data to existing mathematical relationships for natural soils. The relationship developed by Locat and Demers (1988) (Equation 2.1) has been found to approximate the behaviour of tailings (Banas 1991, Beier et al. 2013, Jeeravipoolvarn et al. 2020).

Equation 2.1

$$Su_r(Pa) = \left(\frac{19.8}{I_L}\right)^{2.44}$$

The relationship proposed by Locat and Demers (1988) was developed for Quebec sensitive clays with I_L between 1.5 and 6. The fall cone was used to measure most values

of Su_r with some low-strength values determined by assuming a linear relationship between Su_r and yield stress. The original dataset used to develop this relationship is shown in Figure 2.14. The value of R^2 of 0.95 indicates that there is good agreement between the model (Equation 2.1) and the data. As the difference between the predicted and actual strength decreases, R^2 increases up to a maximum of 1.0, which describes a perfect fit between the model and the data. Lower values of R^2 indicate larger differences between the model and the data. The difference between the model and the data is also shown by plotting pairs of measurements and predictions with the line of equality (y = x) in Figure 2.15. This plot demonstrates that there is some scatter in the dataset and that most of the measurements used to develop this relationship were for very low strength soils (Su_r < 500 Pa or 0.5 kPa).

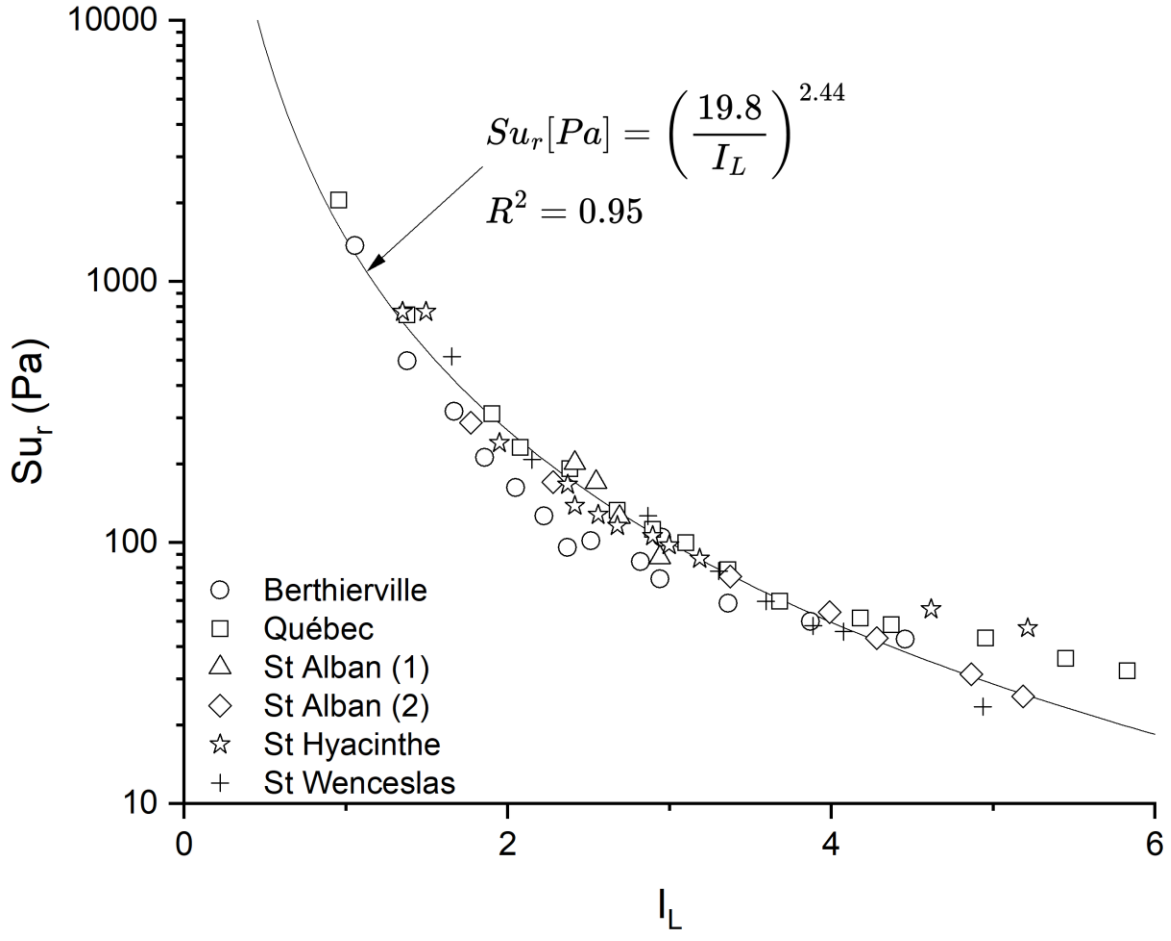

Figure 2.14. Su_r – I_L relationship for Quebec sensitive clays (Locat and Demers 1988)

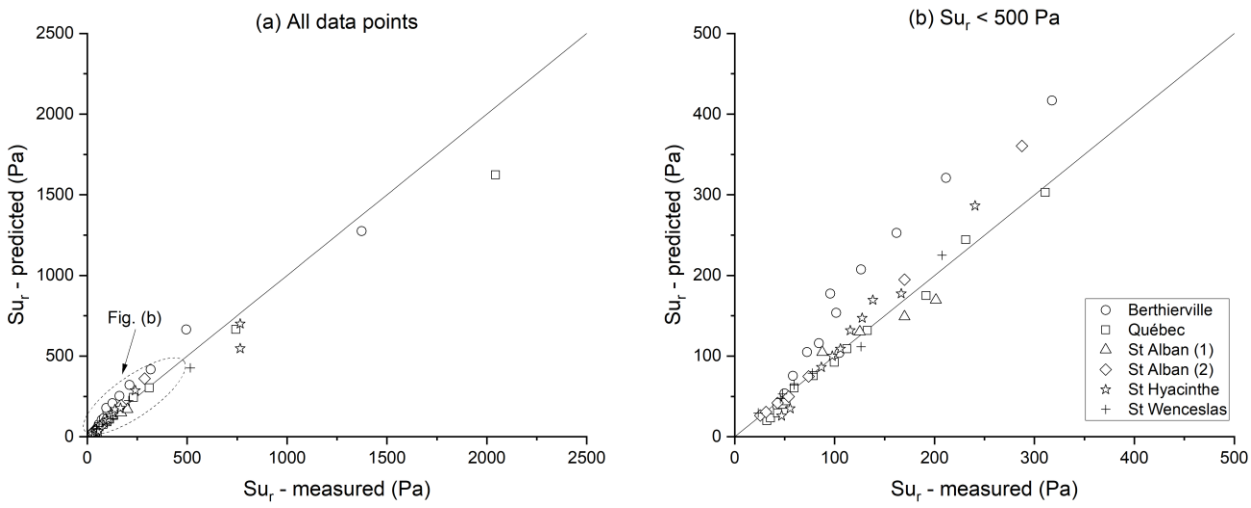

Figure 2.15. Comparison of measured and predicted values from Locat and Demers (1988)

Similar to natural soils, the Su_r of oil sands tailings at the w_L and w_P are often assumed to be approximately 1-2 kPa and 100 kPa, respectively (COSIA 2012, 2014a). The assumed strength at the w_L has been used to inform reporting requirements and regulations. The pond bottom in a tailings storage facility is defined as the point at which the strength approximately corresponds to the w_L (COSIA 2012). *Directive 074: Tailings Performance Criteria and Requirements for Oil Sands Mining Schemes* (which has since been superseded by *Directive 085*) previously specified tailings reclamation requirements and considered the boundary between fluid and solid tailings to be an undrained shear strength of 5 kPa, which was set based on an assumed undrained shear strength at the w_L of around 2 kPa (COSIA 2015).

Publicly available data for Su_r and I_L is plotted in Figure 2.16 with the relationship proposed by Locat and Demers (1988). Sources of data for each type of tailings are presented in Appendix A.

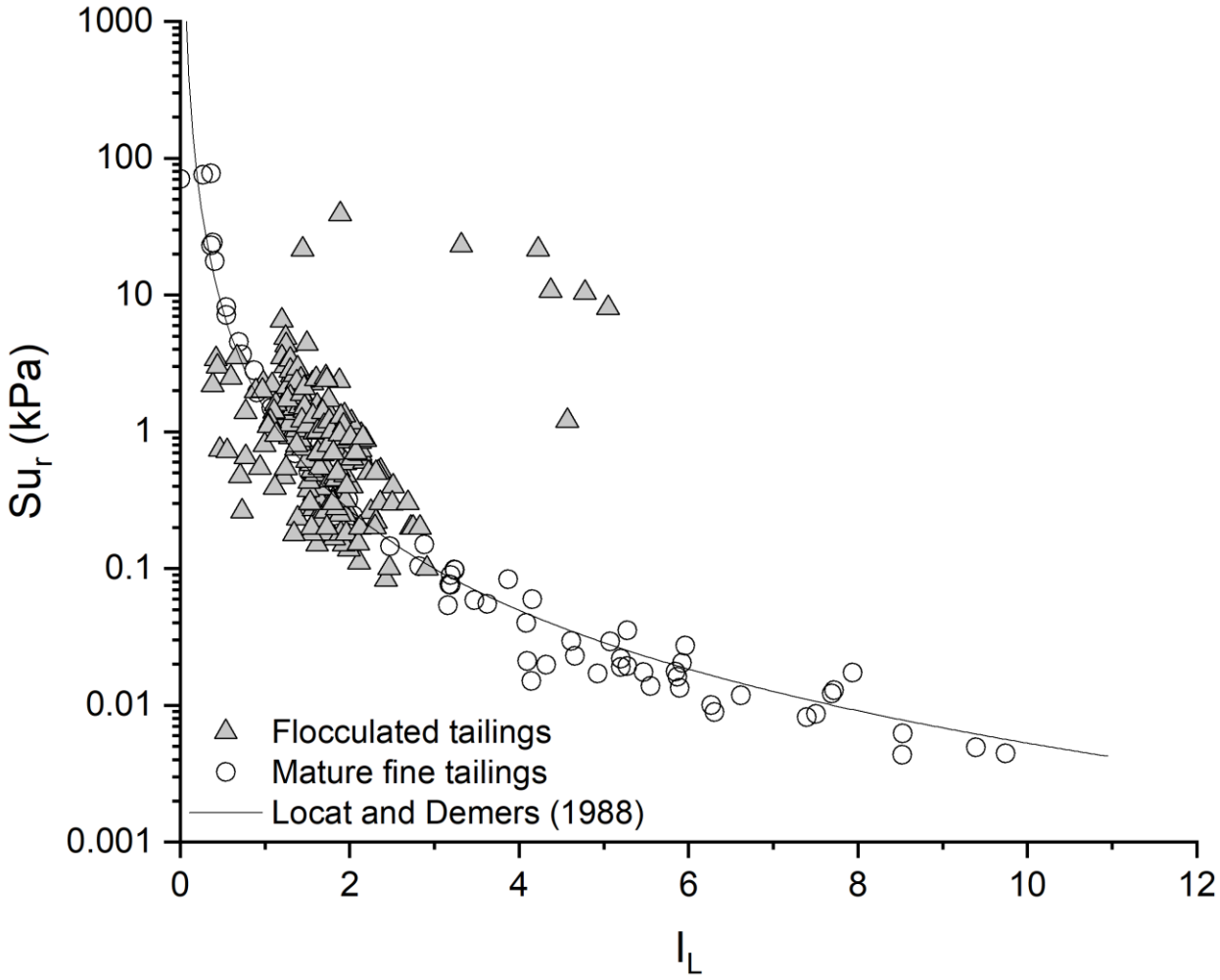

Figure 2.16. Su_r – I_L of oil sands tailings from literature

The Locat and Demers (1988) relationship provides a good overall fit for the data, in particular for MFT. The cause of the scatter in the dataset for flocculated tailings published is unknown but could be the result of thixotropy or pore water chemistry. However, the Locat and Demers (1988) relationship was developed for I_L between 1.5 and 6 and must be extrapolated to fit the tailings dataset. There are also few data points between w_P and w_L (I_L between 0 and 1) (Figure 2.17). It is not feasible to cap tailings at water contents greater than w_L with solid material, meaning that the existing dataset and the Locat and Demers (1988) relationship is of limited use for reclamation as upland or wetland landscapes. The assumption that the Su_r is approximately 1 kPa at w_L does appear to be reasonable, though there is insufficient data to evaluate the strength at w_P.

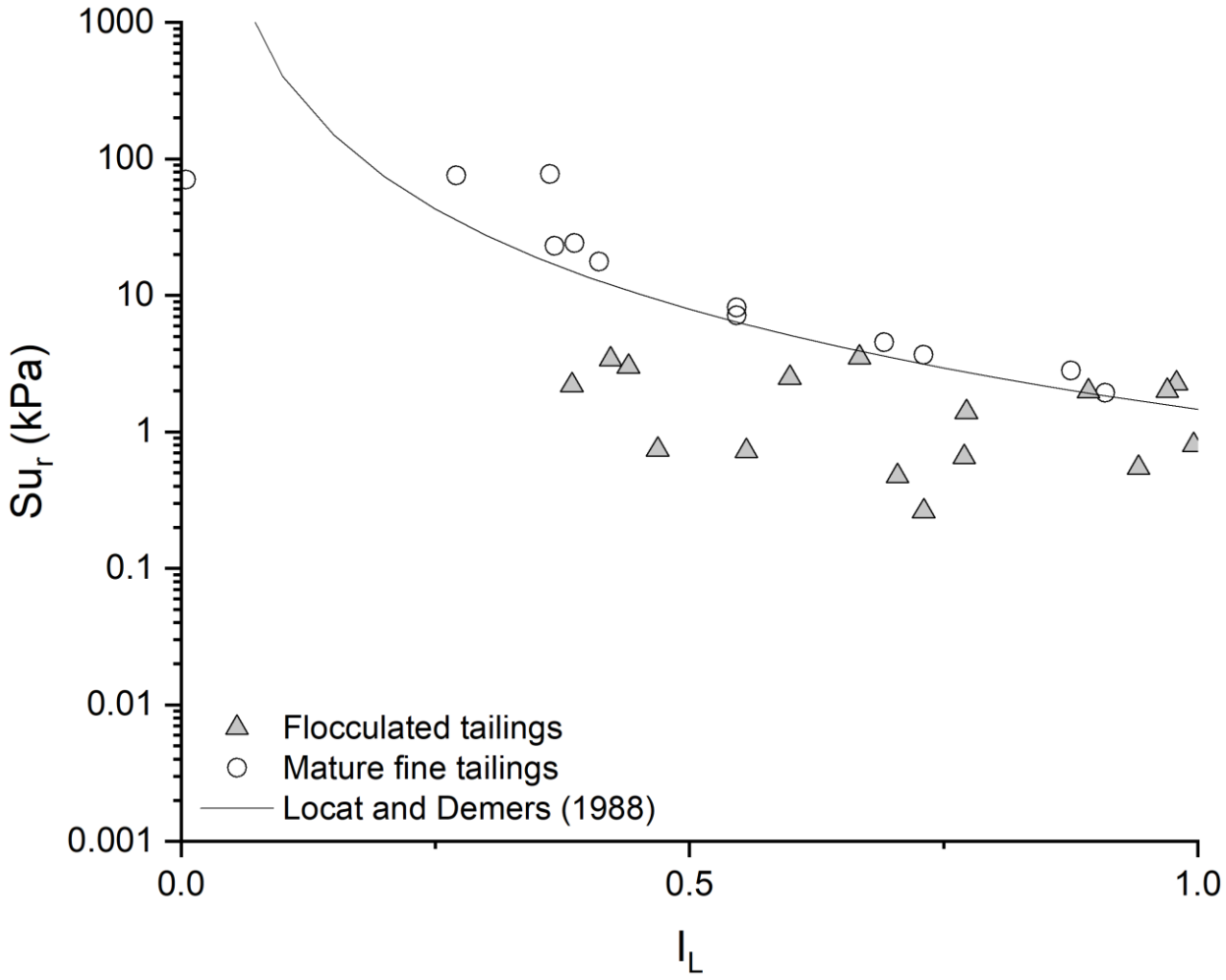

Figure 2.17. Su_r – I_L oil sands tailings from literature between liquid limit and plastic limit

2.4.2 Peak strength of oil sands tailings

While it is generally true that the peak strength *Su* will increase with density (as represented by an increase in I_L), *Su* cannot be predicted from I_L. For oil sands tailings in particular, the range of *Su* possible at a given density spans approximately one order of magnitude (COSIA 2022). Publicly available data on the peak undrained shear strength and density (as represented by solids content) of oil sands tailings is presented in Figure 2.18. Factors that influence the value of *Su* at a given density include process additives (e.g. coagulants, flocculants, and cements), clay minerology, and treatment method (McKenna et al. 2016, COSIA 2022).

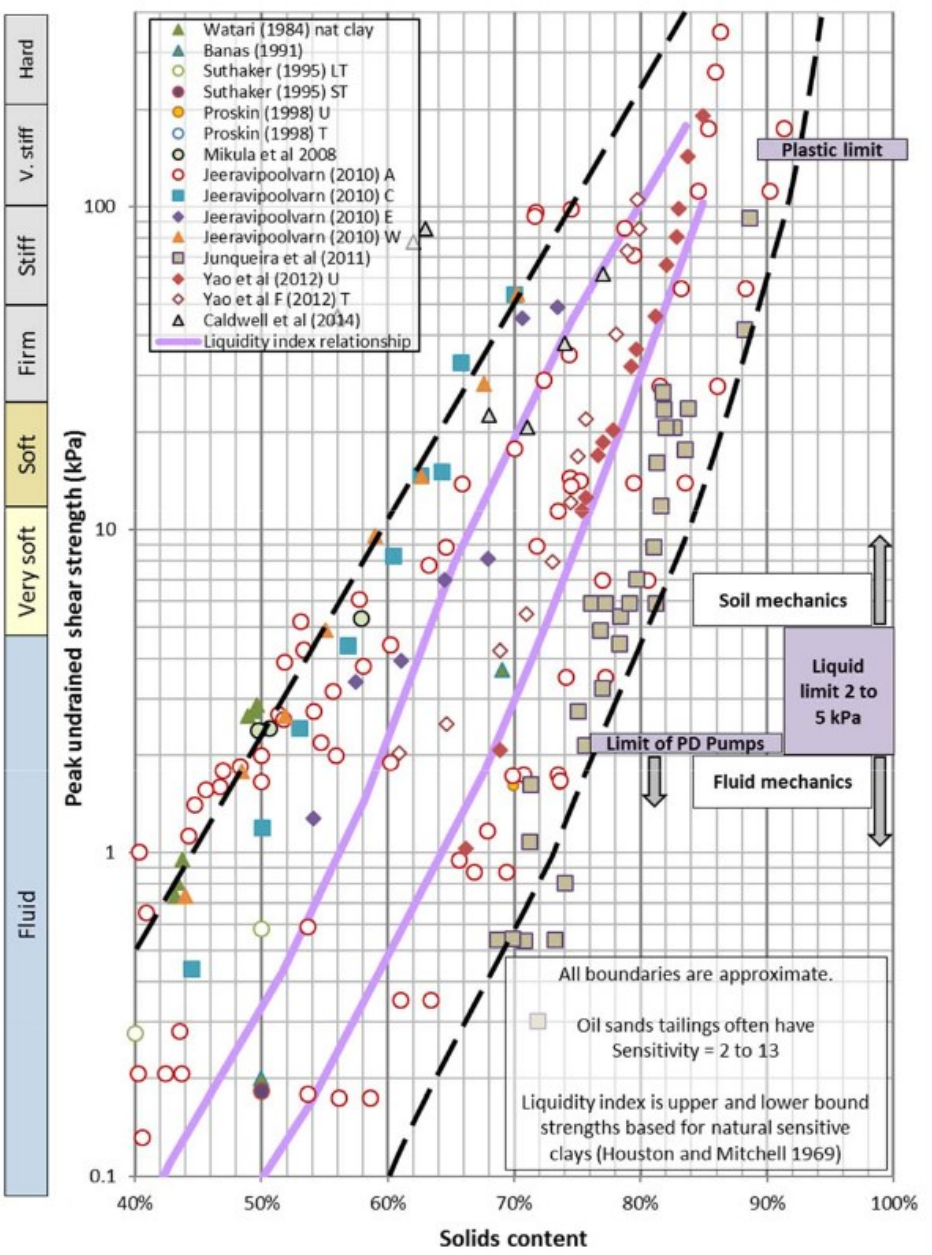

Figure 2.18. Shear strength and density of oil sands tailings (McKenna et al. 2016)

2.5 Relationship between strength and bearing capacity

In addition to strength and density, bearing capacity is a key design parameter for capping oil sands tailings (COSIA 2022). The bearing capacity (q_d or q_{ult}) of a particular soil relates the deformation behaviour of a soil subject to a surface load to a defined failure state. As the soil is loaded, settlement will occur in the direction of loading. This is represented by

a settlement curve (Figure 2.19). The magnitude of settlement under a particular load is influenced by the properties of a soil, including density and stiffness (Terzaghi et al. 1996).

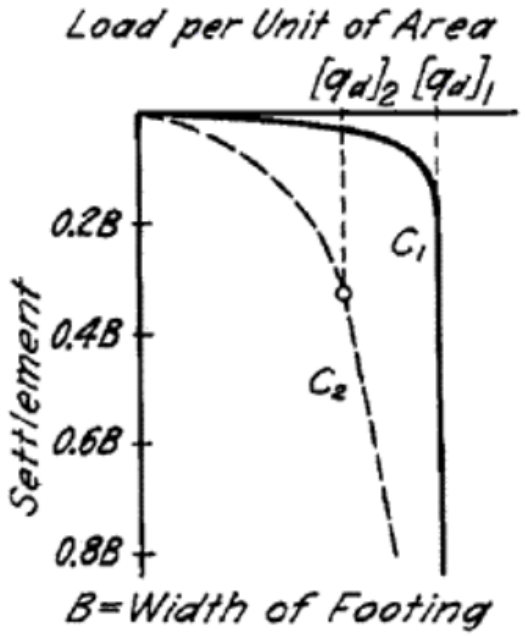

Figure 2.19. Settlement curve for dense/stiff (C_1) and loose/soft (C_2) soils (Terzaghi et al. 1996)

Two methods may be used to estimate the bearing capacity from the settlement curve:

- Bearing capacity is estimated as the stress corresponding to a particular settlement. Cerato and Lutenegger (2007) suggest that the bearing capacity should be estimated at a settlement of 10% for a series of model footing tests performed on compacted sand.
- Bearing capacity is estimated as the intersection point of two tangent lines drawn on the settlement curve. One tangent line is drawn on the initial high-curvature portion of the curve and the second tangent line is drawn on the subsequent low-curvature portion.

2.5.1 Prediction of bearing capacity

The bearing capacity of a continuous footing in homogenous soil above the water table is approximated from Terzaghi et al. (1996). A continuous footing is a footing with a long, rectangular shape and is distinguished from square or circular footings.

Equation 2.2

$$q_{ult} = cN_c + \gamma D_f N_q + \frac{1}{2}\gamma B N_\gamma$$

Where:

- q_{ult} is the bearing capacity of the soil
- c is the shear strength (equal to Su for undrained conditions)
- γ is the unit weight of the soil
- D_f is the depth of the footing (equal to zero for a footing on the surface)
- B is the footing width
- N_c, N_q, and N_γ are bearing capacity factors accounting for the cohesion, surcharge, and weight of the soil, respectively, that depend solely on the friction angle φ' (Figure 2.20)

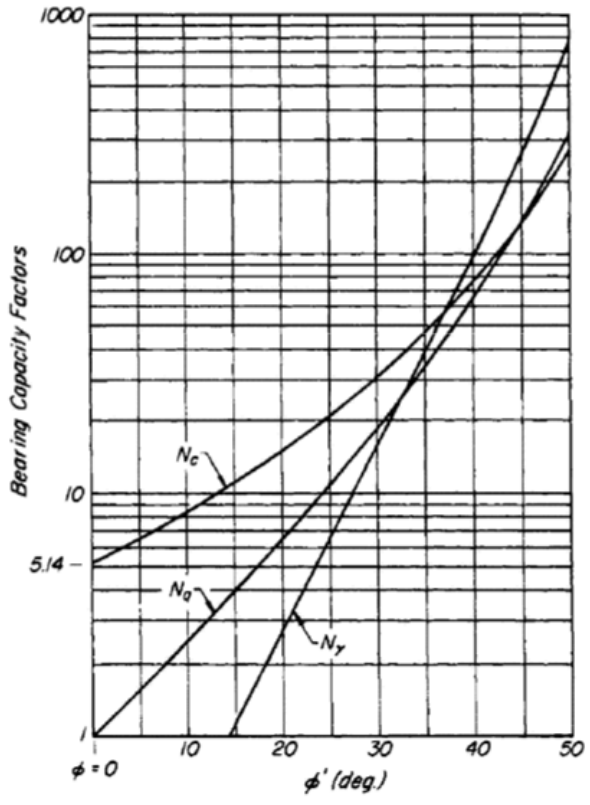

Figure 2.20.Bearing capacity factors as a function of friction angle (Terzaghi et al. 1996)

For undrained failure, φ' is equal to zero. Therefore, for a rectangular footing on the surface failing in undrained conditions, Equation 2.2 becomes Equation 2.3.

Equation 2.3

$$q_{ult} = 5.14Su$$

2.5.2 Bearing capacity of oil sands tailings

Trafficability is governed by the bearing capacity (COSIA 2022). If the bearing pressure of the equipment (defined by the weight and track/tire loading area), exceeds the bearing capacity of the surface, the equipment will punch through. For a deposit to be reclaimed, the surface must be able to support the load of the cap and reclamation cover, as well as the equipment used to place this material, such as trucks and dozers. The ability of equipment to be able to safely operate on the surface without punching through to the weak underlying layer and becoming mired is referred to as trafficability. There are multiple failure modes possible for equipment operating on capped tailings, though punching failure is of specific concern due to the hazards for operators and equipment (Figure 2.21).

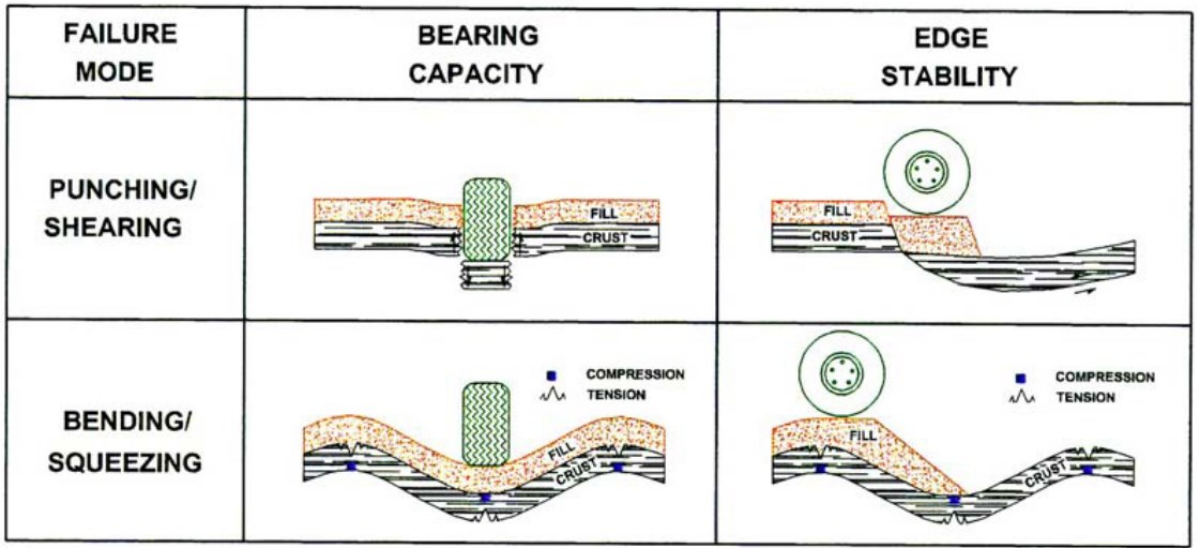

Figure 2.21. Failure modes of equipment on capped tailings (Jakubick et al. 2003)

Field trials (e.g. Wells et al., 2010) are typically used to evaluate the bearing capacity before a cap is placed (McKenna et al. 2016). Current practice for calculating an estimate

of bearing capacity of oil sands tailings is to use Equation 2.3, which describes the bearing capacity of a homogenous, unfrozen soil failing in an undrained manner with a punching failure mode (COSIA 2022). This calculation makes assumptions to reflect practical experience. In practice, tailings deposits are not homogenous, through accounting for layers within the deposit have not provided accurate predictions. The bearing capacity of layered soft soil deposits have previously been studied by Wang and Carter (2002), Park et al. (2010), and Liu et al. (2020).

To assess the trafficability, the bearing pressure at the interface of the cap and the tailings surface is compared against the predicted bearing capacity of the tailings (COSIA 2022). For a sand cap, the bearing pressure at the interface is calculated by assuming a 1H:2V distribution from the surface (Figure 2.22). The strength of the cap is assumed to be negligible, and the stiffness of the cap is assumed to be much greater than the tailings. Results calculated neglecting layers in the tailings deposit, assuming load spreading, and considering peak vane strength have generally provided acceptable field performance. Predictions may be improved with field strength profiles, deformation measurements, and back analysis. Factors such as bearing shape, depth shape, and dynamic effects are also assumed to be negligible, and a factor of safety of 2-3 is commonly applied.

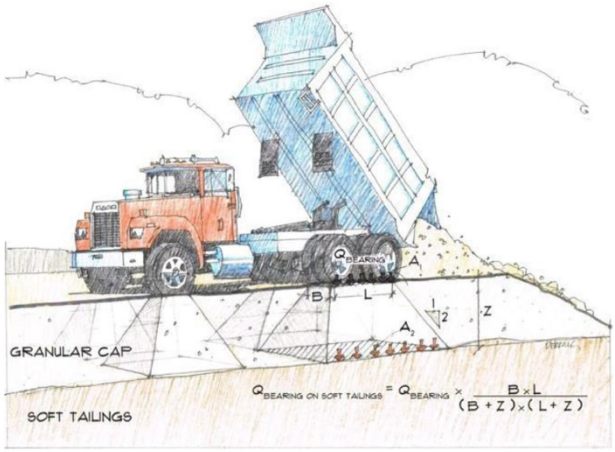

Figure 2.22. 1H:2V load spreading through a sand cap on oil sands tailings (COSIA 2022)

The effect of desiccation is also typically not included in analyses. A crust of dry tailings increases strength and trafficability (Rozina 2013, Williams 2015, COSIA 2022). The effect of matric suction (the difference between the pore air pressure and the pore water

pressure) in unsaturated soils is also not accounted for. Increasing matric suction, such as through drying, increases the bearing capacity of a soil (Fredlund et al. 2012). Similarly, a decrease in matric suction decreases the bearing capacity. Rozina (2013) assessed the bearing capacity desiccated oil sands tailings in the laboratory and found that neglecting matric suction in initial measurements of bearing capacity can over-predict the long-term bearing capacity due to the dissipation of suction. In a numerical modelling study of sand capping centrifuged tailings, Fredlund et al. (2018) also determined that the desiccated crust thickness had little effect on the maximum cap thickness, and that the undrained strength was the dominant factor.

3 Materials and methods

The laboratory test program was developed to study the Atterberg limits, strength, and bearing capacity of oil sands tailings with the overall objective of further understanding the behaviour of capped tailings deposits. A test matrix summarizing the program is found at the end of this chapter (section 3.6).

The program consisted of:

- Characterization (section 3.2): to determine geotechnical index properties.
- Atterberg limits (section 3.3): to investigate the impact of material properties, preparation method, and test method on measurements.
- Su_r - I_L (section 3.4): to develop a mathematical relationship for each sample and investigate the impact of material properties and preparation method.
- Model footing (section 3.5): to measure the bearing capacity of each sample and compare results with predictions based on *Su*.

3.1 Materials

Three types of oil sands tailings and one commercially available clay were used in the laboratory testing program:

- Centrifuge cake (CC)
- Thickened tailings (TT)
- Fluid tailings (FT)
- EPK Kaolin

Oil sands tailings were delivered to the University of Alberta in sealed plastic pails and homogenized prior to testing. In addition to the as-received tailings, subsamples of each tailings stream were amended in the laboratory to evaluate the effect of changing specific properties on the overall behaviour. Each tailings subsample was amended by removing the bitumen through either the Dean Stark method (DS) or cold extraction (CE) for a total of 9 tailings samples, including the as-received tailings. Amendment methods are further described in section 3.2.6.

EPK Kaolin, a commercially available, naturally occurring mineral used in ceramics, agriculture, and manufacturing was also used in the test program (Edgar Minerals Inc.

2018). The kaolin was received initially as a powder and was rehydrated with deionized water prior to further testing. The use of powdered kaolin as a physical analogue to oil sands tailings has previously been studied by Zheng and Beier (2023).

3.2 Characterization

The as-received oil sands tailings (CC, TT, and FT) were characterized by particle size distribution, mass fractions by the DeanStark method, water chemistry, clay content by methylene blue index (MBI), and mineralogy by x-ray diffraction and fluorescence (XRD/XRF). The solids from the amended CC (CC-DS and CC-CE) were characterized by PSD and MBI. The dry solids from the other tailings samples (TT-DS, TT-CE, FF-DS, and FF-CE) were shipped back to the University of Alberta for additional testing. Due to the small quantity of dry solids produced by both methods, the amended CC did not undergo additional laboratory testing, and the amended TT and FT were not characterized. Published properties of EPK Kaolin were used to characterize the material.

3.2.1 Particle size distribution

The particle size distribution describes the gradation of a soil by quantifying the mass fraction that is finer or coarser than a given mineral grain diameter. Of particular interest for oil sands tailings is to quantity the amount of fines (diameter less than or equal to 44 μm) and the sand to fines ratio (SFR), defined as the ratio of the mass of particles with a diameter greater than 44 μm to the mass of fines. The selection of 44 μm as a boundary was originally done out of convenience, as it is a standard sieve size (Mikula 2018). However, this metric has proven useful and continues to be widely adopted in oil sands tailings characterization.

The particle size distribution was measured by sedimentation. In this method, the specific gravity of a dispersed soil solution is measured at regular intervals using a hydrometer (ASTM 2021). The measured specific gravity is then used to calculate the percentage of soil remaining in the suspension and the corresponding particle diameter using Stokes' law. Particle size distribution tests were performed by Bureau Veritas laboratories.

3.2.2 Dean Stark method

The Dean Stark method is used to determine the mass fractions of mineral solids, water, and bitumen in oil sands tailings. In this method, an extraction apparatus is used to

remove bitumen from the mineral solids using vaporized toluene (Figure 3.1) (COSIA 2014b). Toluene is heated to a vapour in the kettle and passes through the sample to remove the bitumen. The toluene-bitumen solution is then condensed such that the liquid toluene can be re-circulated until all of the bitumen is removed from the solids. Water in the sample is also vaporized and subsequently condensed in the water trap separately from the toluene-bitumen solution.

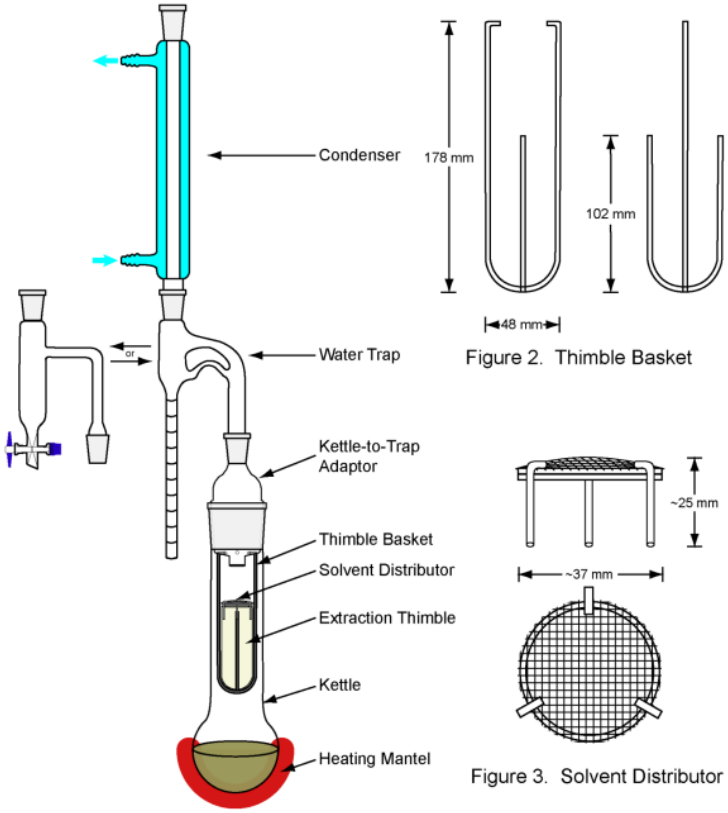

Figure 3.1. Dean Stark extraction apparatus schematic (COSIA 2014b)

At the end of the test, the mass of collected water and solids (after drying at 105˚C) are measured, and a subsample of the toluene-bitumen solution is used to measure the mass fraction of bitumen. Mass fractions by the Dean Stark method were performed by Bureau Veritas laboratories.

3.2.3 Methylene blue index

The methylene blue test is used to determine the clay mineral fraction in a sample by titration with a methylene blue solution (Wells and Kaminsky 2015). The methylene blue

index (MBI) is determined by the titration endpoint and is then used to calculate the percent clay by mass using an empirical correlation developed by Sethi (1995) (Equation 3.1). The correlation used is specific to oil sands tailings. In addition to the percent clay, MBI can also be used to determine the surface area (Equation 3.2) (Hang and Brindley 1970). The methylene blue test was performed by Bureau Veritas laboratories.

Equation 3.1

$$\%\ Clay\ [\%\ wt] = \frac{MBI\ \left[\frac{meq}{100\ g}\right] + 0.04}{0.14}$$

Equation 3.2

$$Surface\ area\ \left[\frac{m^2}{g}\right] = MBI\ \left[\frac{meq}{100\ g}\right] * 130 * 0.06002$$

3.2.4 Water chemistry

The geotechnical behaviour of oil sands tailings is strongly influenced by interactions between negatively charged clay minerals and ions in the pore water (Mikula and Omotoso 2006, Kaminsky and Omotoso 2016). Sources of ions include the addition of caustic NaOH for bitumen extraction (Na^+ and HCO_3^-), chemical amendments to improve tailings properties (SO_4^{2-}), and naturally occurring species in oil sands pore water (Ca^{2+}, Mg^{2+}, K^+, Cl^-, SO_4^{2-}) (Kaminsky and Omotoso 2016, Cossey et al. 2021). Clays in oil sands tailings will tend to disperse in environments with high concentrations of Na^+ and pH values around 8 (Miller et al. 2010, Vietti 2018). The sodium absorption ratio (SAR, Equation 3.3) of the pore water is often used to evaluate the degree of clay dispersion; a high SAR (20 or above) indicates high dispersion, and a low SAR (5 or below) indicates little dispersion (Miller et al. 2010). Water chemistry analysis was performed by Bureau Veritas laboratories.

Equation 3.3

$$SAR = \frac{[Na^+]}{\sqrt{\frac{[Ca^{2+}] + [Mg^{2+}]}{2}}}$$

3.2.5 XRD/XRF

The specific clay minerals present in tailings influence how they interact with the surrounding environment and in turn the overall geotechnical properties. The clay minerology was determined by X-ray diffraction (XRD) and X-ray fluorescence (XRF). Both methods involve subjecting the sample to X-ray radiation. In XRD, X-rays diffract upon interacting with the sample to produce a characteristic pattern from the constructive interference of the scattered beams (Kaminsky 2008). The angle between the X-ray source and the sample is changed during the test to generate peaks of intensity with respect to the angle of incidence, which is interpreted as the mineralogical composition (e.g. quartz, illite, kaolinite). In X-ray fluorescence (XRD), X-rays are used to excite electrons in the sample. This causes the sample itself to emit X-rays in a characteristic pattern that is interpreted as the elemental composition. The elemental composition can in turn be related to the mineralogical composition from the atomic formula of each species to interpret XRD and XRF together. XRD/XRF analysis was performed by the Northern Alberta Institute of Technology.

3.2.6 Amendment methods

Subsamples of the as-received tailings were amended by the Dean Stark method (DS) and cold extraction (CE) to evaluate the effect of changing different properties on the geotechnical behaviour. These amendment methods were selected because they are existing methods used to remove bitumen from tailings or ore samples. In general, both involve using a solvent to remove the bitumen from the solid matrix. Both methods were performed by Bureau Veritas laboratories, and solids were shipped back to the University of Alberta for additional testing. A summary of the amendment methods is presented in Table 3.1.

Table 3.1. Summary of amendment methods

	Dean Stark (DS)	Cold Extraction (CE)
Solvent	Toluene	Toluene (74%) Isopropyl alcohol (26%)
Method of bitumen removal	Extracted from solids by vaporized toluene	Mixed with solvent and centrifuged to separate from solids
Solids treatment after testing	Oven-drying at 105˚C	Air-drying at room temperature

Dean Stark solids were prepared as described in section 3.2.2. A key consideration for the Dean Stark method is that the solids are oven-dried at a temperature of 105˚C. The effect of oven drying on Atterberg limits has been previously studied by Basma et al. (1994). To remove the bitumen by cold extraction, the tailings are mixed with a solution of 74% toluene and 26% isopropyl alcohol. The sample is then spun in a centrifuge to separate the bitumen from the solid matrix (COSIA 2014b). After centrifuging, the tailings solids are air-dried at room temperature.

3.3 Atterberg limits

Atterberg limits tests were performed using different test procedures and sample preparation methods to evaluate the impact on test results. The as-received tailings samples (CC, TT, FT) were prepared by both air-drying the sample from w_L to w_P ("drying down") and rewetting the sample from w_P to w_L ("wetting up"). Samples of kaolin and amended tailings (TT-DS, TT-CE, FT-DS, FT-CE) were rehydrated from dry powder with deionized water to a consistency above w_L, then air-dried at room temperature to measure the Atterberg limits.

The fall cone and the Casagrande apparatus were used to measure w_L of different samples. For as-received samples, the fall cone and Casagrande apparatus were used

for the “dried down” samples, and the fall cone was used for the rewetted sample. For the rehydrated samples, w_L was measured using only the fall cone. The procedure to determine w_P (defined as the water content at which a thread crumbles at 3.2-mm) remained the same for all samples.

3.3.1 Casagrande apparatus – liquid limit

The Casagrande apparatus was used to determine w_L according to ASTM D4318-17 (ASTM 2017). The water content at which a groove made using a standard grooving tool closes at 25 drops of the cup from a 1-mm height is defined as w_L. The water content at w_L is determined by plotting points of water content and number of drops at 3 points: 15-25 drops, 20-30 drops, and 25-35 points. A linear fit through these data points can then be used to determine the water content at which 25 drops are needed to close the gap. The Casagrande apparatus used in this testing program used an electric motor that dropped the cup at a consistent rate. The drop height was regularly re-calibrated during testing.

3.3.2 Fall cone – liquid limit

The fall cone was used to measure w_L as the water content at which a 60g/60˚ cone penetrates 10 mm into the sample (BNQ 2023a). This is determined by plotting 3-4 points of water content and penetration between penetration depths of 8 mm and 15 mm. Each point is determined according to the following procedure:

1. The sample is thoroughly remoulded and placed in a cup. The sample is pressed into the cup to remove air pockets and the surface is smoothed.
2. The fall cone is dropped from the surface into the sample and the penetration depth is measured. This is repeated until two penetrations are measured that are within 0.3 mm. Penetrations must be at least 1 cm away from each other and the container wall.
3. The average of the two acceptable penetrations is noted and a subsample of the surface is taken for a water content measurement. The remainder of the sample is removed from the cup.
4. Steps 1 through and 3 are repeated to generate a second set of two penetrations within 0.3 mm.

5. The average of the first and second set of penetrations must be within 0.3 mm. If this criterion is met, the penetration is taken to be the average of all four acceptable penetrations and the average of the two water contents. If this criterion is not met, the procedure is repeated.

Multiple trials may be required to plot a single point. A linear fit of penetration depth and water content is used to calculate the water content corresponding to a penetration depth of 10 mm. A dataset of 4 points was used in this test program to determine w_L.

3.3.3 Plastic limit

The water content at which a thread of soil crumbles at a water content crumbles at a diameter of 3.2 mm is defined as w_P (ASTM 2017). A metal rod is used to compare the soil to the target diameter. This is determined by rolling and re-rolling a small mass (~2g) of soil into a thread 3.2 mm in diameter until it is too dry to be formed back into a single mass and re-rolled. This is repeated multiple times to produce a minimum of 6g of solids for a water content measurement.

In this test program, only thread segments measuring 3.2 mm in diameter that could not be re-rolled were taken for the water content (Figure 3.2). Acceptable threads were kept in a sealed plastic during the test to prevent moisture loss by evaporation. The average of 3 water content measurements of at least 6g each was used to determine w_P.

Figure 3.2. Standard (3.2 mm) rod and sample at w_P

3.3.4 Drying and rewetting

As-received tailings were initially at a very fluid consistency much higher than w_L. To determine w_L and w_P, it was necessary to reduce the water content. The tailings were placed in an open container on the lab bench to air-dry at room temperature. A benchtop fan and a hand-dryer on the coldest setting was used to increase the rate of drying without increasing the temperature. The fall cone and Casagrande cup were used to determine when the sample had dried to a consistency slightly above w_L (~15 mm of penetration with the 60g/60˚ cone or ~15 drops of the Casagrande cup).

As the sample continued to air-dry, measurements were taken using both methods as the water content was reduced to and then past w_L. The sample was mixed by hand to homogenize the moisture content and remould the sample immediately prior to each measurement. Using the Casagrande cup, the first measured point was at the highest number of drops (15-25) and the final measured point was at the lowest number of drops (25-35). Similarly, the first measured point on the fall cone was the highest penetration (~15 mm) and the final measured point was the lowest penetration (~8 mm). After w_L was measured, the sample was left to continue drying until it achieved a consistency slightly above w_P as determined by rolling test threads, then w_P was measured as described in section 3.3.3. The sample was then re-hydrated with deionized water and w_L and w_P were measured again. Only the fall cone was used to measure the w_L of the rewetted sample.

A schematic of the drying and rewetting process is shown in Figure 3.3. The same sample was used for both drying and rewetting for CC and TT. For the FT, two subsamples from the same pail were used for drying and rewetting (one subsample per method).

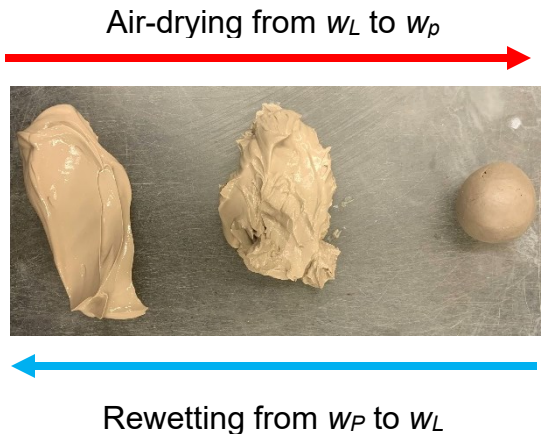

Figure 3.3. Drying and rewetting to Atterberg limits

3.4 Remoulded strength – liquidity index

A Su_r - I_L relationship was developed for all samples using the same material as was used to measure the Atterberg limits. For the as-received samples (CC, TT, and FT), measurements of Su_r and water content were taken using the fall cone as sample was dried and rewetted. This water content was then used to determine I_L. All samples were remoulded by hand immediately prior to the measurement. For the amended samples (TT-DS, TT-CE, FT-DS, FT-CE) and EPK Kaolin, the samples were rehydrated from dry powder, then measurements were also taken as the sample air-dried. The water content for each fall cone measurement was used to determine the I_L of each data point.

3.4.1 Measurement of remoulded undrained shear strength using the fall cone

The fall cone may be used to measure the peak (Su) or remoulded (Su_r) strength. In this test program, all samples were remoulded immediately prior to the measurement, to the measured strength is Su_r. The use of the fall cone to measure Su_r is described in CAN/BNQ 2501-110 (BNQ 2023b). Similar to the measurement of w_L, the tip of the cone is dropped from the surface of the sample (Figure 3.4) and the penetration is measured. Multiple penetrations at least 1 cm away from each other and the container wall can be taken in the same sample (Figure 3.5).

Figure 3.4. Fall cone at surface of sample

Figure 3.5. Sample after multiple fall cone penetrations

A number of standard cones are available including 10g/60˚, 60g/60˚, 100g/30˚, and 400g/30˚ (Figure 3.6; left to right: 400g/30˚, 100g/30˚, 60g/60˚). Different cones are used depending on the consistency of the sample; if a penetration less than 5 mm is measured, the cone mass must be increased.

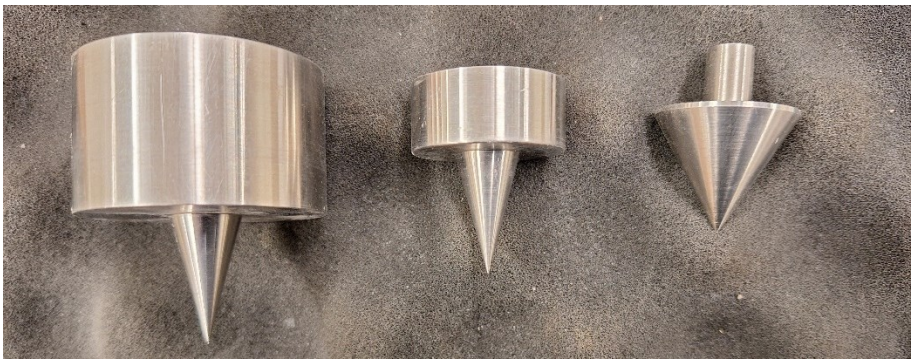

Figure 3.6. Fall cones used in laboratory test program

Su_r is calculated using Equation 3.4 where K is an empirical constant related to the cone angle (equal to 1.0 for 30˚ and 0.3 for 60˚) and m is the cone mass in grams (Hansbo 1957). The mean square penetration $\overline{P}^2$ of all measurements taken in the same sample is used to calculate the shear strength in kPa. The mean square penetration is calculated using Equation 3.5 where P_i are the penetrations (mm) and is the number of penetrations.

Equation 3.4

$$Su\ [kPa] = \frac{9.8Km}{\overline{P}^2}$$

Equation 3.5

$$\overline{P}^2 = \frac{\sum P_i}{N}$$

In this test program, all samples were remoulded by hand immediately before being tested. Between 6-8 penetrations were taken for each measurement of Su_r. After the last penetration for each sample, a subsample was taken from the surface to measure water content. Measurements were taken at random time intervals as the samples air-dried at room temperature. The cone used was changed from 60g/60˚ to 100g/30˚ to 400g/30˚ once the measured penetration from each cone was less than 5 mm, and the test was stopped once the 400g/30˚ penetrated less than 5 mm. The measured mass of each cone was used to calculate the strength. Penetrations and water contents from w_L tests were also used in the dataset.

3.5 Bearing capacity

The bearing capacity of the as-received CC and TT and EPK Kaolin was measured using a model footing test in a procedure developed by Zheng (2023) (note that this source is not publicly available). In these tests, a triaxial loading frame was used to push a 14.5-mm footing into a dewatered sample at a rate of 1 mm/min and measure the load. Samples were prepared to the target moisture content using Tempe cells. The use of Tempe cells to dewater samples of oil sands tailings is detailed in Kabwe et al. (2023a, 2023b). Following the model footing test, the fall cone was used to measure *Su* and Su_r.

Model footing tests were not performed on as-received FT or any amended tailings samples. FT must be treated using some other technology (e.g. centrifuging, thickening, etc.) before being capped, therefore bearing capacity data is of little use.

3.5.1 Sample preparation in Tempe cells

The purpose of the Tempe cell is typically to measure the soil water characteristic curve (SWCC). The SWCC describes how the amount of water in a soil changes as the matric suction (defined as the difference between pore water and pore gas pressure) changes, and is commonly used in unsaturated soil mechanics (Fredlund et al. 2012). A typical SWCC with key points and zones is shown in Figure 3.7.

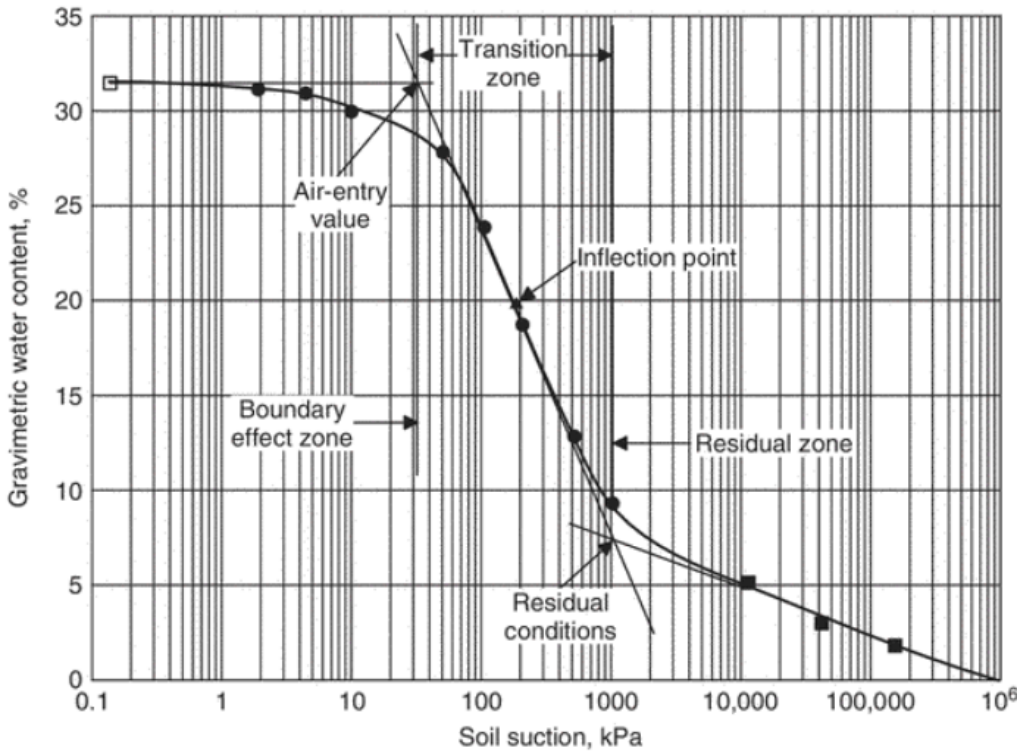

Figure 3.7. Typical SWCC with labeled points and zones (Fredlund et al. 2012)

A key parameter determined from the SWCC is the air entry value (AEV) which is defined as the suction at which the soil transitions from saturated to unsaturated behaviour. The amount of water in a soil can be described in multiple ways, including the degree of saturation (*S)*, the gravimetric water content (*w*), the volumetric water content based on the initial sample volume (θ), and the instantaneous volumetric water content based on the sample volume at the moment of measurement (θ_i) to plot the *S*-SWCC, *w*-SWCC, θ-SWCC, and θ_i-SWCC, respectively. For coarse-grained materials, the *S*-SWCC, *w*-SWCC, θ-SWCC, and θ_i-SWCC are approximately equal (Fredlund et al. 2011). However, this is not the case for fine-grained materials such as oil sands tailings that undergo a significant volume change when suction is increased. Unsaturated properties (including the AEV) must be determined from the *S*-SWCC for these materials.

A Tempe cell (Figure 3.8) is a pressure cell used to measure the *w*-SWCC. While in the Tempe cell, a sample of known initial water content in the cell body (A) experiences different levels of matric suction through the application of an air pressure beyond atmospheric pressure. Because the pore water pressure remains at atmospheric

pressure, increasing the air pressure beyond atmospheric pressure creates an equivalent matric suction (e.g. an air pressure of 100 kPa is equivalent to a matric suction of 100 kPa) (ASTM 2016). The air pressure causes pore fluid to move down and out of the sample in the cell body (A) through the porous stone (B) at the bottom of the cell and into the plastic bottle (C) through a drainage tube.

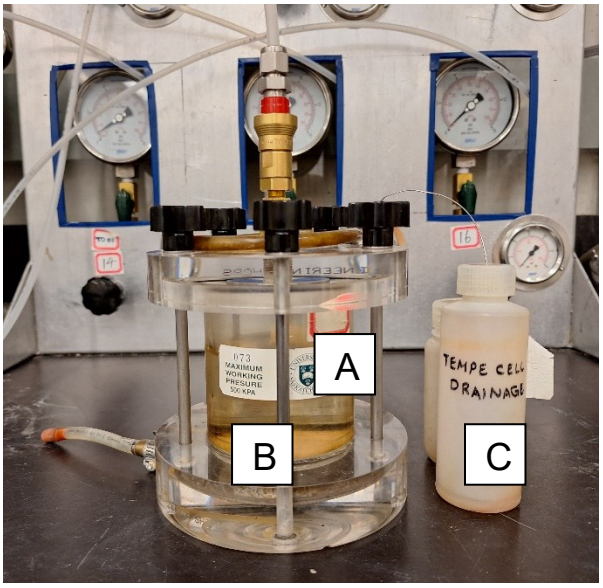

Figure 3.8. Tempe cell with labelled components

To determine the w-SWCC, the water content at different values of matric suction is determined by applying an air pressure and allowing water to drain from the sample until the mass has equilibrated (considered to be a change less than 0.2g in 24 hours). This process is then repeated with increasing air pressures to determine points of matric suction and water content which are plotted as the *w*-SWCC. For high volume change materials, the *S*-SWCC is determined from the *w*-SWCC by calculating the corresponding degree of saturation for each water content using the specific gravity and the void ratio as determined from the shrinkage curve. This method is further described in section 3.5.2.

In this test program, the air pressure in the Tempe cells was used as a consolidating load to dewater samples from an initially weak, fluid consistency to a plastic consistency (between w_L and w_P). The tailings were dewatered under air pressures of 100 kPa, 200 kPa, or 400 kPa, and were considered to be fully consolidated when the mass had equilibrated. Consolidation for each sample took 1-2 weeks. Samples were removed from

the Tempe cells when consolidation was complete, then wrapped in plastic wrap and placed in resealable plastic bags in a controlled temperature and humidity environment until model footing testing. Samples during different stages of this procedure are shown in Figure 3.9 and Figure 3.10.

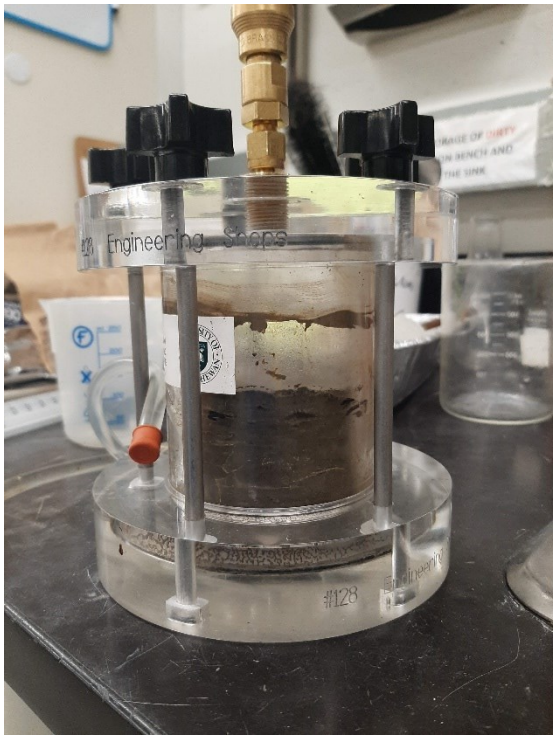

Figure 3.9. Model footing sample in Tempe cell at equilibrium

Figure 3.10. Model footing sample after removal from Tempe cell

3.5.2 Degree of saturation of Tempe cell samples

The degree of saturation of the Tempe cell samples at matric suctions of 100 kPa, 200 kPa, and 400 kPa were calculated to determine if matric suction was present that could influence the measured bearing capacity. The method used is based on the calculation of the *S*-SWCC from the *w*-SWCC for high volume change materials. The degree of saturation (*S*) for of a soil with specific gravity (G_s), void ratio (*e*), and water content (*w*) may be calculated using Equation 3.6.

Equation 3.6

$$S = \frac{G_s w}{e}$$

The shrinkage curve describes the relationship between *e* (defined as the ratio of the volume of voids to the volume of solids) and *w* as a undergoes volume change (shrinkage) during drying. Shrinkage curves were determined by measuring the mass and volume change of samples as they were air-dried on the laboratory bench (Figure 3.11). The mass and dimensions of the sample were taken as the sample dried to calculate points of water content and *e*.

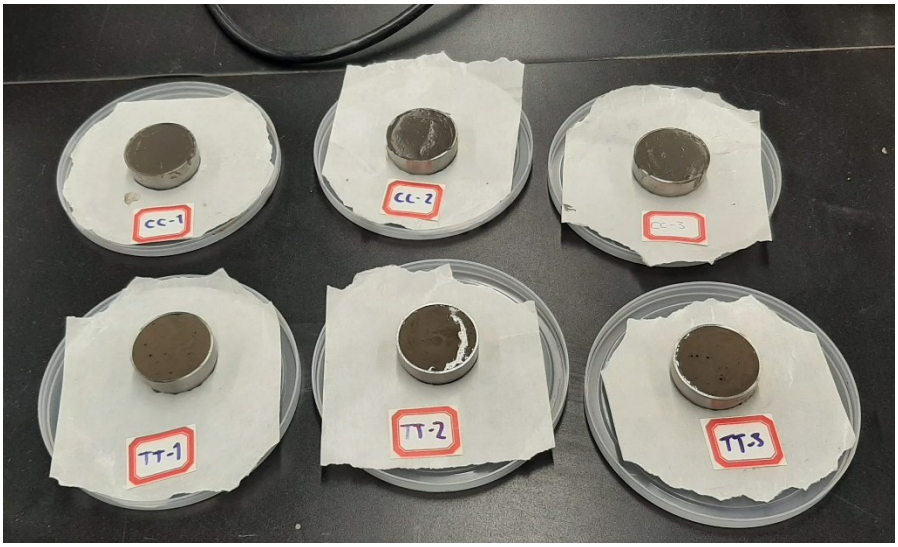

Figure 3.11. Shrinkage curve samples

Equation 3.7 was proposed by Fredlund (1999) as a general equation of the hyperbolic shrinkage curve where a_{sh} is the minimum *e*, b_{sh} is the slope of the line of tangency, and

c_{sh} is the curvature. For a specific soil, a constant ratio of S to G_s is also defined as in Equation 3.8. The SOLVER function in Microsoft Excel was used to fit Equation 3.7 to the measured points of e and water content.

Equation 3.7

$$e(w) = a_{sh}\left[\frac{w^{c_{sh}}}{b_{sh}^{c_{sh}}} + 1\right]^{\frac{1}{c_{sh}}}$$

Equation 3.8

$$\frac{a_{sh}}{b_{sh}} = \frac{G_s}{S}$$

The shrinkage curve was used to determine the corresponding e for the water content of each Tempe cell sample. Equation 3.5 was then used to determine the degree of saturation of each sample. The shrinkage curve can also be used to determine the shrinkage limit (w_s), defined as the water content at which a further decrease in water content does not result in any additional decrease in volume. The intersection point of the initial linear portion of the shrinkage curve under saturated conditions (line AB) and the minimum void ratio (D) is w_s (Figure 3.12). The slope of line AB is also equal to G_s.

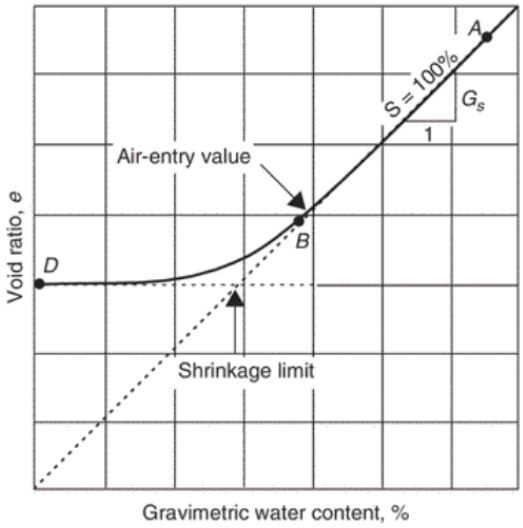

Figure 3.12. Determination of shrinkage limit from shrinkage curve (Fredlund et al. 2012)

3.5.3 Specific gravity

The specific gravity of the as-received CC and TT was determined according to ASTM D854-14 (ASTM 2014). A vacuum was used to de-air samples in pycnometers (Figure 3.13). The samples were tested at the as-received water content and included bitumen. Published properties of EPK Kaolin were used for G_s of this material.

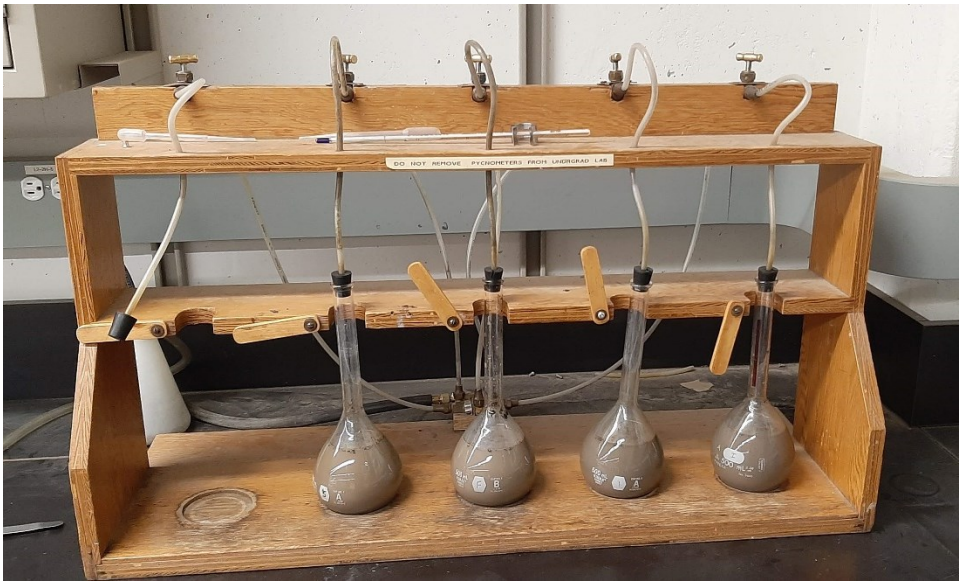

Figure 3.13. Samples in pycnometers

3.5.4 Model footing tests

Model footing tests were conducted using a pocket penetrometer footing with a diameter of 14.5 mm attached to a triaxial loading frame. The loading frame moved the sample upwards such that the footing penetrated the sample at a rate of 1 mm/min. This rate was selected to ensure that the test occurred under undrained conditions. The effect of penetrometer loading rates on drainage conditions has been previously studied by Randolph (2004) and Garcia Martinez et al. (2016). The experimental setup is shown in Figure 3.14 and Figure 3.15.

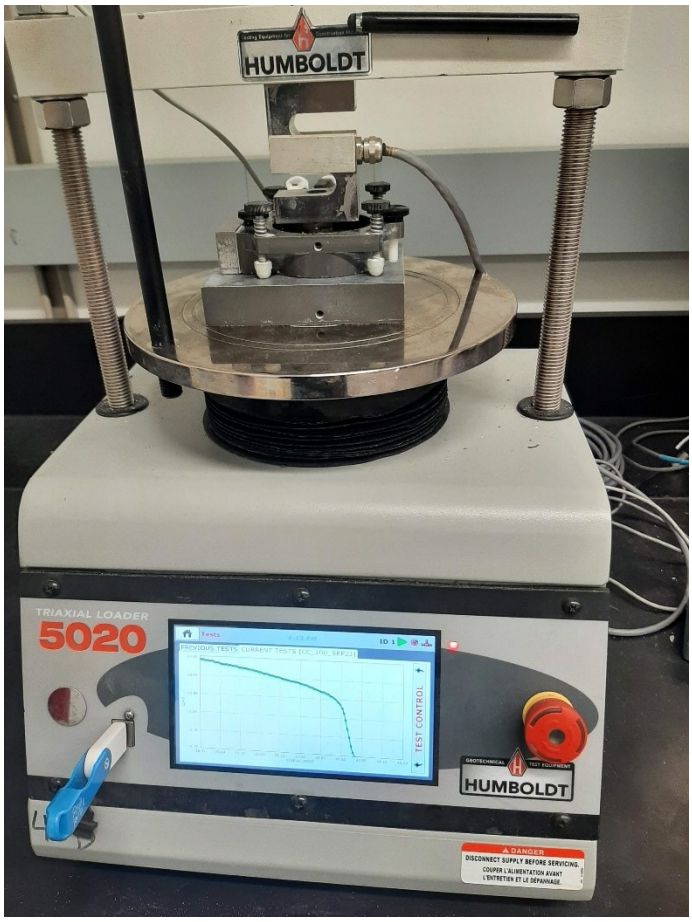

Figure 3.14. Triaxial loading frame setup for model footing tests

Figure 3.15. Footing penetrating sample

Samples were prepared for testing by trimming with a Shelby ring and extracting them into a confining box, which ensured that the sample was laterally constrained during the model footing tests. Measurements were taken before and after trimming to determine the density and water content of the sample.

The footing was manually positioned approximately at the surface of the sample before the test began. The triaxial loading frame recorded measurements of load and displacement at 10 second intervals, and the test was manually stopped once the penetration depth was approximately equal to the footing diameter (~15 mm). The measured load was converted to a stress using the area of the footing. The bearing capacity was then determined from a plot of stress and displacement using the slope-tangent and 0.1B methods (Cerato and Lutenegger 2007).

3.5.5 Undrained shear strength of model footing samples

Su and Su_r of each model footing sample were measured immediately after the model footing test using the fall cone (Figure 3.16). To measure *Su*, the sample was measured either in the confining box or was carefully removed from the box into a Shelby ring (to prevent the cone hitting the confining box edge). Water contents were taken at the surface

(cone penetration depth), middle (footing penetration depth), and bottom (below footing penetration depth). The remainder of the sample was the remoulded by hand to Su_r. A water content of the surface of the remoulded sample was also taken. All fall cone measurements of model footing samples were taken using the 400g/30˚ cone. Multiple penetrations were taken for each sample.

Figure 3.16. Fall cone test on model footing sample

3.6 Summary

A summary of the laboratory program is presented in Table 3.2 below.

Table 3.2. Test matrix

		CC			TT			FT			EPK Kaolin
		AR*	DS	CE	AR	DS	CE	AR	DS	CE	
Characterization		X	X	X	X			X			
Atterberg limits											
Dried	w_L - FC†	X			X			X			
	w_L - C‡	X			X			X			
	w_P	X			X			X			
Rewetted	w_L - FC	X			X			X			
	w_P	X			X			X			
Rehydrated	w_L - FC		X	X		X	X		X	X	X
	w_P		X	X		X	X		X	X	X
Su_r vs. I_L											
Dried		X			X			X			
Rewetted		X			X			X			
Rehydrated						X	X		X	X	X
Bearing capacity											
Shrinkage curve		X			X						X
G_s		X			X						
Model footing		X			X						X
Fall cone		X			X						X

* As-received
† Fall cone
‡ Casagrande apparatus

4 Results and discussion

4.1 Characterization

Characterization results for all samples tested are summarized in section 4.1.1 through 4.1.5 below. Complete results are presented in Appendix B.

4.1.1 Particle size distribution

The particle size distributions of all samples are presented in Figure 4.1. The particle size distribution of EPK Kaolin was determined by hydrometer by Darbari et al. (2017).

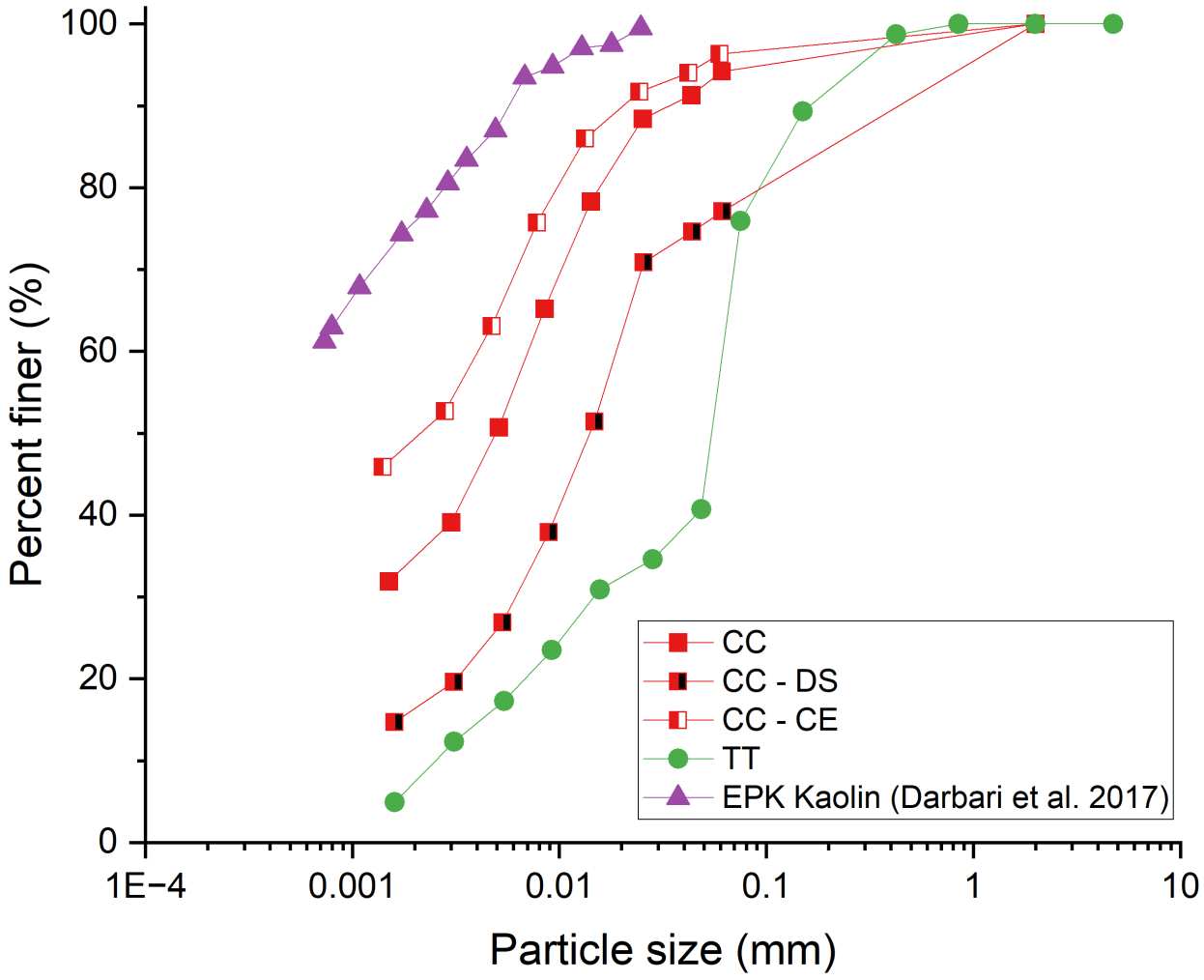

Figure 4.1. Particle size distribution

The fines content of the tailings samples was determined from the particle size distribution as the percentage of solids with a particle size less than 44 μm (Table 4.1). The sand to

fines ratio (SFR) was calculated as the ratio of the percentage of solids with a particle size greater than 44 μm to the percentage of solids with a particle size less than 44 μm.

Table 4.1. Fines content and SFR

	Fines (<44 μm) content (%)	SFR
CC	91.4	0.1
CC-DS	74.6	0.3
CC-CE	94.2	0.1
TT	39.3	1.5
FT	82.0	0.2

The particle size distribution indicates that the TT has the lowest percentage of fine particles (<44 μm) by mass and that the CC has the highest percentage. The effect of the amendment methods (DS and CE) is also shown. Relative to the as-received CC, the CC-DS has a larger amount of coarse particles and the CC-CE has a larger amount of fine particles. The change in CC-DS is proposed to be the result of particle aggregation from drying and washing out of fines through the thimble (Basma et al. 1994, COSIA 2014b). Centrifugation in the cold washing procedure tends to aggregate the particles, which then must be broken apart (e.g. by mortar and pestle), and it is proposed that disaggregation may have caused the particle size distribution to become slightly finer by particle crushing (COSIA 2014b). However, the difference is so small and could be attributed to sample heterogeneity.

4.1.2 Mass fractions

The mass fractions of the as-received tailings samples from the Dean Stark method are reported in Table 4.2. All samples have a similar fraction of bitumen.

Table 4.2. Dean Stark results

	Solids (wt%)	Water (wt%)	Bitumen (wt%)
CC	49.1	49.1	1.53
FT	22.2	77.4	1.20
TT	44.9	53.7	1.29

4.1.3 Methylene blue index

The MBI of the samples is presented in Table 4.3. The clay mineral fraction and specific surface area for the tailings were calculated from the MBI using the correlations developed by Sethi (1995) (Equation 3.1) and Hang and Brindley (1970) (Equation 3.2), respectively. Previously published properties were used for the EPK Kaolin.

Table 4.3. Methylene blue index test results

	MBI (meq/100g)	% Clay	Specific surface (m^2/g)
CC	13.6	97.7	106
CC-DS	11.5	82.4	90
CC-CE	11.9	85.6	93
FT	8.29	59.5	65
TT	8.9	64.1	70
EPK Kaolin	3.7†	99.0-99.9*	25.6†

† MatWeb (n.d.)

* Edgar Minerals Inc. (2018)

The results in Table 4.3 seem to indicate that both the Dean Stark method and the cold extraction method decreased the amount of clay in the sample, which does not agree with the fines content of CC-CE. Kaminsky (2014) states it is difficult to disperse samples that have been amended by Dean Stark extraction or flocculation, which is a critical step in the procedure. It is suggested that the CC-CE may not have been completely dispersed, affecting the measured MBI. Further, it is also possible that the MBI of the TT may have been impacted by the presence of flocculant. However, there is overall good agreement

between the MBI and fines content measurements between the as-received tailings samples (CC has the highest fraction of clay and fines, and TT has the least).

The MBI results also demonstrate the different properties between clay mineral types. Kaolin has a small specific surface relative to other clay minerals and is therefore expected to have a smaller MBI than a sample of oil sands tailings, which contains both kaolin and other clay minerals (illite and smectite) with larger specific surfaces (Kaminsky 2014).

4.1.4 Water chemistry

Results of water chemistry analysis are summarized in Table 4.4. The effect of tailings treatment methods is illustrated by higher SAR and therefore higher degree of clay dispersion of FT relative to the CC and TT (Miller et al. 2010). The CC also has a higher conductivity and concentration of cations.

Table 4.4. Water chemistry of as-received tailings samples

	Ion concentrations (mg/L)								SAR	Conductivity (µS/cm)	pH
	Na^+	K^+	Ca^{2+}	Mg^{2+}	Cl^-	HCO_3^-	SO_4^{2-}	CO_3^{2-}			
CC	388	30.5	90.6	48.4	123	250	705.7	12	8.2	2390	8.4
FT	321	20.0	31.6	23.1	124	390	279.1	28	10.6	1540	8.6
TT	256	23.3	70.5	35.9	12.4	300	403.4	33	6.2	1520	8.6

The amended samples of CC were also tested for soluble conductivity (Table 4.5). The reduction in conductivity between the as-received CC and the amended CC suggests that ions have been removed through these processes. Different subsamples of as-received CC were used for this test and water chemistry testing, so measured values of conductivity differ slightly from Table 4.4.

Table 4.5. Conductivity of as-received and amended CC

	Conductivity (dS/m)
CC	2.1
CC-DS	1.4
CC-CE	1.5

4.1.5 XRD/XRF

The results of XRD testing are shown in Table 4.6. The clay fraction consists of kaolinite and illite, as is typical for oil sands tailings (Kaminsky et al. 2006). The results of XRF testing are shown in Table 4.7. All samples have a similar elemental composition.

Table 4.6. Bulk XRD results

	Mineral phases (wt%)					
	Quartz	K-Feldspars	Siderite	Anatase	Kaolinite	Mica/Illite
CC	30.7	6.5	1	0.8	46.4	13.6
FT	30.7	6.0	1.6	-	41.0	20.0
TT	37.9	6.1	1.2	0.8	40.7	13.3

Table 4.7. Bulk XRF results

	Oxides (wt%)							
	Na_2O	MgO	Al_2O_3	SiO_2	K_2O	CaO	TiO_2	Fe_2O_3
CC	0.3	0.9	24.6	67.4	2.6	0.2	0.8	3.2
FT	0.3	0.8	25.2	67.4	2.4	0.2	0.7	3.0
TT	0.3	0.9	24.2	67.4	2.6	0.2	0.8	3.2

4.2 Atterberg limits

4.2.1 Overall results and comparison with literature data

The w_L and I_P of each sample for all preparation methods test procedures used in this study are plotted with the literature data in Figure 4.2. The laboratory data plots within the range of the literature data, and the EPK Kaolin has properties similar to those of the tailings. For the tailings samples, the overall trend seems to most closely reflect the fines content as measured from the particle size distribution; w_L generally increases and w_P generally decreases as the fines content of the as-received tailings increases. Similar results have previously been observed by Jeeravipoolvarn et al. (2008), Jeeravipoolvarn (2010), Sorta (2015), and Kabwe et al. (2019, 2021). Notably, the fines content isn't necessarily the amount of clay in the sample as measured by the MBI. The samples of TT showed the greatest sensitivity to the preparation method relative to the other tailings samples tested. In all cases, the dried down sample acts as a lower bound for w_L and I_P. It is proposed that the dried preparation should be generally adopted as the method to determine the Atterberg limits of oil sands tailings. This method best preserves the properties of the as-received tailings and is straightforward to perform, meaning that methods will be consistent between laboratories and operators.

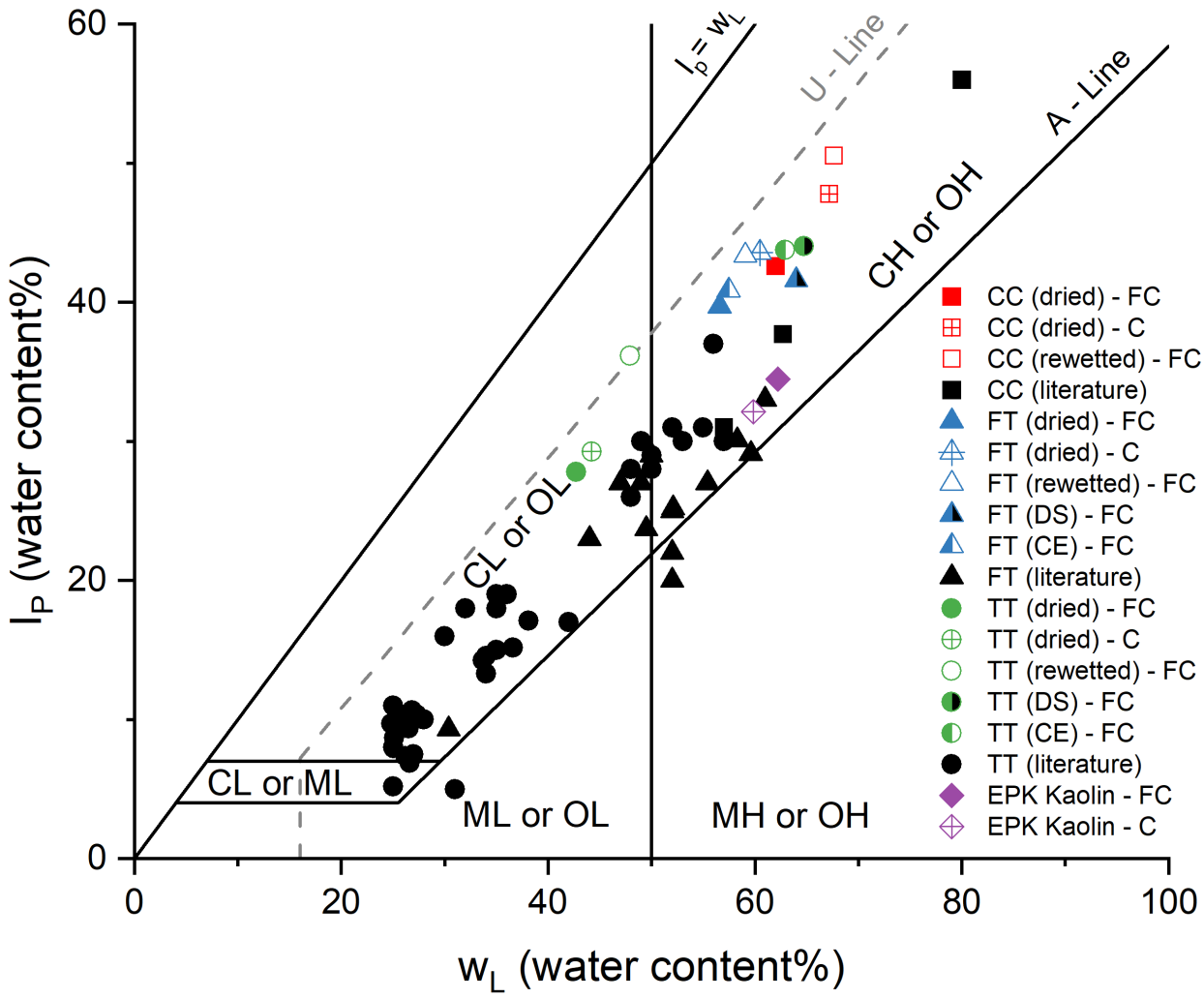

Figure 4.2. Plasticity chart - laboratory and literature data

While the Atterberg limits are sensitive to the test procedure, the exact influence of individual factors cannot be accurately determined from the limited number of data points. This is because of the embedded uncertainty of the test method in addition to competing factors (e.g. fines content, water chemistry, bitumen content, etc.). To evaluate the laboratory results against the embedded uncertainty, Atterberg limits data from literature was reviewed to determine the variation in measurements performed on the same tailings using the same method (Table 4.8).

Table 4.8. Variation in Atterberg limits data for oil sands tailings reported in literature

Source	Sample	# of pairs	w_L (% Diff.)			w_P (% Diff.)		
			Min.	Max.	Avg.	Min.	Max.	Avg.
Banas (1991)	MFT-1	1	-	-	6.6	-	-	4.9
	MFT-2	1	-	-	6.6	-	-	21.3
Yuan and Lahie (2009)	TT	1	-	-	1.9		N/A	
Stianson et al. (2016)	Flocc. tailings	3	0.0	2.1	1.4	7.4	19.6	13.1
Yao (2016)	MFT	4	1.8	15.4	8.0	0.0	11.8	5.9
	TT	15	1.8	15.4	7.6	0.0	23.3	11.9
Gidley and Moore (2013)	MFT-A (Air-dried)	91	0.0	7.3	2.9	0.0	31.3	10.0
	MFT-A (Dean Stark)	120	0.0	19.7	7.1	0.0	34.4	9.3
	MFT-A (DI water)	36	2.6	37.8	15.8	0.2	21.7	10.0
	MFT-A (Process water)	120	0.0	27.3	9.8	0.1	39.2	13.1
	Flocc. MFT-A (Air-dried)	120	0.0	17.7	6.8	0.0	33.6	10.7
	Flocc. MFT-A (Dean Stark)	136	0.0	16.5	5.6	0.0	58.1	21.8
	Flocc. MFT-A (DI water)	21	0.0	36.0	16.0	0.6	31.9	12.3
	Flocc. MFT-A (Process water)	120	0.0	18.3	6.7	0.0	49.5	15.6
	MFT-B (Air-dried)	28	0.0	8.9	3.3	0.0	14.8	6.3
	MFT-B (DI water)	1	-	-	4.4	-	-	12.8
	Flocc. MFT-B (Air-dried)	36	0.0	21.9	6.6	0.0	12.5	5.3
	Flocc. MFT-B (DI water)	36	0.1	21.1	7.5	0.2	21.0	8.6
All pairs for each sample		892	0.0	37.8	7.1	0.0	58.1	12.6

A histogram of the percent difference between pairs of measurements for all samples shows that this data follows a log-normal distribution (Figure 4.3). For both w_L and w_P, small values of percent difference between duplicate measurements are more common than large values.

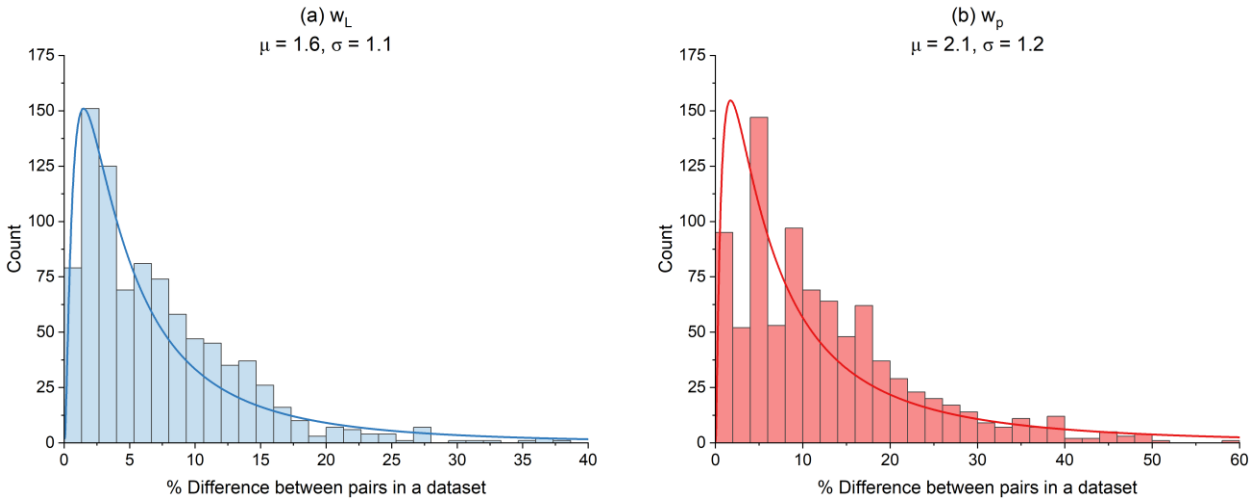

Figure 4.3. Distribution of percent difference between duplicate measurements of w_L (a) and w_P (b)

The laboratory data is compared to the variation in the literature data in Figure 4.4 and Figure 4.5. For each sample, w_L and w_P for all sample preparation methods and test procedures are plotted with ranges representing the average percent difference and maximum percent difference (Table 4.8). Percent difference ranges are calculated based on the dried preparation measured with the fall cone. If the measured Atterberg limits from different preparation methods and test procedures plots within the expected range of the percent difference between duplicate measurements, it is possible to attribute the difference between methods the embedded uncertainty of the test. Most laboratory data for CC, FT and EPK Kaolin plots around the average percent difference from literature except for FT-DS. However, the different amendment methods for TT (DS and CE) appear to have resulted in a significant difference in behaviour.

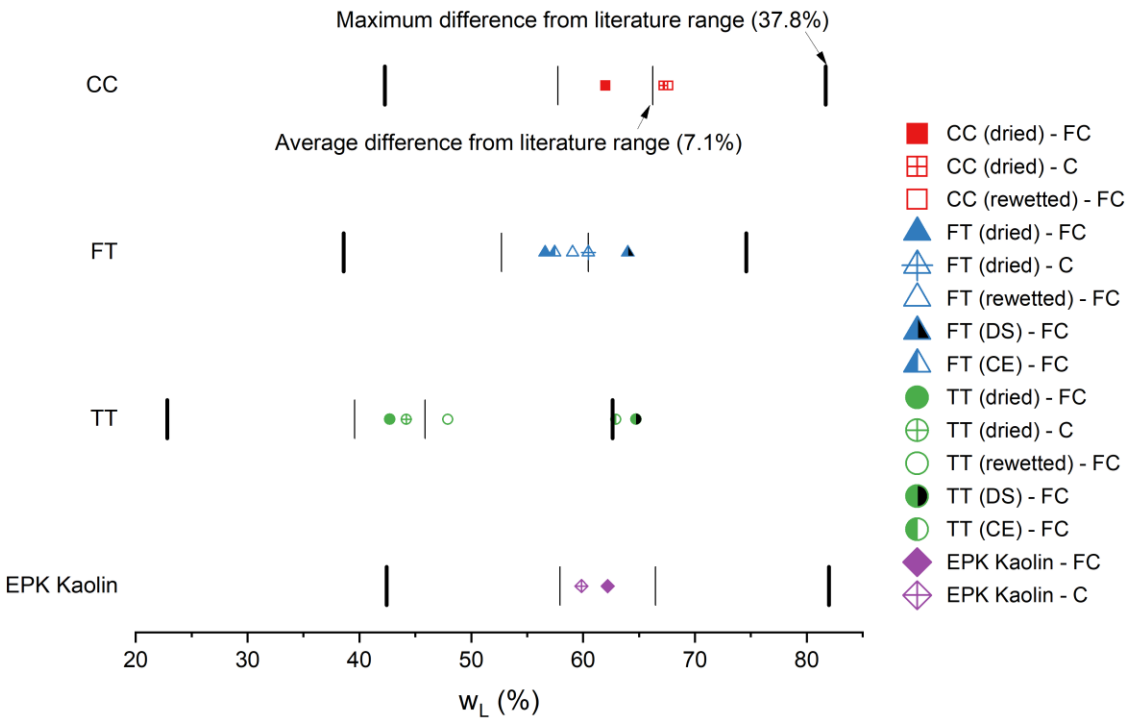

Figure 4.4. Comparison of measured w_L with variation in literature data

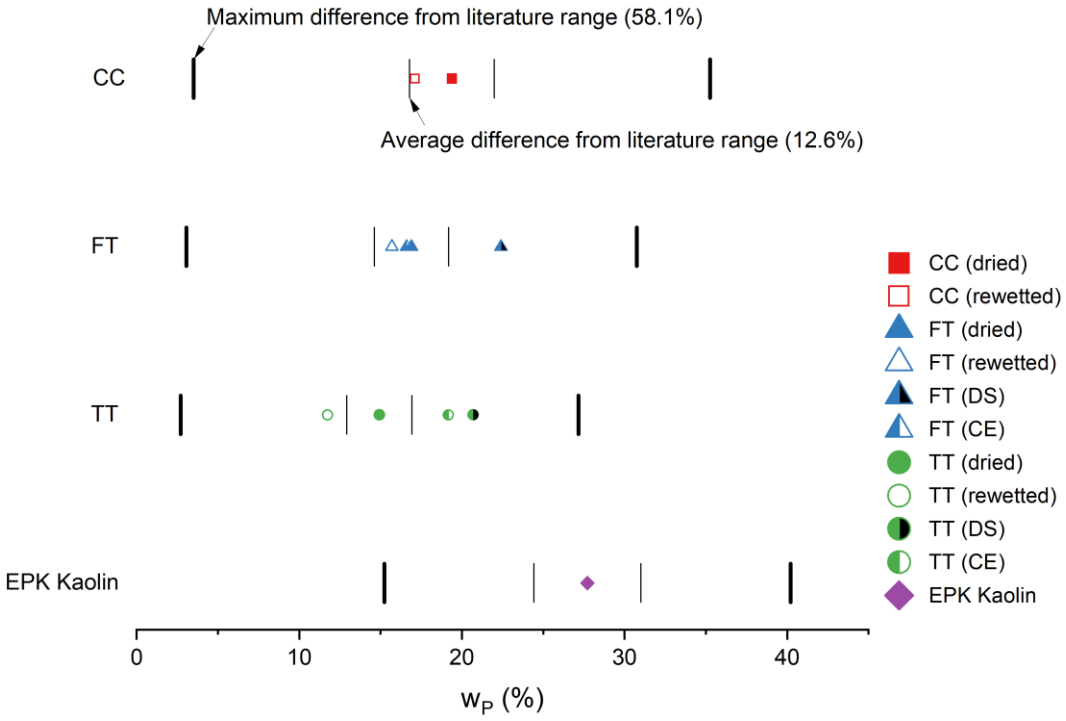

Figure 4.5. Comparison of measured and w_P with variation in literature data

4.2.2 Fall cone vs. Casagrande apparatus

Atterberg limits for w_L determined with the fall cone and Casagrande apparatus are shown in Figure 4.6 with measured values presented in Table 4.9. The same w_P was used to calculate I_p.

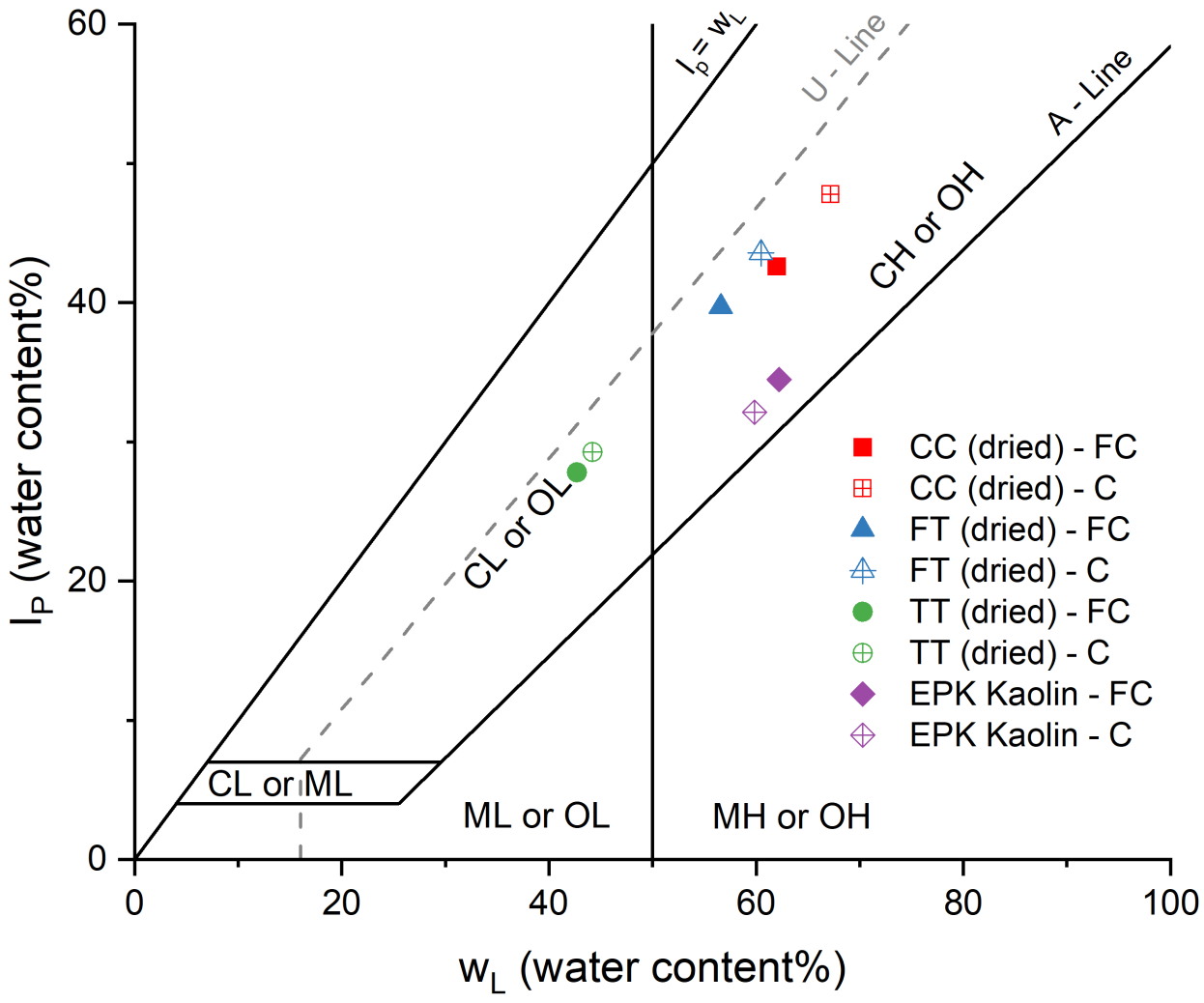

Figure 4.6. Plasticity chart - fall cone vs. Casagrande apparatus

Table 4.9. Liquid limit measured using fall cone and Casagrande apparatus with plastic limit used to determine plasticity index

	w_L (%)			w_P (%)
	Fall cone	Casagrande	%Diff.	
CC	62.0	67.2	8.0	19.4
FT	56.6	60.5	6.6	16.9
TT	42.7	44.2	3.4	14.9
EPK Kaolin	62.2	59.8	-3.9	27.7

There is overall good agreement between both methods, as has been determined by previous authors (e.g. Claveau-Mallet et al., 2010). For all tailings samples, w_L measured using the Casagrande cup was greater than that measured using the fall cone, while the opposite was true for the EPK Kaolin. This is proposed to be the result of operator bias; one individual performed the liquid limit test on all tailings samples and another performed the tests on the EPK Kaolin. Operator bias is most relevant to the Casagrande cup method because the operator must visually determine when the groove has closed ~1 cm. The measurement is also dependent how the operator prepares the material (i.e. sufficient remoulding, eliminating air bubbles when placing in the cup, using the grooving tool) and calibrates the machine. Errors in these steps are often not obvious while the test is being performed. Conversely, while operator bias is possible with the fall cone, the measurement of w_L is a result of 16 penetration measurements, and more are measured during the test to meet the criterion for an acceptable measurement (penetrations are within 0.3 mm for each point). The operator can therefore assess the precision (operator can assess the degree of scatter of the penetrations) and accuracy (operator can assess if penetrations are erroneously high or low) of the test while it is being performed. For example, if the operator observes that penetrations in a particular sample are highly variable, they can remould the sample and re-do the measurement.

4.2.3 Drying vs rewetting

Results of Atterberg limits tests for samples that were dried down at room temperature and rewetted with deionized water are presented in Figure 4.7. For all samples, rewetting with deionized water increased w_L and decreased w_P (Table 4.10). Tests on natural and amended soils have also found that repeated drying and wetting with deionized or distilled water tends to increase w_L and decrease w_P (e.g. Bouazza et al., 2007; Ye et al., 2018). This is attributed to the destruction of the particle microstructure and associated increase in fines content. Gidley and Moore (2013) also observed that samples of MFT tested with deionized water had greater w_L than air-dried samples, though the average w_P of the sample increased.

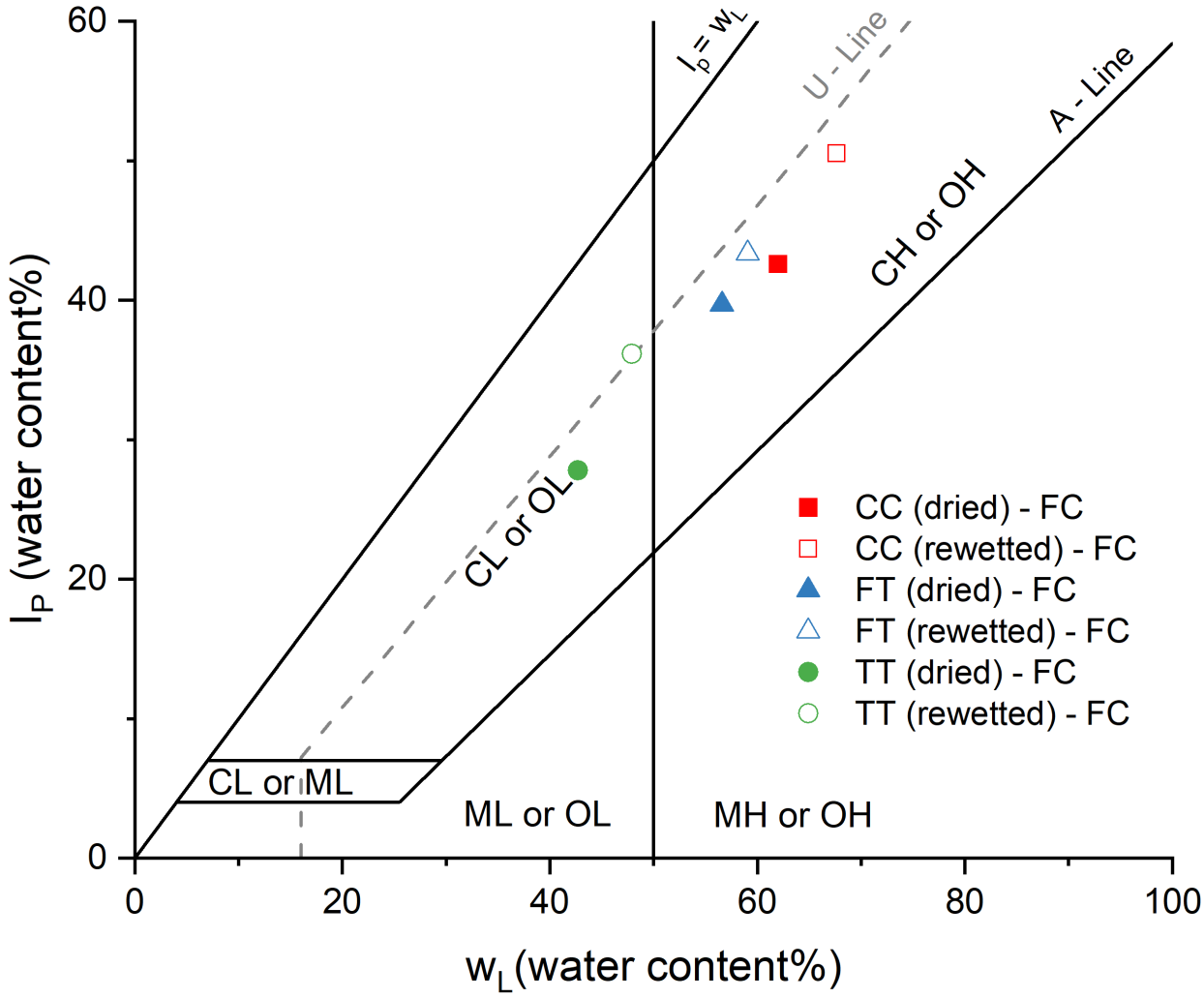

Figure 4.7. Plasticity chart - dried vs. rewetted

Table 4.10. Atterberg limits measured on dried and rewetted tailings

	w_L (%)			w_P (%)		
	Dried	Rewetted	%Diff.	Dried	Rewetted	%Diff.
CC	62.0	67.6	8.7	19.4	17.1	-12.5
FT	56.6	59.1	4.3	16.9	15.7	-7.4
TT	42.7	47.9	11.4	14.9	11.7	-23.9

4.2.4 Amendment methods

Atterberg limits of samples that were amended using the Dean Stark and cold extraction methods are presented in Figure 4.8. As compared to the as-received dried sample, FT experienced a small change in w_L and w_P. while both values significantly increased for TT (Table 4.11).

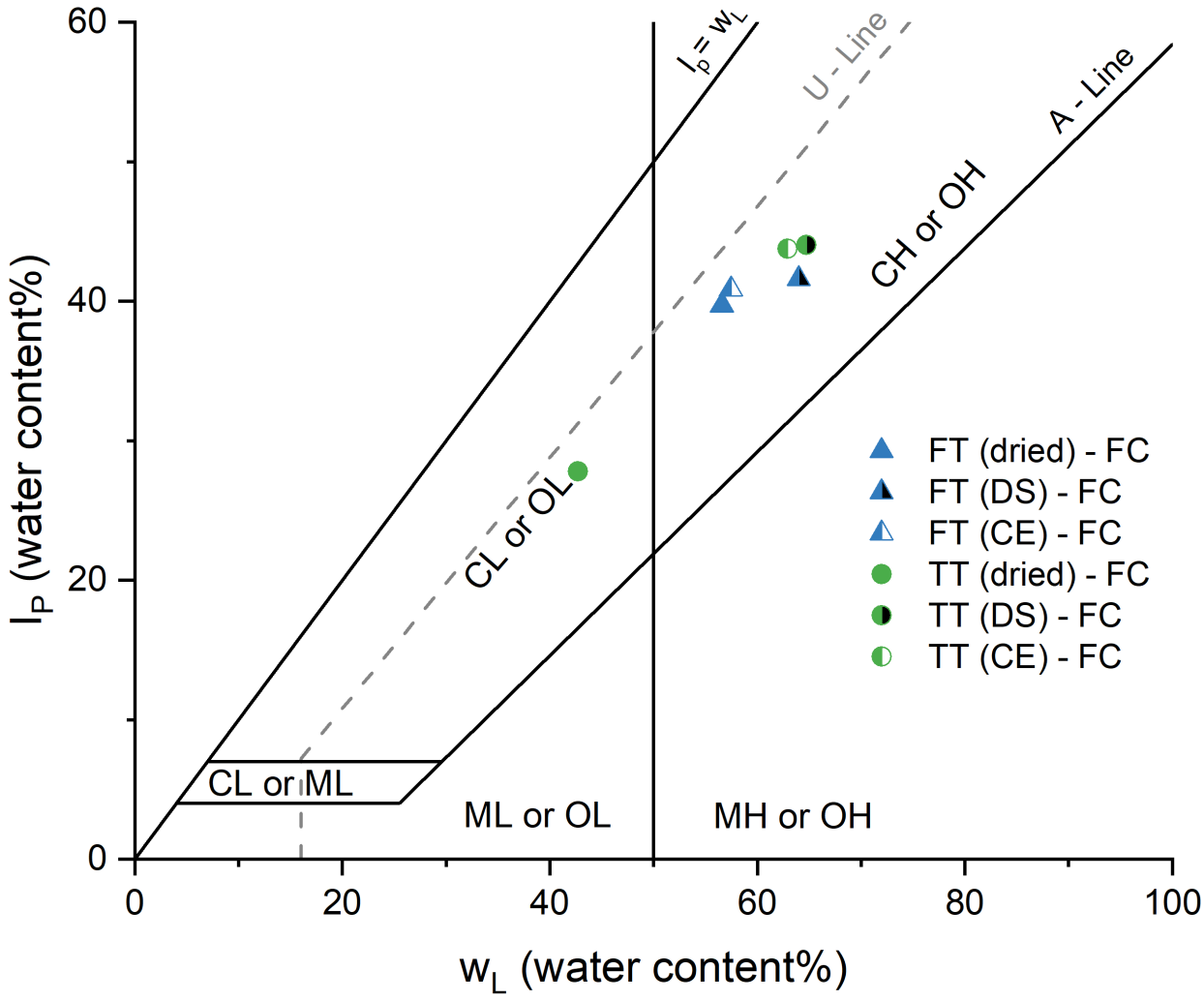

Figure 4.8. Plasticity chart - dried (as-received) vs. amended

Table 4.11. Atterberg limits measured on dried (as-received) and amended tailings

	w_L (%)					w_P (%)				
	Dried (as-received)	DS	% Diff.†	CE	%Diff.†	Dried (as-received)	DS	% Diff.†	CE	%Diff.†
FT	56.6	64.0	12.3	57.4	1.5	16.9	22.4	28.0	16.6	-1.8
TT	42.7	64.7	41.0	62.9	38.2	14.9	20.7	32.3	19.2	24.8

† %Diff. measured between dried (as-received) and amended sample

It was observed that effect of the Dean Stark method was to increase both w_L and w_P, however, the expected effect of this method is complicated by competing factors. The Dean Stark method removes bitumen and promotes particle aggregation through drying (Basma et al. 1994). In this study, it was also observed that the Dean Stark method reduced the fines content and clay content (as measured by MBI) and removed ions (as indicated by a reduction in conductivity). Considering w_L, removing ions is expected to increase w_L (Mitchell and Soga 2005, Miller et al. 2010), while oven-drying and removing bitumen is expected to decrease w_L (Scott et al. 1985, 2013, Basma et al. 1994). Gidley and Moore (2013) observed that the w_L of MFT decreased (opposite to this study) and w_P increased after Dean Stark extraction.

The effect of cold extraction in this study was to increase w_L of both samples and increase w_P of TT. There was no significant effect of cold extraction on w_P of FT. The primary difference between the cold extraction method and the Dean Stark method is that bitumen and ions are removed without oven drying, through these are still competing factors.

4.3 Remoulded strength – liquidity index

4.3.1 Overall results

The measured Su_r and water content of all samples is plotted in Figure 4.9. The range of measured strengths at a particular water content varies by approximately one order of magnitude. As was observed in the Atterberg limits, the TT shows the greatest sensitivity to the preparation method.

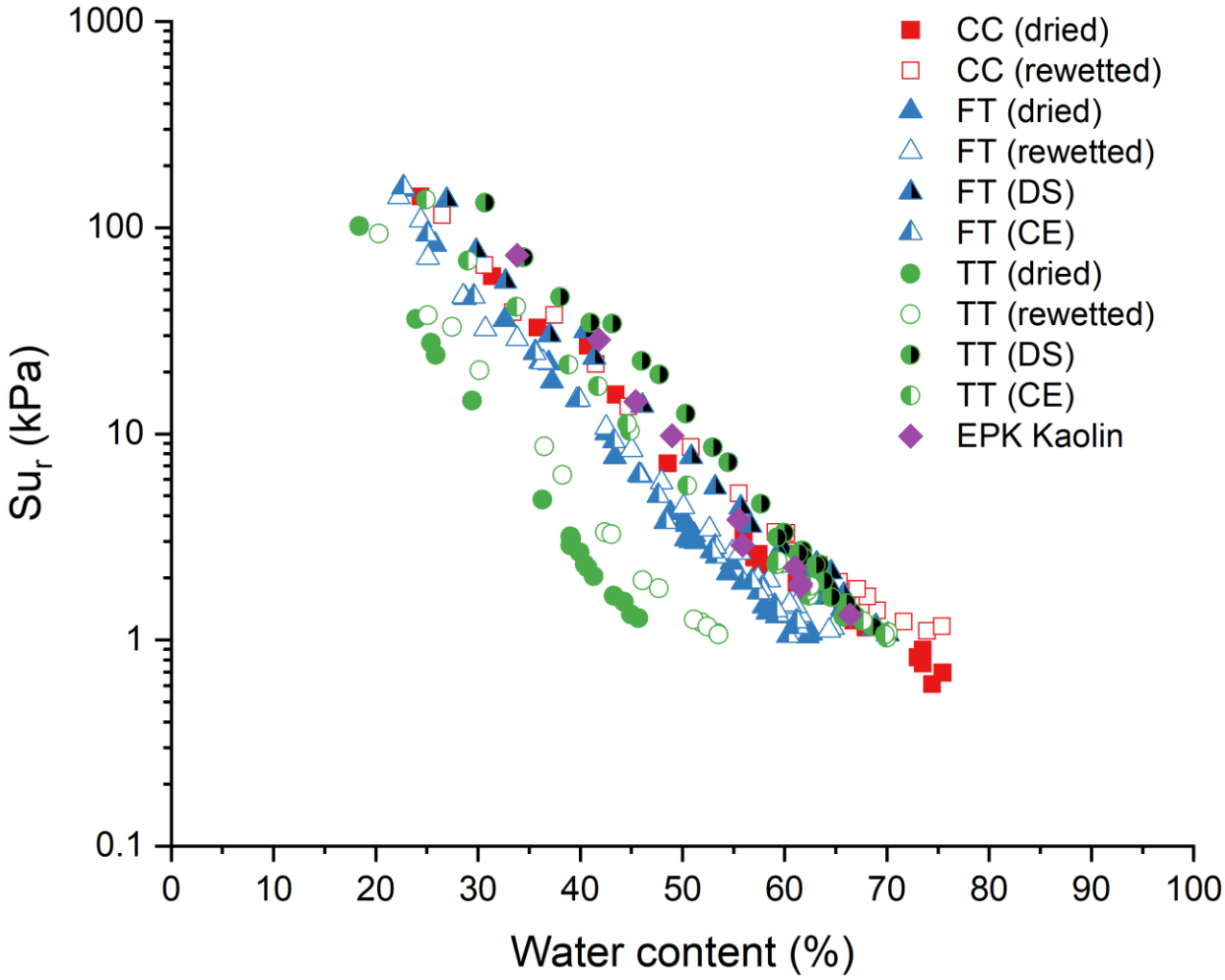

Figure 4.9. Su_r vs. water content – all samples

The measured Su_r and the I_L calculated from the water content and the appropriate Atterberg limits are plotted in Figure 4.10. When normalized to I_L, the measured Su_r shows a consistent trend that deviates from the behaviour predicted by the Locat and Demers (1988), which has been extrapolated to fit this dataset. A new relationship is proposed to predict Su_r from I_L (Equation 4.1). This relationship was determined from all samples in the test program for I_L ranging from 0.1 to 1.3. The measured Su_r are plotted with the data from literature and Equation 4.1 in Figure 4.11. While this relationship does not extend to w_P ($I_L = 0$), the dataset appears to support the rule of thumb that Su_r at w_P is approximately 2 orders of magnitude (100 times) greater than Su_r at w_P (e.g. Sharma and Bora 2003, Mitchell and Soga 2005).

Equation 4.1

$$Su_r = \left(\frac{21.8}{2.78I_L + 18.7}\right)^{36.2}$$

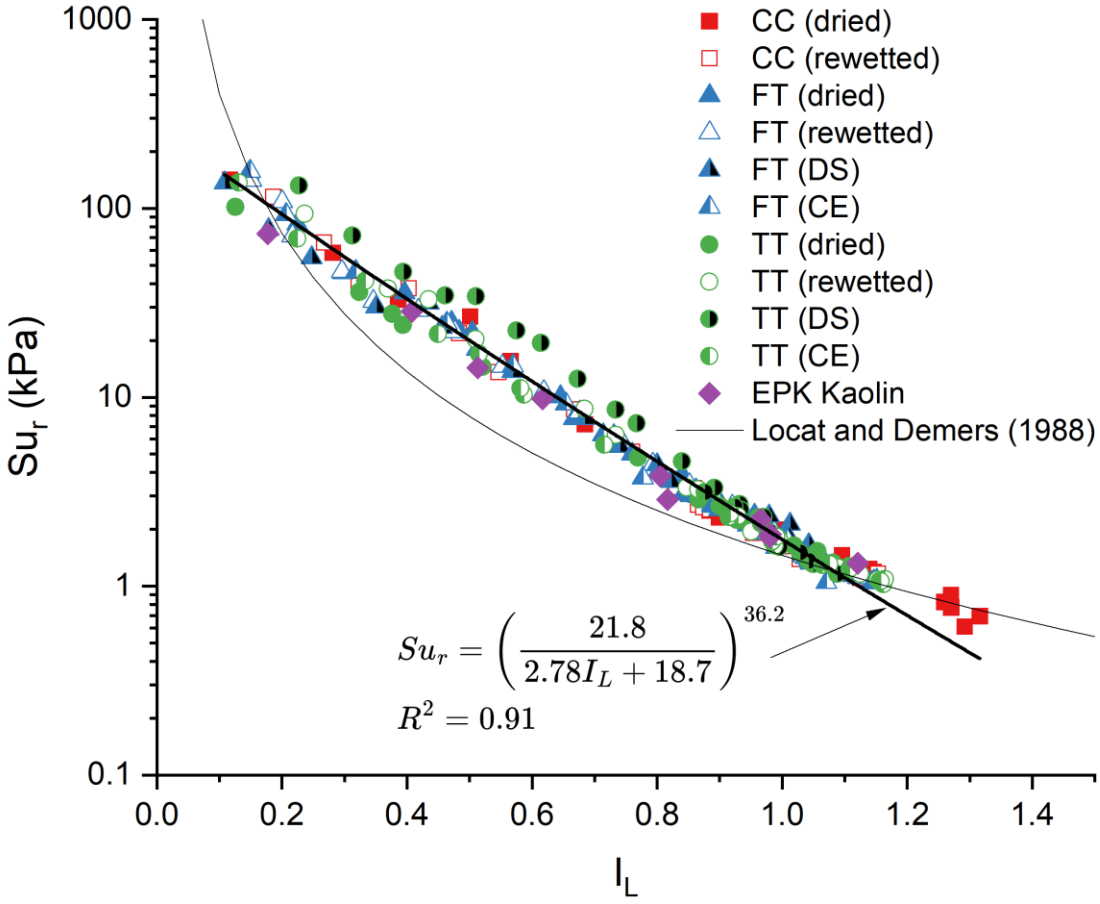

Figure 4.10. Su_r vs I_L - measured data with curve fit (log scale)

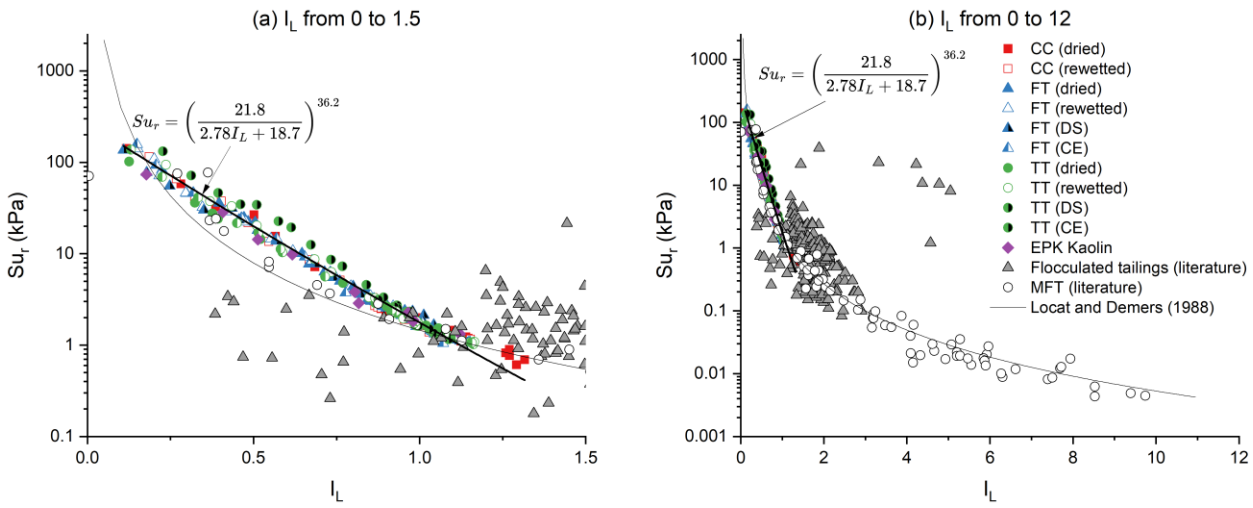

Figure 4.11. Su_r and I_L of lab and literature data with fitted curve

The measured Su_r is compared to the predicted Su_r from the Locat and Demers (1988) relationship and Equation 4.1 (Paul 2024) in Figure 4.12. The results indicate that Equation 4.1 is a better fit of the measured data (R^2 = 0.91) than the relationship proposed by Locat and Demers (1988) (R^2 = 0.52). The value of R^2 for the proposed relationship is also similar to the value calculated for the original Locat and Demers (1988) relationship (R^2 = 0.95). Most data points in Figure 4.12(b) also plot below the line of equality (y = x), indicating that strengths calculated from the Locat and Demers (1988) relationship are typically less than the measured strength.

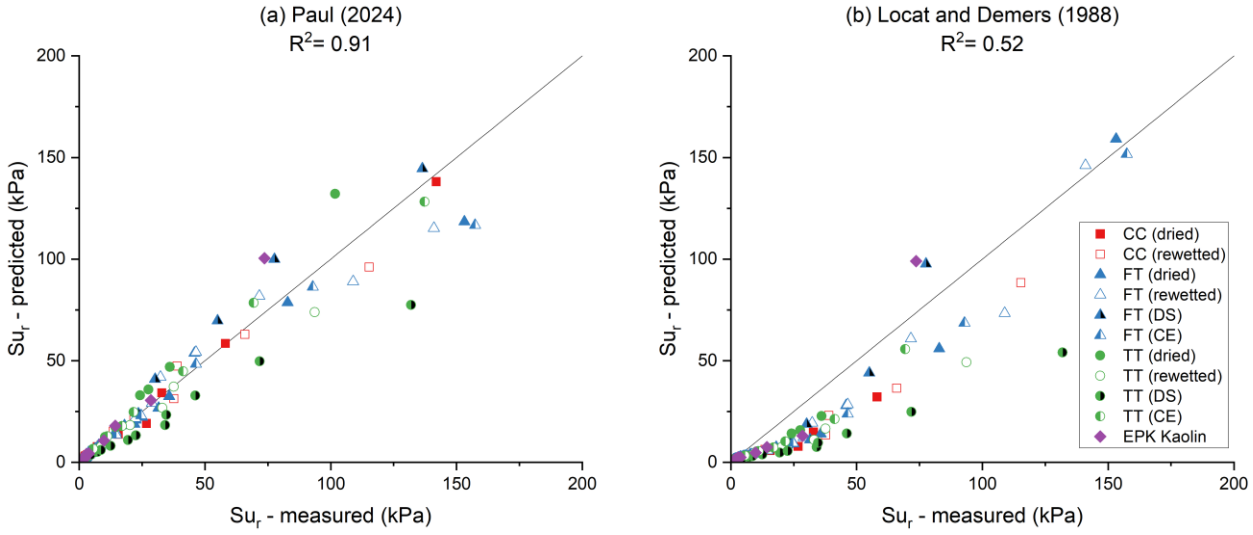

Figure 4.12. Comparison of lab Su_r with Paul (2024) (a) and Locat and Demers (1988) (b)

Figure 4.12 (a) also shows that the difference between the measured and predicted strength using Equation 4.1 increases for larger Su_r. This is a result of the higher degree of scatter at low I_L, which is clearly visible in a linear plot of the data (Figure 4.13). A conservative assumption based on the measured dataset is that it is possible for the predicted strength to be 50% larger than the measured strength, meaning that a factor of safety of at least 2 should be applied.

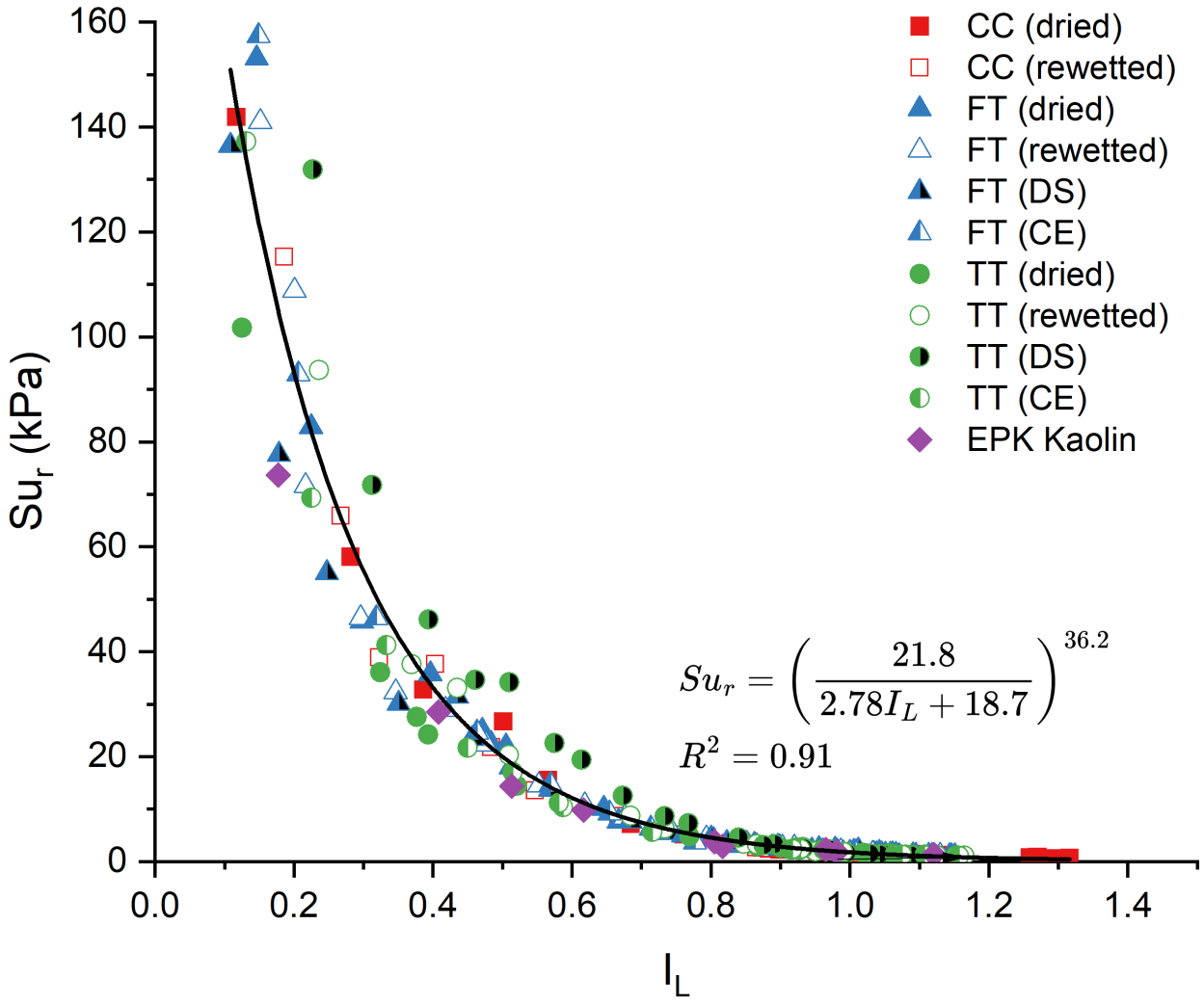

Figure 4.13. Su_r vs I_L - measured data with fitted curve (linear scale)

Values of Su_r reported in the literature are compared to both models in Figure 4.14. Both models show a similar correlation between the predicted and measured Su_r when considering all of the data points. However, there are significant differences between the two tailings. The strength data for the flocculated tailings is highly scattered and is not

well predicted by either model, as demonstrated by the negative value of R^2. The strength of the MFT is comparatively well predicted by Equation 4.1 (R^2 = 0.73) and is poorly predicted by Locat and Demers (1988) (R^2 = 0.37). The scatter of the MFT data is also similar to the laboratory values (Figure 4.15). This suggests that Equation 4.1 can be used to predict the strengths of samples outside of the laboratory test data used to develop the model.

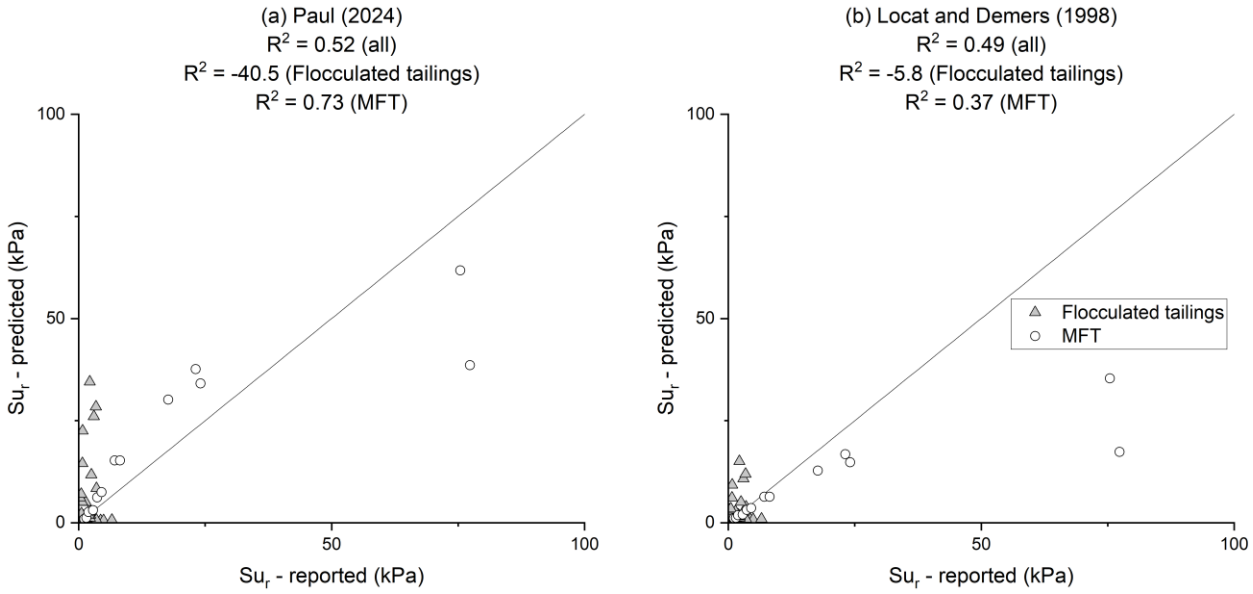

Figure 4.14. Comparison of literature Su_r with Paul (2024) (a) and Locat and Demers (1988) (b)

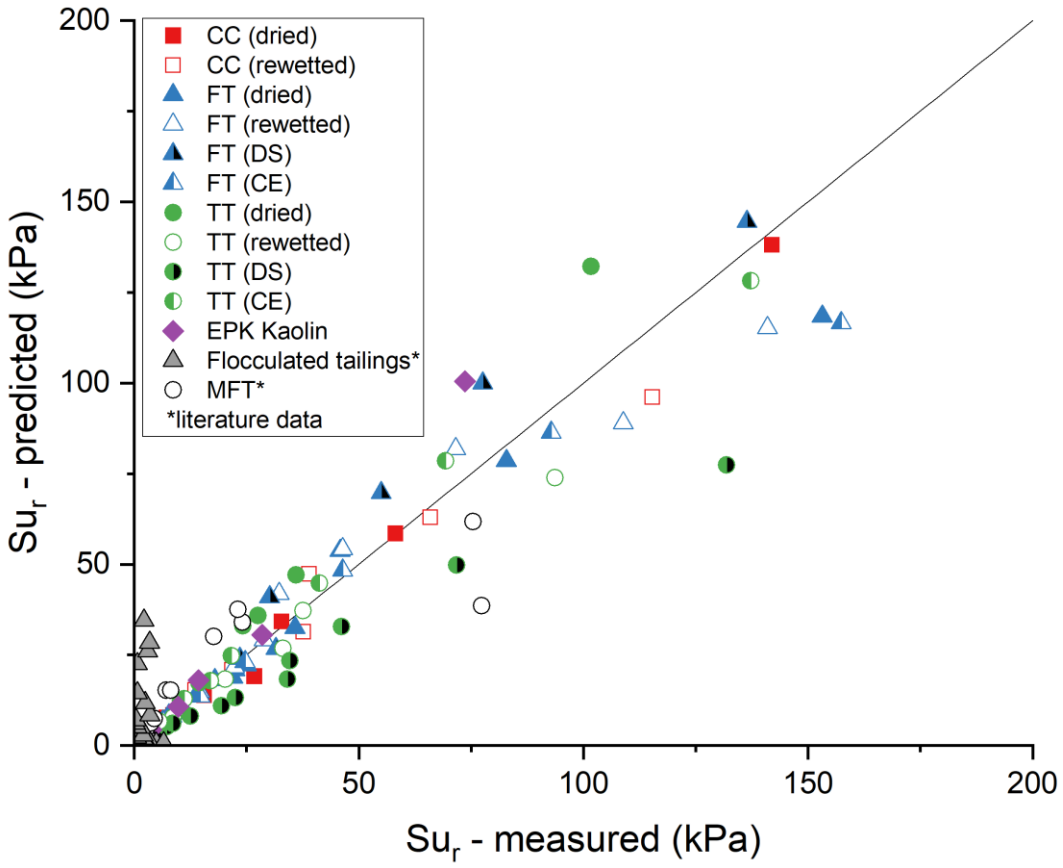

Figure 4.15. Comparison of lab and literature Su_r with Paul (2024)

4.3.2 Drying vs. rewetting

The measured Su_r for dried and rewetted samples are plotted against I_L and water content in Figure 4.16. The Atterberg limits for each preparation method were used to determine I_L. At a given water content, the rewetted Su_r is slightly stronger than the dried Su_r at higher water contents (around w_L), and this difference reduces as the water content reduces (approaches w_P). This behaviour is analogous to atmospheric drying to increase the strength of tailings deposits. When the water content is normalized as the I_L using the Atterberg limits, the Su_r is similar and closely matches Equation 4.1 for both dried and rewetted samples.

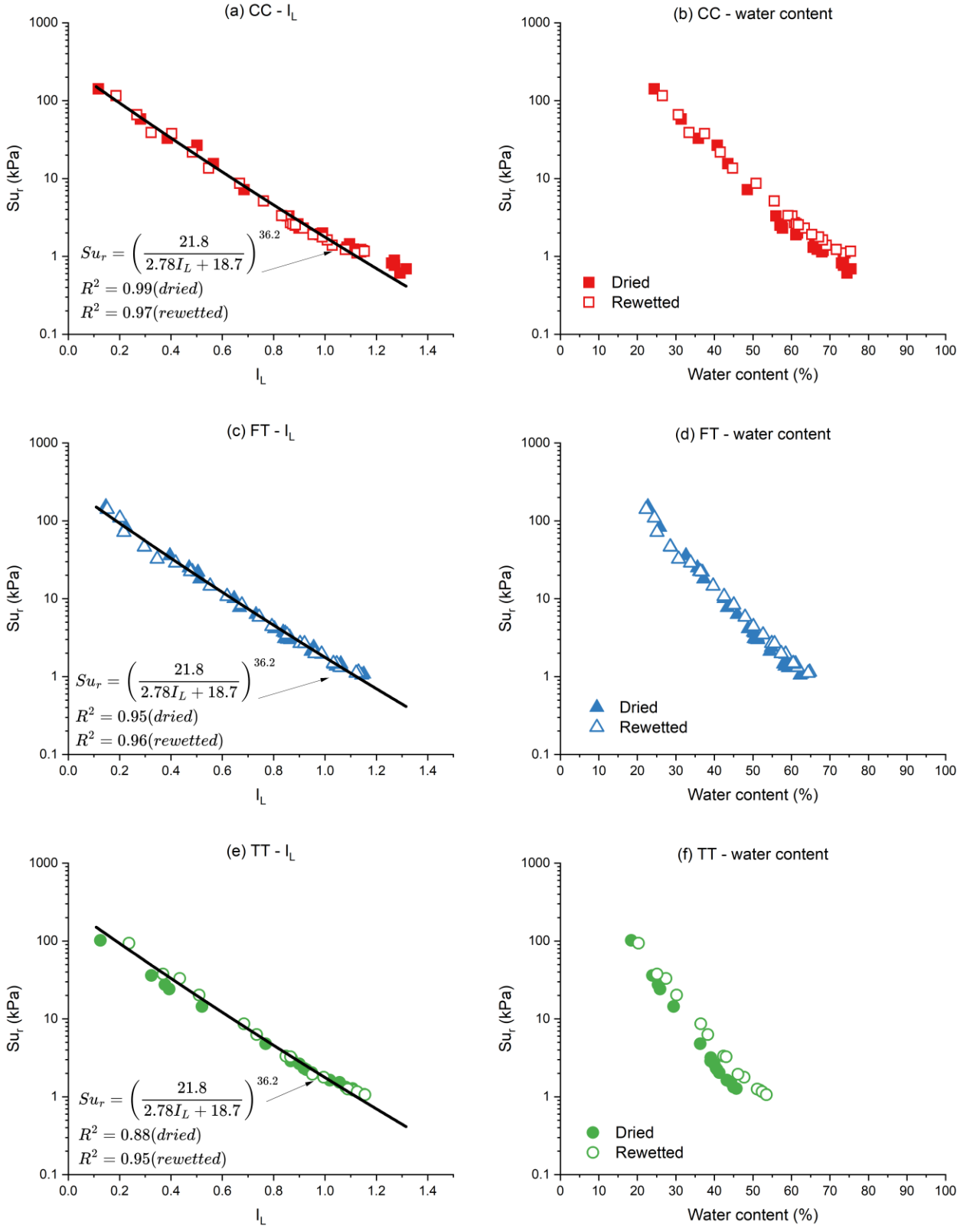

Figure 4.16. Dried and rewetted Su_r vs. I_L and water content (all samples)

4.3.3 Amendment methods

The measured Su_r for amended samples are plotted against I_L and water content in Figure 4.17. The Su_r of the dried samples are also plotted to describe the behaviour of the as-received tailings. Both amendment methods increased the strength of the tailings at the same water content. The Dean Stark method caused the highest strength increase. The cold extraction method also increased the strength, but this effect was less significant for the FT. The dried and amended TT also showed the poorest correlation with Equation 4.1 of the tailings samples. These results demonstrate that as-received and amended tailings samples show a similar strength behaviour when the appropriate Atterberg limits are used to calculate I_L.

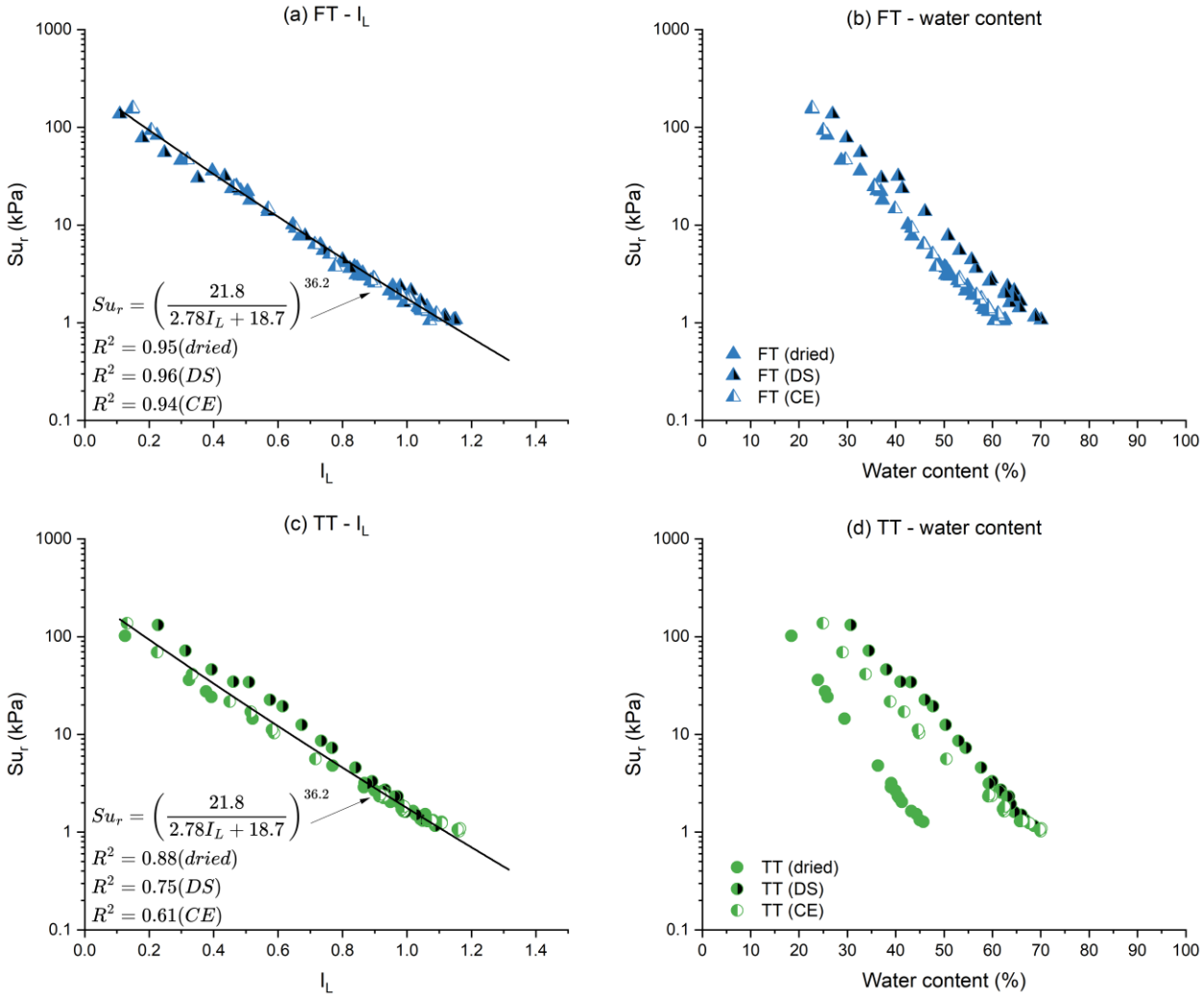

Figure 4.17. Amended Su_r vs. I_L and water content (all samples)

4.3.4 Effect of changing Atterberg limits

If Equation 4.1 is to be used to predict the Su_r from I_L, it is relevant to understand the effect of changing the Atterberg limits on the model. This is illustrated in Figure 4.18 by plotting the same strength data (dried) against different sets of I_L. These I_L are determined by normalizing the water content corresponding to the measured Su_r against Atterberg limits matching either the preparation method" (dried) or other preparation methods (rewetted, DS, or CE). For example, "Dried-rewetted" indicates that the rewetted Atterberg limits were used to calculate the I_L for the dried Su_r. The effect of changing the Atterberg limits on the model is related to the magnitude of the difference between the matching and mis-matched Atterberg limits. This effect is demonstrated in Figure 4.18(c) in which large changes between the dried and amended Atterberg limits for TT cause the model to not fit the data. Small differences between the actual and measured Atterberg limits such as the dried and rewetted CC (Figure 4.18[a]) do not appear to significantly effect the fit. This suggests that material specific Atterberg limits should be used to calculate I_L, and that sensitivity testing may be appropriate where there is uncertainty. This would be the case in a TSF in which deposits are highly heterogeneous and changes in material properties over time will result in changes to the Atterberg limits.

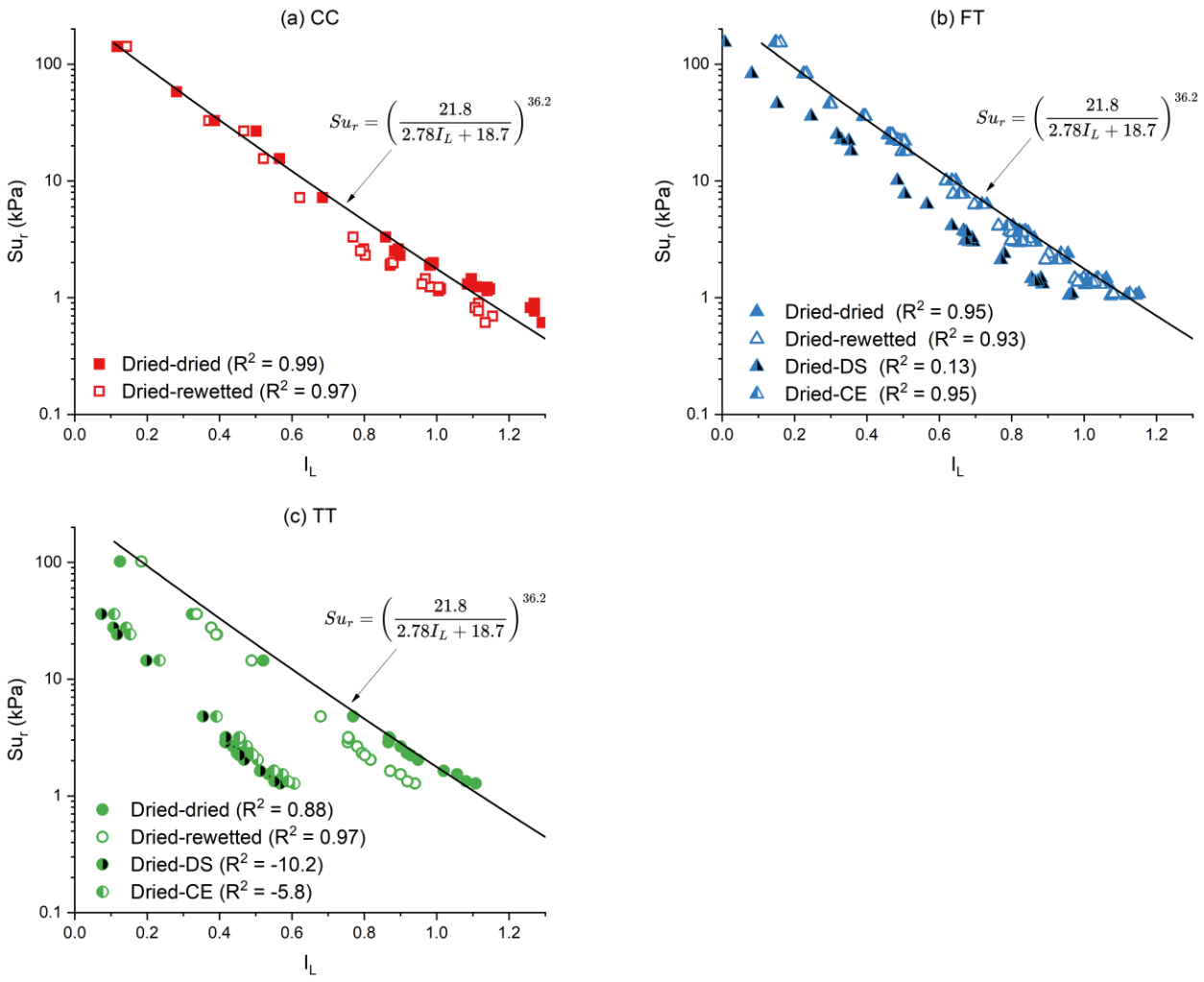

Figure 4.18. Effect of changing rewetted and amended Atterberg limits to dried Atterberg limits

4.4 Bearing capacity

4.4.1 Properties of model footing samples

Key parameters of each model footing sample are presented in Table 4.12. Water content measurements of the top, middle, and bottom of each model footing sample were approximately equal, indicating that the samples are homogenous. Samples are differentiated by the pressure applied in the Tempe cell (100 kPa, 200 kPa, or 400 kPa), and the number of days between when they were removed from the Tempe cell and when the model footing test was performed. The samples were stored wrapped in plastic under controlled temperature and humidity conditions during this period. For the tailings samples (CC and TT), I_L was calculated using the as-received dried Atterberg limits (w_L

measured with the fall cone). The I_L of the kaolin was calculated using the w_L measured with the fall cone. The density of each sample was also calculated from the mass and volume measurements.

Table 4.12. Properties of model footing samples

Sample	G_s	w (%)	I_L	e	S	Density (g/cm^3)
CC (100 kPa) - 277 days	2.28	40.9	0.50	0.85	1	1.68
CC (100 kPa) - 24 days	2.28	41.2	0.51	0.85	1	1.66
CC (200 kPa) - 278 days	2.28	36.0	0.39	0.74	1	1.74
CC (200 kPa) - 29 days	2.28	36.5	0.40	0.76	1	1.73
CC (400 kPa) - 281 days	2.28	30.3	0.26	0.63	1	1.78
CC (400 kPa) - 28 days	2.28	31.3	0.28	0.65	1	1.79
TT (100 kPa) - 66 days	2.53	27.8	0.46	0.70	1	1.83
TT (100 kPa) - 9 days	2.53	27.8	0.46	0.70	1	1.82
TT (200 kPa) - 64 days	2.53	23.9	0.32	0.60	1	1.66
TT (200 kPa) - 9 days	2.53	24.4	0.34	0.62	1	1.86
TT (400 kPa) - 103 days	2.53	19.7	0.17	0.50	0.99	1.91
TT (400 kPa) - 8 days	2.53	20.4	0.20	0.52	0.99	1.91
EPK Kaolin (100 kPa) - 45 days	2.65†	47.6	0.58	1.20	1	1.77
EPK Kaolin (200 kPa) - 110 days	2.65†	41.0	0.38	1.03	1	1.72
EPK Kaolin (400 kPa) - 74 days	2.65†	37.9	0.30	0.95	1	1.78

† Edgar Minerals Inc. (2018)

The properties of the model footing samples demonstrate the effect of consolidation in the Tempe cell. The pressure applied in the Tempe cell to dewater the sample also acts as a consolidating load. As the pressure is increased, more pore fluid is pushed out of the sample and the water content and I_L decrease. The density also follows a general increasing trend as the water content decreases. All samples were completely saturated except for the TT (400 kPa), which was determined to be marginally unsaturated (S of 0.99).

The degree of saturation of each model footing sample was calculated from specific gravity, void ratio, and water content (Equation 3.6). Shrinkage curves used to determine void ratio corresponding to the water content each sample are plotted in Figure 4.19. Curve fitting was used to determine the equation of the curve according to the form proposed by Fredlund (1999). The shrinkage curves were also used to determine w_s of each sample (Table 4.13). The samples were assumed to be completely saturated, and the intersection point with the minimum void ratio was determined from both a line of slope G_s and a slope determined from curve fitting.

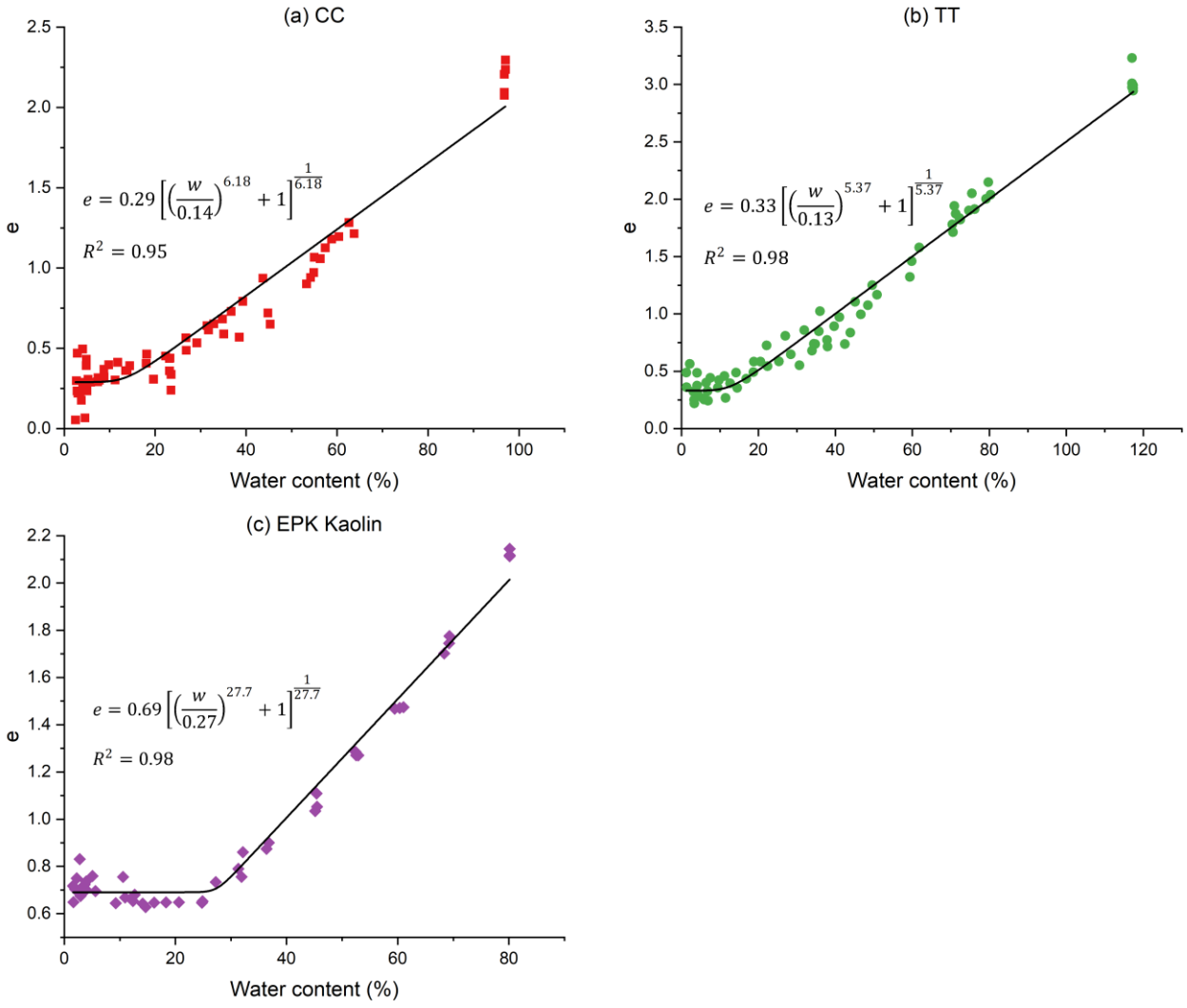

Figure 4.19. Shrinkage curves

Table 4.13. Shrinkage limit of samples used for model footing tests

Sample	e_{min}	Slope from curve fit	G_s	w_s (%)		
				From curve fit	From G_s	% Diff.
CC	0.29	2.07	2.28	14.0	12.7	9.7
TT	0.33	2.58	2.53	12.8	13.0	1.9
EPK Kaolin	0.69	2.58	2.65	26.8	26.0	2.7

4.4.2 Model footing tests

The measured stress and displacement for the model footing tests is presented in Figure 4.20. Tests are differentiated by sample type (CC, TT, or EPK Kaolin) and aging time. Aging had a significant effect on the behaviour of CC as demonstrated by the increase in strength and stiffness of the samples with a longer aging. The behaviour of TT was not influenced by aging, and this is proposed to be result of a lower clay content compared to CC. For the TT and EPK Kaolin, the strength and stiffness of the sample increased as the I_L decreased, as illustrated by the higher value of approximately constant stress and initial slope. For a given aging period (~30 days vs. ~280 days), the CC followed a similar trend.

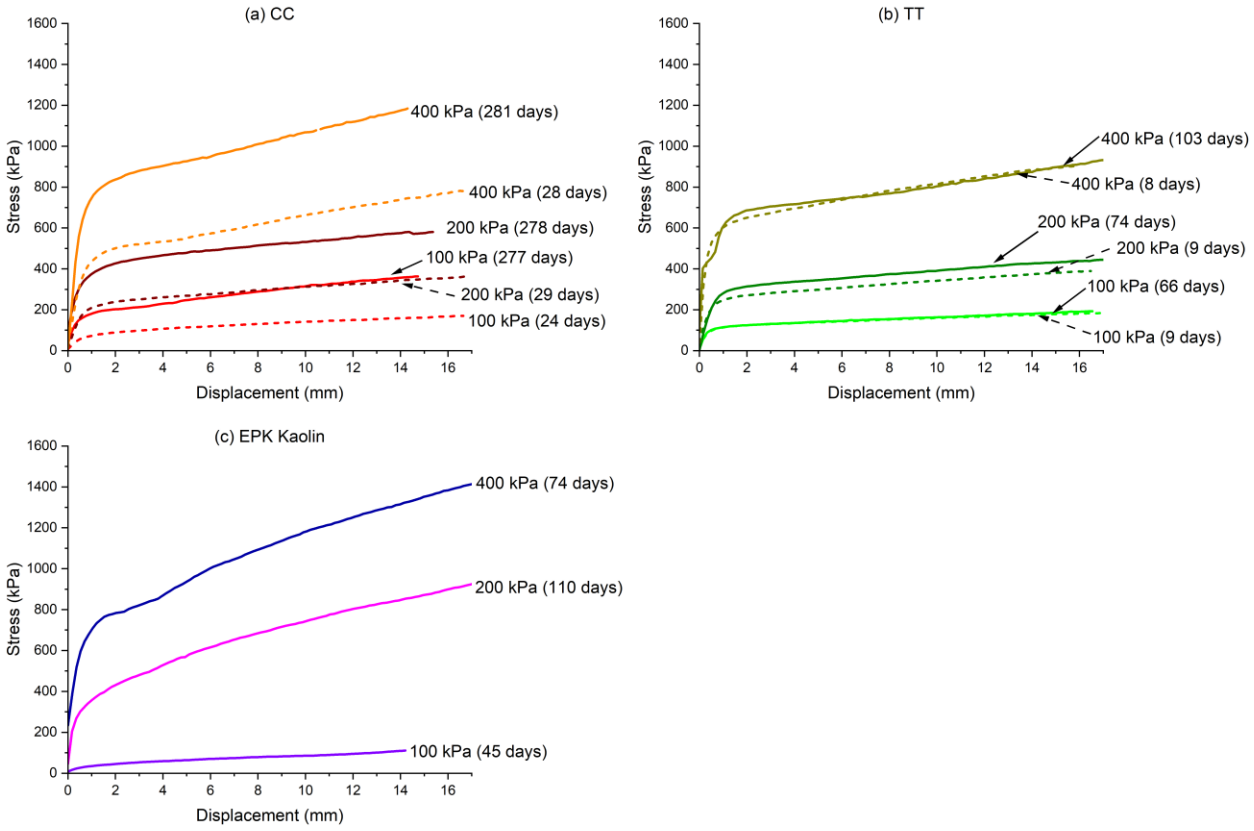

Figure 4.20. Model footing test results

The slope-tangent and 0.1B methods were used to determine q_{ult} of each model footing sample. These values are summarized in Table 4.14 and plotted in Figure 4.21. The high value of R^2 (0.99) indicates that both methods produce approximately identical results.

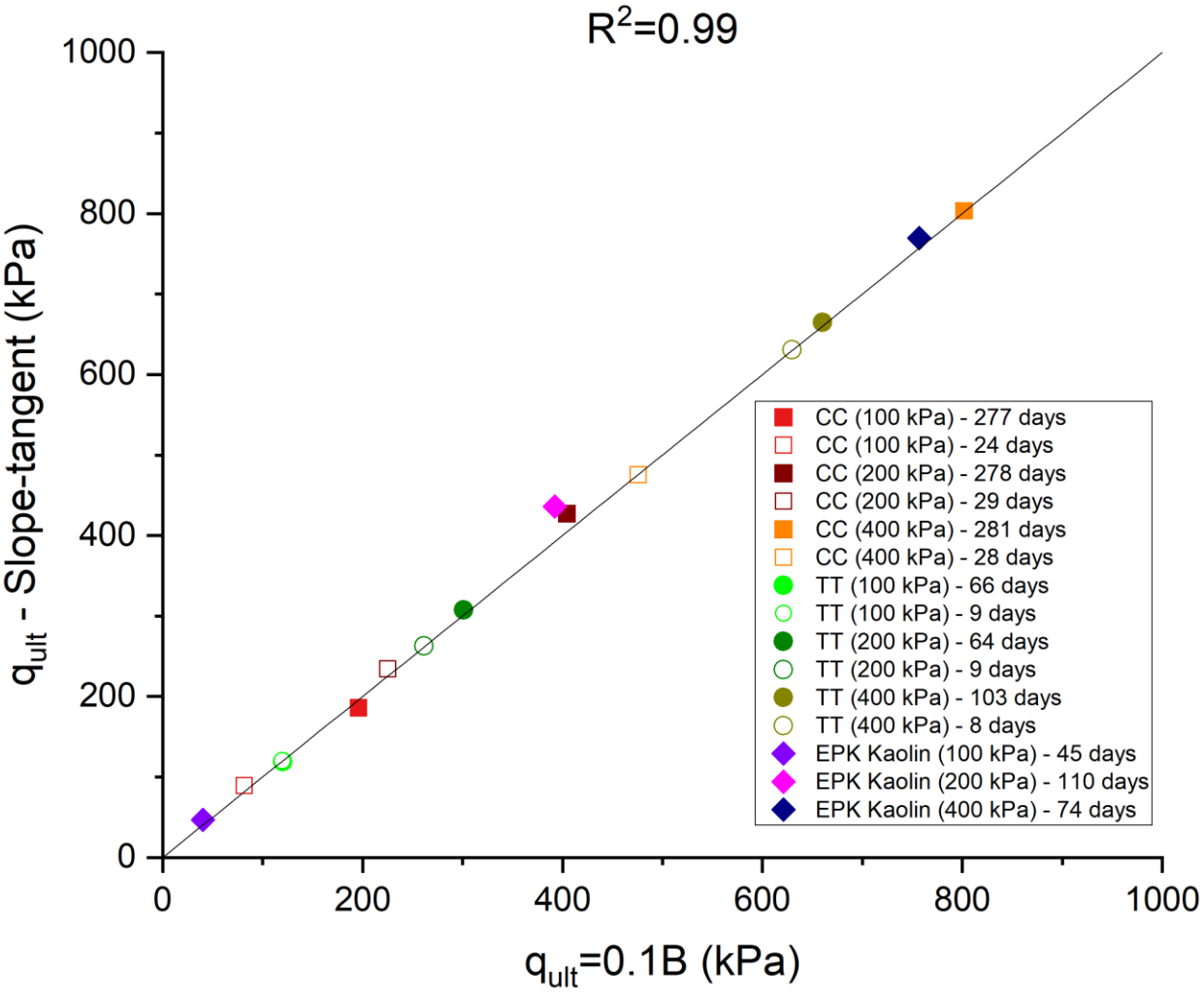

Figure 4.21. Comparison of model footing q_{ult} determined with slope-tangent and 0.1B methods

Table 4.14. Measured q_{ult} of model footing samples

Sample	q_{ult} (kPa)	
	0.1B	Slope-tangent
CC (100 kPa) - 277 days	196	186
CC (100 kPa) - 24 days	81.8	89.3
CC (200 kPa) - 278 days	404	427
CC (200 kPa) - 29 days	225	234
CC (400 kPa) - 281 days	802	803
CC (400 kPa) - 28 days	476	475
TT (100 kPa) - 66 days	120	119
TT (100 kPa) - 9 days	120	120
TT (200 kPa) - 64 days	301	308
TT (200 kPa) - 9 days	261	263
TT (400 kPa) - 103 days	660	665
TT (400 kPa) - 8 days	630	631
EPK Kaolin (100 kPa) - 45 days	40.2	46.6
EPK Kaolin (200 kPa) - 110 days	392	436
EPK Kaolin (400 kPa) - 74 days	757	770

4.4.3 Predicting bearing capacity from peak undrained shear strength

The q_{ult} predicted from *Su* (Equation 2.3) is plotted against the q_{ult} determined from the 0.1B and slope-tangent methods in Figure 4.22. After the model footing test, the fall cone was used to measure *Su* of each sample and is presented with the measured and predicted q_{ult} in Table 4.15. The predicted q_{ult} shows reasonably good agreement with the measured q_{ult} (R^2 of 0.65), however, this relationship tends to over-predict q_{ult} with an average ratio of the predicted to measured q_{ult} of 1.3 and a range of 0.8 to 2.2 (when using the average measured q_{ult} between the two methods). This may be considered acceptable considering of safety of 2-3 that is typically applied to predictions of q_{ult} (COSIA 2022). The TT (400 kPa) in particular shows a significant difference between the measured and predicted q_{ult}.

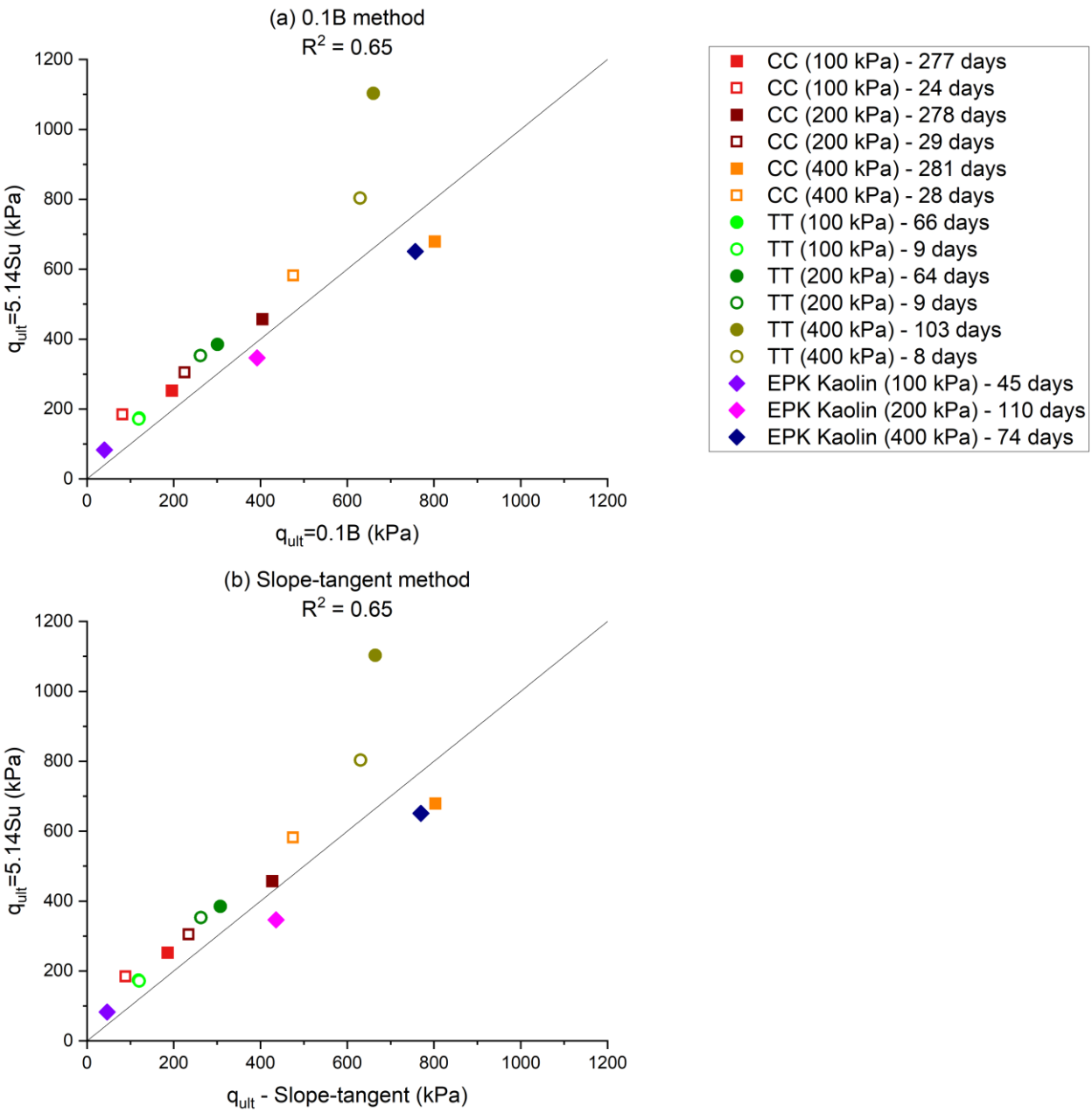

Figure 4.22. Comparison between q_{ult} determined from 0.1B (a) and slope-tangent (b) methods and predicted from *Su*

Table 4.15. Measured q_{ult} and predicted q_{ult} from *Su*

Sample	*Su* (kPa)	q_{ult} (kPa)		
		5.14*Su*	0.1B	Slope-tangent
CC (100 kPa) - 277 days	49.1	252	196	186
CC (100 kPa) - 24 days	35.9	184	81.8	89.3
CC (200 kPa) - 278 days	88.9	457	404	427
CC (200 kPa) - 29 days	59.3	305	225	234
CC (400 kPa) - 281 days	132	679	802	803
CC (400 kPa) - 28 days	113	582	476	475
TT (100 kPa) - 66 days	33.9	174	120	119
TT (100 kPa) - 9 days	33.4	172	120	120
TT (200 kPa) - 64 days	74.8	385	301	308
TT (200 kPa) - 9 days	68.7	353	261	263
TT (400 kPa) - 103 days	215	1103	660	665
TT (400 kPa) - 8 days	156	804	630	631
EPK Kaolin (100 kPa) - 45 days	16.1	83.0	40.2	46.6
EPK Kaolin (200 kPa) - 110 days	67.3	346	392	436
EPK Kaolin (400 kPa) - 74 days	127	651	757	770

4.4.4 Predicting bearing capacity from sensitivity and liquidity index

By linking Su_r to *Su* via the sensitivity ratio (S_t), it is possible to link Su_r to q_{ult}. Further, Equation 4.1 relates Su_r and I_L, making it possible to predict q_{ult} from S_t and I_L using Equation 4.2. The measured strengths for each model footing sample are plotted with the datasets used to develop the Su_r *and* I_L relationship in Figure 4.23. *Su* plots above the rest of the as-received data.

Equation 4.2

$$q_{ult} = 5.14 * S_t * Su_r = 5.14 * S_t * \left(\frac{21.8}{2.78I_L + 18.7}\right)^{36.2}$$

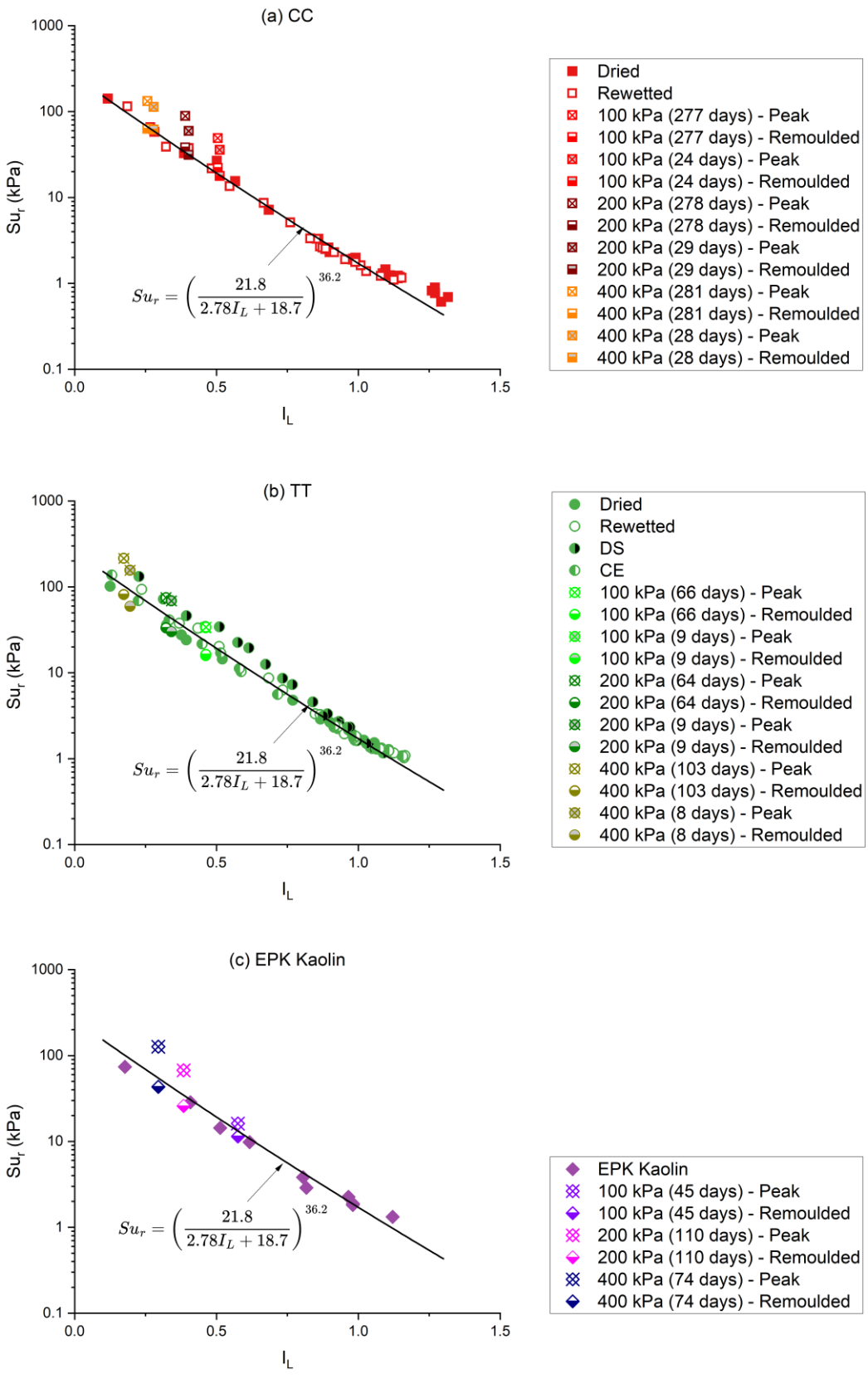

Figure 4.23. Peak and remoulded *Su* of model footing samples

Su_r is reasonably well predicted by Equation 4.1 (R^2 = 0.64 when considering all datapoints) (Figure 4.24), however, there are significant differences between the sample types. CC is very well predicted by the model (R^2 = 0.97) while the difference between the predicted and measured strengths are larger for the other samples, in particular for TT (R^2 = 0.41). This may be the result of the high degree of scatter in the model at higher values of Su_r, though it is unclear why predictions for some sample types are more variable than others. It is suggested that the low fines content of TT relative to the other samples may be causing a different pattern of behaviour. The results of this analysis further support the use of a factor of safety of 2 or more for the use of this model in practice as this would reduce the predicted strength to less than the actual strength for all samples, including TT.

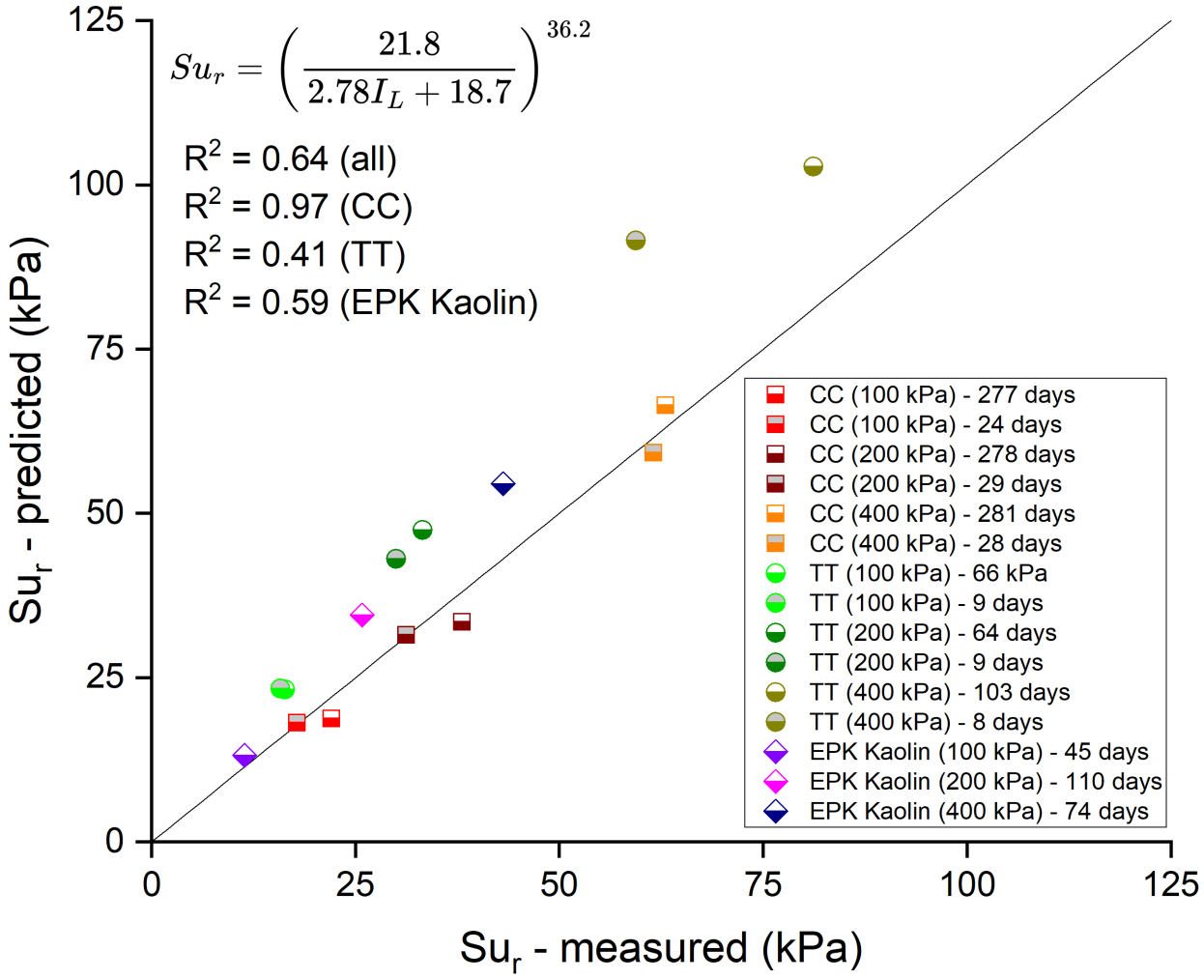

Figure 4.24. Comparison between measured and predicted Su_r of model footing samples

Methods of measuring and predicting values of q_{ult} are compared in Figure 4.25 with values presented in Table 4.16. The value of q_{ult} predicted from Equation 4.2 does not match the measured values of q_{ult} from both the 0.1B (R^2 = -0.26) and slope-tangent methods (R^2 = -0.22) when the entire dataset is considered, though the agreement between the model and the measured data varies significantly between samples. Similar to the behaviour observed in Figure 4.24, CC showed very good agreement with the model considering all methods of predicting and measuring q_{ult} (R^2 > 0.9). The measured q_{ult} of TT was not predicted by the model (R^2 < 0) (Figure 4.25[a,b]). Values of q_{ult} predicted from Equation 4.2 tend to be larger than the measured q_{ult}, which suggests that the prediction is not conservative, though a factor of safety of at least 2 would reduce the predicted q_{ult} to the measured q_{ult} for all samples, including the TT. There is also relatively

good agreement between q_{ult} predicted from Equation 2.3 and Equation 4.2 (Figure 4.25[c]). The average values of the percent difference between all methods of measuring and predicting q_{ult} are presented in Table 4.17.

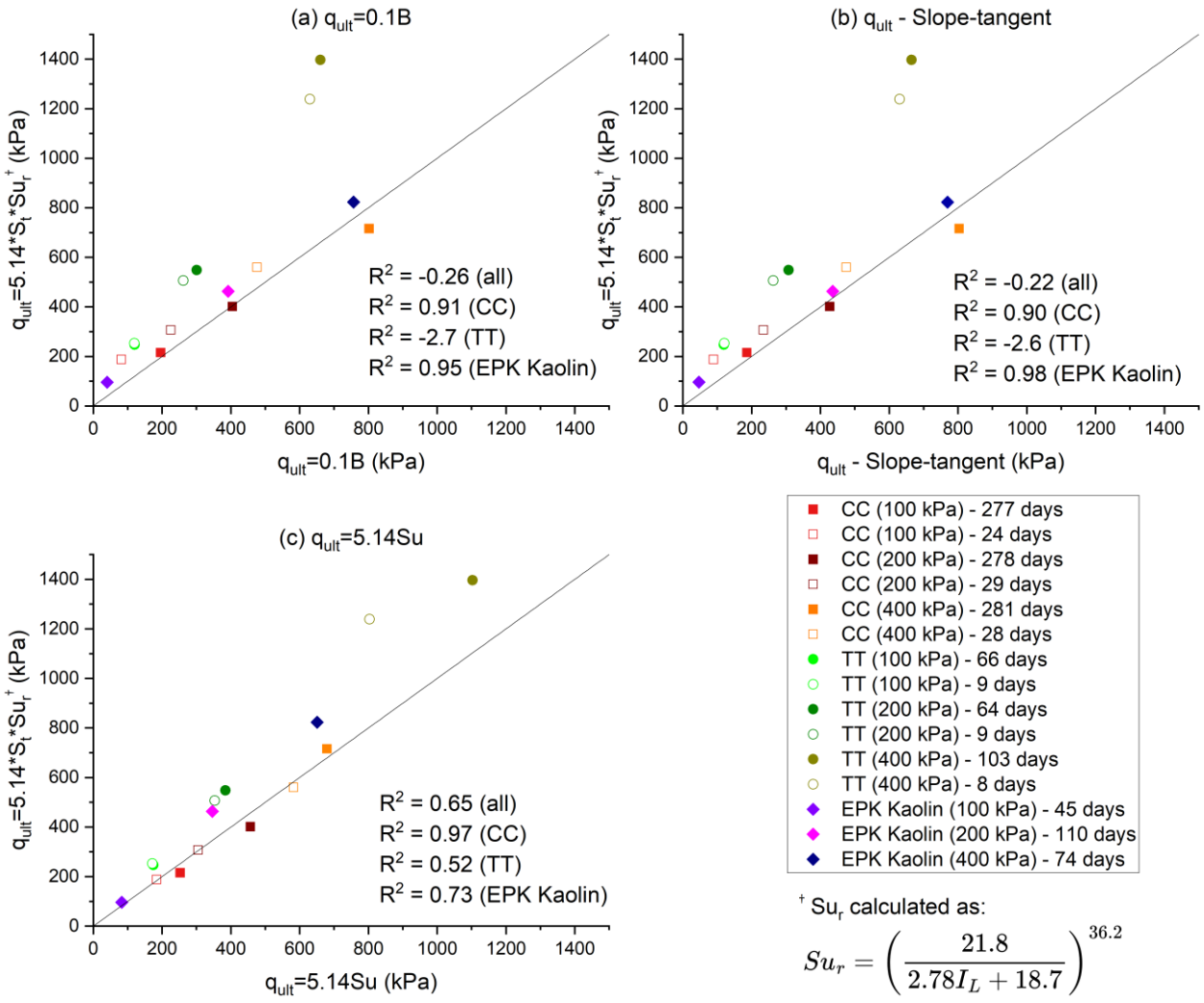

Figure 4.25. Comparison between q_{ult} predicted from I_L and S_t and 0.1B (a), slope-tangent (b), and 5.14*Su* (c) methods

Table 4.16. Measured and predicted q_{ult} (all methods) with S_t and I_L

Sample	S_t	I_L	q_{ult} (kPa)			
			5.14*St*Su_r[†]	5.14Su	0.1B	Slope-tangent
CC (100 kPa) - 277 days	2.2	0.5	215	252	196	186
CC (100 kPa) - 24 days	2.0	0.5	188	184	81.8	89.3
CC (200 kPa) - 278 days	2.3	0.4	402	457	404	427
CC (200 kPa) - 29 days	1.9	0.4	307	305	225	234
CC (400 kPa) - 281 days	2.1	0.3	716	679	802	803
CC (400 kPa) - 28 days	1.8	0.3	560	582	476	475
TT (100 kPa) - 66 days	2.1	0.5	247	174	120	119
TT (100 kPa) - 9 days	2.1	0.5	253	172	120	120
TT (200 kPa) - 64 days	2.2	0.3	548	385	301	308
TT (200 kPa) - 9 days	2.3	0.3	506	353	261	263
TT (400 kPa) - 103 days	2.6	0.2	1400	1103	660	665
TT (400 kPa) - 8 days	2.6	0.2	1240	804	630	631
EPK Kaolin (100 kPa) - 45 days	1.4	0.6	96.0	83.0	40.2	46.6
EPK Kaolin (200 kPa) - 110 days	2.6	0.4	463	346	392	436
EPK Kaolin (400 kPa) - 74 days	2.9	0.3	823	651	757	770

[†] Su_r calculated from I_L using Equation 4.1

Table 4.17. Average percent difference between measured and predicted q_{ult} (all methods)

	5.14*St*Su_r	5.14Su	0.1B	Slope-tangent
5.14*St*Su_r	-	21.1	43.6	41.7
5.14Su	21.1	-	31.9	30.9
0.1B	43.6	31.9	-	3.7
Slope-tangent	41.7	30.9	3.7	-

A plot (Figure 4.26) can be developed to relate I_L and q_{ult} based on Equation 4.2. Varying S_t produces a series of parallel lines. The predicted q_{ult} for all model footing samples is plotted on

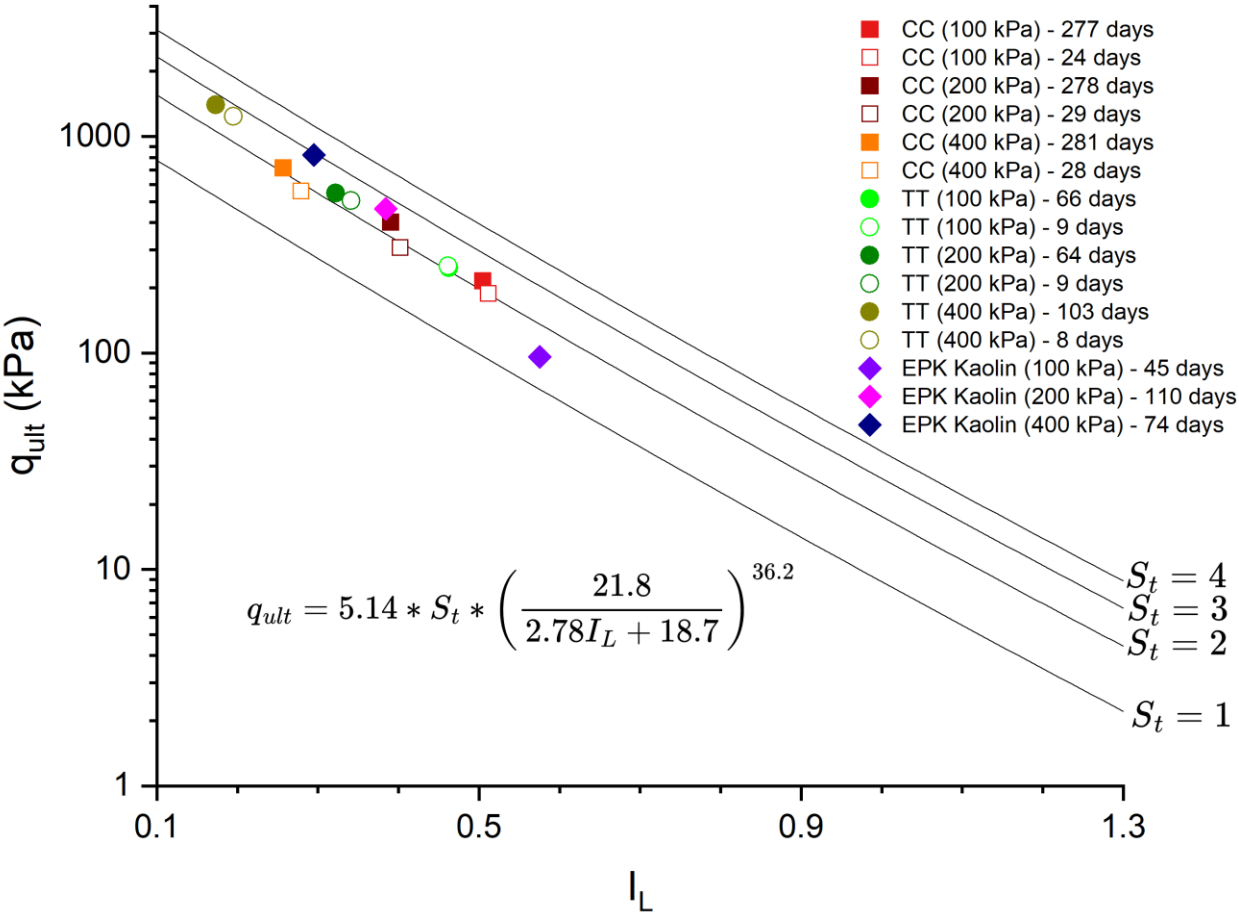

Figure 4.27 using the measured I_L and S_t.

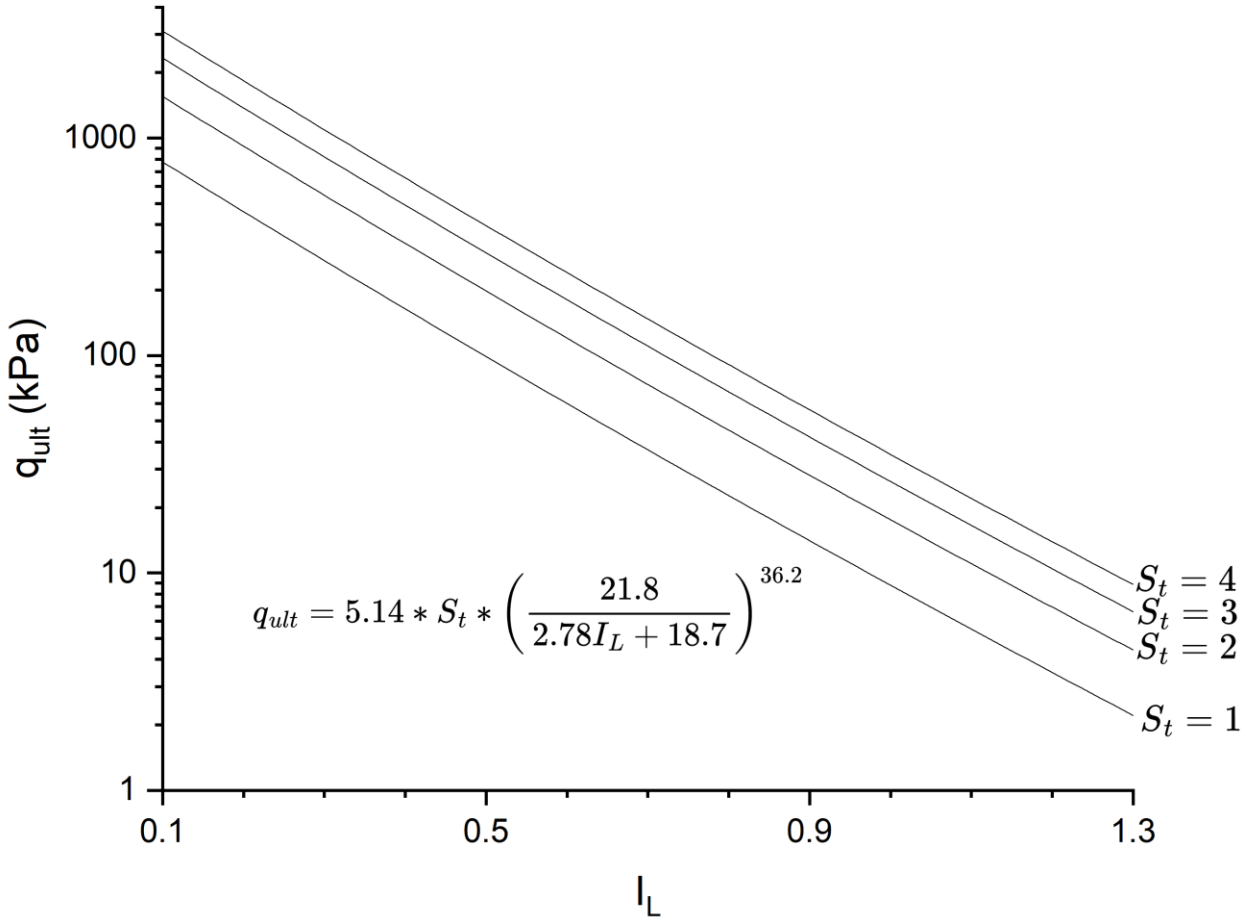

Figure 4.26. Prediction of q_{ult} from I_L and S_t

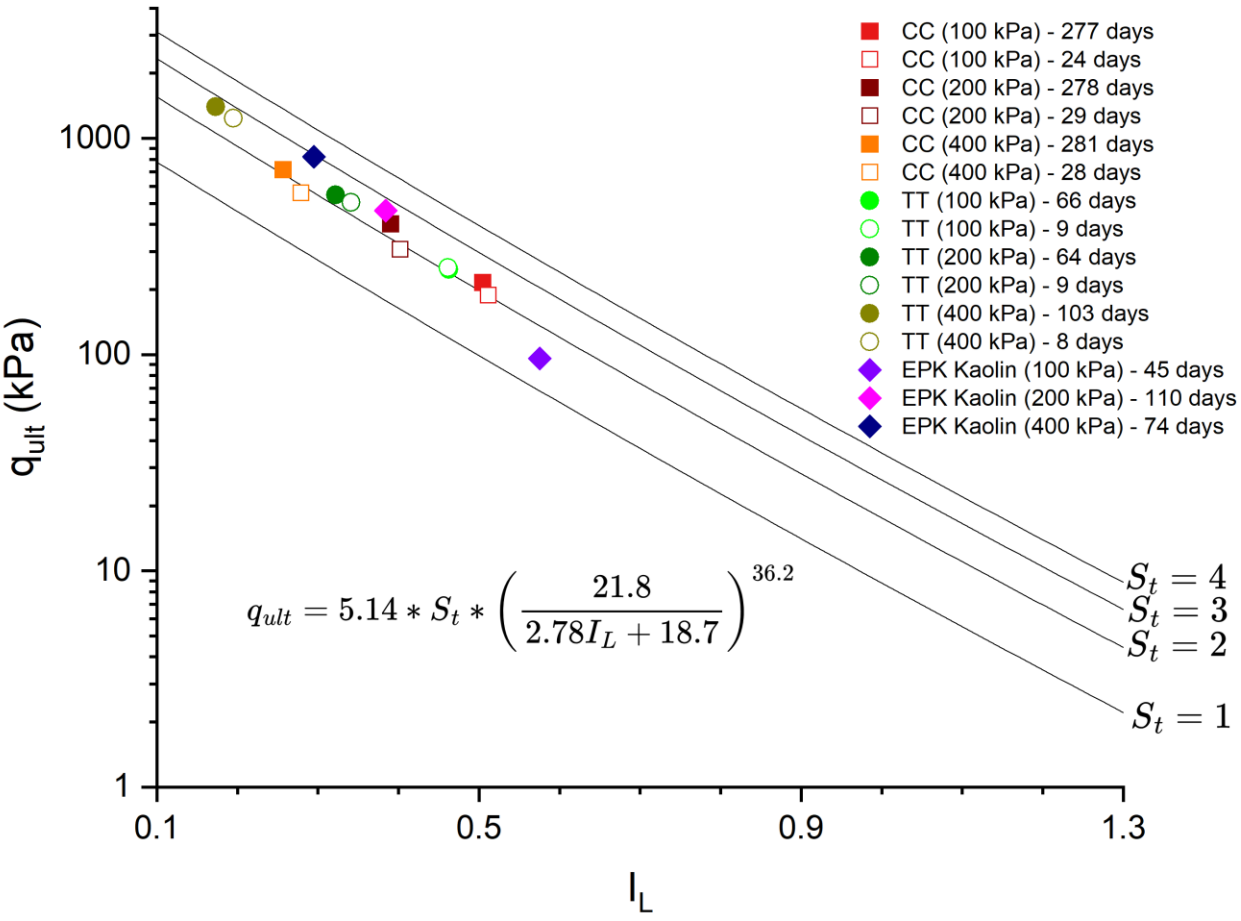

Figure 4.27. Prediction of q_{ult} from I_L and S_t for model footing results

Figure 4.26 provides a straightforward method to estimate q_{ult} from basic tailings properties. This could be used to determine the water content or I_L necessary to achieve a target capping strength. Examples of I_L needed to achieve the bearing capacity for different loads as calculated from Equation 4.2 (without a factor of safety) are presented in Table 4.18. This could also be coupled with consolidation models to assess the length of time needed to reach a specific strength value based on the I_L.

Table 4.18. I_L required for bearing pressure of various types of equipment

Load	Bearing pressure (kPa)†	I_L		
		S_t = 1	S_t = 2	S_t = 3
Foot traffic	50	0.6	0.8	0.9
Small dozer (Cat D6N LGP)	35	0.7	0.9	0.9
Medium dozer (Cat D9R)	115	0.5	0.6	0.7
Large dozer (Cat D11T)	160	0.4	0.5	0.6
Pickup truck (Ford F-150)	240	0.3	0.5	0.5
40-ton haul truck (Cat 740)	450	0.2	0.3	0.4
100-ton haul truck (Cat 777C)	750	0.1	0.2	0.3

† COSIA (2022)

This method would be most appropriate for long-term monitoring and the preliminary design of capped oil sands tailings deposits. This preliminary design would then be updated over time according to the observational method as the properties and behaviour are measured. In particular, the accuracy of this method depends on the accuracy of the Atterberg limits, which may very over time and throughout the deposit (e.g. changes in pore water chemistry, heterogeneity of tailings, etc.). This method was also developed on saturated, homogenous tailings. It was also shown in Table 4.16 that the value of q_{ult} calculated from Equation 4.2 is not conservative when compared to the measured q_{ult} from the model footing test. A factor of safety of 2-3 is proposed for bearing capacity based on the ratio of the measured and predicted strength, which is consistent with existing methods for predicting q_{ult} (COSIA 2022). This factor of safety is also sufficient to account for the possible difference between the predicted and measured strength at low I_L. It is suggested that a larger factor of safety within this range be adopted for lower values of I_L to account for increased scatter in the dataset in this region.

4.5 Summary

The overall results of the laboratory test program are summarized below:

- Preparation method, test procedure, and sample properties have an effect on the measured Atterberg limits. However, it is challenging to separate the effect of individual factors from the embedded uncertainty of the test.
- Air-drying the tailings from the w_L to the w_P is recommended as a standard preparation method for measuring the Atterberg limits as it best preserves the properties of the tailings and is straightforward to perform.
- Results determined using the fall cone and Casagrande cup methods for measuring w_L appear to reflect operator bias. It is proposed that the fall cone method is more accurate and precise. However, results determined using both methods are similar.
- When considering as-received tailings samples, w_L generally increases and w_P generally decreases as the fines content increases. Drying and rewetting with deionized water also increased w_L and decreased w_P. Determining the effect of bitumen removal is complicated by other changes in properties (reduction in fines, oven-drying, and/or reduction in ions) that occur as a result of the bitumen extraction process through either the Dean Stark or cold extraction method.
- A new relationship (Equation 4.1) is proposed to predict Su_r of oil sands tailings for values of I_L between 0.1 and 1.3. A factor of safety of at least 2 should be applied to account for the observed scatter of the dataset at low I_L.
- The effect of drying and rewetting is to slightly increase Su_r at the same water content, though this effect tends to decrease as the water content approaches w_P. The effect of the Dean Stark and the cold extraction method was to increase Su_r at the same water content.
- Using Atterberg limits that do not match the preparation method to calculate I_L in Equation 4.1 impacts the prediction of Su_r. It is suggested that Atterberg limits corresponding to the material and the preparation method should be used to calculate I_L, and that sensitivity testing may be appropriate where there is uncertainty.

- In model footing tests, the effect of decreasing $I_{L:}$ (and therefore reducing water content) was to increase q_{ult}. The effect of aging on CC was also observed to increase $q_{ult.}$
- The 0.1B and slope-tangent methods produced near-identical results for determining q_{ult} from measured plots of stress and displacement.
- Predictions of q_{ult} from Su generally over-predicted q_{ult}, though this may be considered acceptable when the typical factor of safety of 2-3 is applied (COSIA 2022).
- A method was proposed to calculate q_{ult} from I_L and S_t (Equation 4.2) by combining Equation 4.1 and Equation 2.3. This method provided a reasonably good prediction of q_{ult} of model footing samples, though was not conservative. A factor of safety of 2-3 for this method is proposed, which is consistent with existing methods for predicting q_{ult} (COSIA 2022). It is suggested that a larger factor of safety within this range be adopted for lower values of I_L to account for increased scatter in the model dataset in this region.

5 Conclusions and recommendations

5.1 Conclusions

This research program involved a review of existing data and a laboratory test program to investigate the Atterberg limits, strength, and bearing capacity of oil sands tailings with the goal of improving reclamation outcomes of capped terrestrial tailings deposits. The laboratory test program was performed on three types of oil sands tailings (centrifuge cake, CC; untreated fluid tailings, FT; and thickened tailings, TT) and a commercially available clay (EPK Kaolin). The conclusions of this study are summarized under their relevant objective as defined in Chapter 1:

1. Investigate the effect of material properties, preparation method, and test procedure on the Atterberg limits of oil sands tailings through a laboratory test program and a review of existing published data.

- Based on the results of the literature review and laboratory test program, material properties, preparation method, and test procedure have an effect on the measured Atterberg limits of oil sands tailings. However, it is challenging to determine the effect of individual factors compared to the intrinsic variability of the test (as quantified using data from literature).
- Air-drying the tailings from above the w_L to the w_P is proposed to be the preferred preparation method for measuring the Atterberg limits. This method preserves the properties of the as-received tailings and is straightforward to perform, facilitating consistency in measurements between different test operators.
- The fall cone is proposed as a preferred method to determine w_L due to its accuracy (ability for the operator to judge if measurements are erroneously high or low during the test) and precision (operator can assess the degree of scatter). However, results determined using the Casagrande cup are similar.
- In general, w_L increases and w_P decreases as the fines content increases for as-received tailings samples. Drying and rewetting with deionized water also increased w_L and decreased w_P. Determining the effect of bitumen removal by the Dean Stark or cold extraction method is complicated by other changes in

properties (reduction in fines, oven-drying, and/or reduction in ions) that also occur as a result of these processes.

2. Develop a mathematical correlation between Su_r and I_L for oil sands tailings between the liquid limit (w_L) and plastic limit (w_P) using laboratory test data and compare this to the relationship developed by Locat and Demers (1988).

- A new relationship (Equation 4.1) is proposed for predicting Su_r for I_L for I_L between 0.1 and 1.3. This equation was developed by using the fall cone to measure Su_r of as-received (air-dried and rewetted) and amended (Dean Stark and cold extraction) tailings and EPK Kaolin at different water contents.

Equation 4.1

$$Su_r = \left(\frac{21.8}{2.78I_L + 18.7}\right)^{36.2}$$

- The proposed relationship better fits the laboratory test data compared to the Locat and Demers (1988) relationship. A factor of safety of at least 2 should be applied to predictions to account for scatter in the Su_r at low I_L. This relationship was also observed to provide a good fit for some literature data.
- The effect of drying and rewetting is to slightly increase Su_r at the same water content, though this effect tends to decrease as the water content approaches w_P. The effect of the Dean Stark and the cold extraction method was to increase Su_r at the same water content. However, all samples demonstrated a similar behaviour when the water content was normalized as I_L using Atterberg limits that matched the preparation method (air-dried, rewetted, Dean Stark, or cold extraction).
- Using Atterberg limits that do not match the preparation method to calculate I_L in Equation 4.1 impacts the prediction of Su_r. It is suggested that Atterberg limits corresponding to the material and the preparation method should be used to calculate I_L, and that sensitivity testing may be appropriate where there is uncertainty.

3. *Evaluate predictions of q_{ult} from Su at the benchtop scale and compare laboratory results to predictions of q_{ult} from S_t and Su_r (using the relationship developed in objective 2).*

- The effect of decreasing I_L (and therefore reducing water content) of the sample was observed to increase q_{ult} for benchtop model footing tests performed on as-received oil sands tailings (CC and TT) and EPK Kaolin. The effect of aging on CC was also observed to increase q_{ult}.
- The 0.1B and slope-tangent methods produced near-identical results for determining q_{ult} from measured plots of stress and displacement.
- Predictions of q_{ult} from *Su* generally over-predicted q_{ult} based on laboratory measurements of q_{ult} and *Su*, though this may be considered acceptable when the typical factor of safety of 2-3 is applied (COSIA 2022).
- A method was proposed to calculate q_{ult} from I_L and S_t (Equation 4.2) by combining Equation 4.1 and Equation 2.3. This method provided a reasonably good prediction of q_{ult} of model footing samples, though was not conservative. A factor of safety of 2-3 for this method is proposed, which is consistent with existing methods for predicting q_{ult} (COSIA 2022). It is suggested that a larger factor of safety within this range be adopted for lower values of I_L to account for increased scatter in the model dataset in this region.

Equation 4.2

$$q_{ult} = 5.14 * S_t * Su_r = 5.14 * S_t * \left(\frac{21.8}{2.78I_L + 18.7}\right)^{36.2}$$

- The samples of TT were observed to behave differently relative to the other samples when comparing the measured q_{ult} to the predicted q_{ult} (Equation 2.3 and Equation 4.2). Additionally, Atterberg limits and Su_r indicated that TT was significantly more sensitive to the preparation method relative to the other tailings samples. Taken together, it is proposed that the low fines content of TT relative to the other samples may be a different pattern of behaviour.

5.2 Recommendations for future research

- The effect of sample preparation methods on the measured Atterberg limits should be further investigated. Conclusions drawn from this study were limited by the number of data points measured. Future studies should aim to produce multiple data points from a single method (similar to Gidley and Moore, 2013) and use statistical methods of analysis.
- Collecting previously published Atterberg limits and $Su_r - I_L$ data (Chapter 1) and performing statistical analysis on duplicate Atterberg measurements (Chapter 4) provided useful context for interpreting laboratory results. It is recommended that similar methods be used in a review of other tailings properties, and that characterization measurements should published whenever possible to facilitate this.
- The air-dried preparation method was recommended as a general method for measuring the Atterberg limits of oil sands tailings. However, this method is only possible if the tailings are initially above the w_L. Methods for measuring the Atterberg limits of tailings below the w_L (e.g. rewetting with process water) should be investigated. This will be necessary for the long-term monitoring of in-situ tailings as the water content decreases.
- Equation 4.1 should be further tested using laboratory and field data to assess the performance of the model predictions. This should include investigating the behaviour of other low fines content tailings streams to further evaluate the behaviour of TT. Validation is currently limited by the few $Su_r - I_L$ datasets publicly available.
- Similarly, Equation 4.2 should be validated using laboratory and field data. In particular, this method should be tested on unsaturated, heterogeneous deposits.

References

Abusaid, A., and Pollock, G. 2011. An Update to the Construction of the Suncor Oil Sands Tailings Pond 5 Cover. *In* Proceedings of the 15th International Conference on Tailings and Mine Waste. Vancouver, British Columbia, Canada.

Alberta Energy Regulator (AER). 2017. Directive 085: Fluid Tailings Management for Oil Sands Mining Projects. Available from: https://static.aer.ca/prd/documents/directives/Directive085.pdf. Accessed on May 26, 2022.

Alberta Energy Regulator (AER). 2020a. Oil Sands Mining [online]. Available from: https://www.aer.ca/providing-information/by-topic/oil-sands/oil-sands-mining. Accessed on November 13, 2023.

Alberta Energy Regulator (AER). 2020b. Oil Sands [online]. Available from https://www.aer.ca/providing-information/by-topic/oil-sands. Accessed on November 13, 2023.

Alberta Energy Regulator (AER). 2023. State of Fluid Tailings Management for Mineable Oil Sands, 2022. Available from: https://static.aer.ca/prd/documents/reports/State-Fluid-Tailings-Management-Mineable-OilSands.pdf. Accessed January 11, 2024.

Alberta Government. 2015. Lower Athabasca Region - Tailings Management Framework for the Mineable Athabasca Oil Sands.

Anstey, D., and Guang, R. 2017. Relationship between in-line polymer dose and tailings index properties. *In* Proceedings of the 21st International Conference on Tailings and Mine Waste. University of Alberta, Banff, Alberta, Canada.

ASTM. 2014. ASTM D854 − 14: Standard Test Methods for Specific Gravity of Soil Solids by Water Pycnometer. ASTM International, West Conshohocken, Pennsylvania, United States.

ASTM. 2016. ASTM D6836-16: Standard Test Methods for Determination of the Soil Water Characteristic Curve for Desorption Using Hanging Column, Pressure Extractor, Chilled Mirror Hygrometer, or Centrifuge. ASTM International, West Conshohocken, Pennsylvania, United States.

ASTM. 2017. ASTM D4318-17: Standard Test Methods for Liquid Limit, Plastic Limit, and Plasticity Index of Soils. ASTM International, West Conshohocken, Pennsylvania, United States.

ASTM. 2021. ASTM D7928-21: Standard Test Method for Particle-Size Distribution (Gradation) of Fine-Grained Soils Using the Sedimentation (Hydrometer) Analysis. ASTM International, West Conshohocken, Pennsylvania, United States.

Atterberg, A. 1911. The behavior of clays with water, their limits of plasticity and their degrees of plasticity [in Swedish]. Kungliga Lantbruksakademiens Handlingar och Tidskrift, **50**(2).

Bajwa, T.M. 2015. Microstructure and macroscopic behaviour of polymer amended oil sands mature fine tailings. PhD Thesis, Carleton University, Ottawa, Ontario, Canada.

Banas, L.C. 1991. Thixotropic behaviour of oil sands tailings sludge. MSc Thesis, University of Alberta, Edmonton, Alberta, Canada.

Basma, A., Alhomoud, A., and Altabari, E. 1994. Effects of methods of drying on the engineering behavior of clays. Applied Clay Science, **9**(3): 151–164. doi:10.1016/0169-1317(94)90017-5.

Beier, N., Wilson, W., Dunmola, A., and Sego, D. 2013a. Impact of flocculation-based dewatering on the shear strength of oil sands fine tailings. Canadian Geotechnical Journal, **50**(9): 1001–1007. doi:10.1139/cgj-2012-0262.

BGC Engineering Inc. 2010. Oil Sands Tailings Technology Review. OSRIN Report, Oil Sands Research and Information Network, University of Alberta, School of Energy and the Environment, Edmonton, Alberta, Canada. Available from: https://era.library.ualberta.ca/items/d54a3e22-cf15-4c3b-baeb-2ee10578a259/view/ad8166dd-861d-4162-afac-949a5ac82582/Tailings-20Technology-20Review-20--202010-2007-2019.pdf. Accessed May 30, 2022.

Bureau de normalisation du Québec (BNQ). 2019. CAN/BNQ 2501-090: Determination of Liquid Limit by the Casagrande Apparatus and Determination of Plastic Limit. BNQ, Québec, Canada.

Bureau de normalisation du Québec (BNQ). 2023a. CAN/BNQ 2501-092: Determination of Liquid Limit by a Fall Cone Penetrometer and Determination of Plastic Limit. BNQ, Québec, Canada.

Bureau de normalisation du Québec (BNQ). 2023b. CAN/BNQ 2501-110: Determination of Undrained Shear Strength and Sensitivity of Cohesive Soils Using a Fall Cone Penetrometer. BNQ, Québec, Canada.

Bouazza, A., Jefferis, S., and Vangpaisal, T. 2007. Investigation of the effects and degree of calcium exchange on the Atterberg limits and swelling of geosynthetic clay liners when subjected to wet–dry cycles. Geotextiles and Geomembranes, **25**(3): 170–185. doi:10.1016/j.geotexmem.2006.11.001.

British Standards Institution (BSI). 2022. BS 1377-2:2022: Methods of test for soils for civil engineering purposes - Classification tests and determination of geotechnical properties. BSI, United Kingdom.

Casagrande, A. 1932. Research on the Atterberg limits of soils. Public Roads, **18**(8): 121–136.

Cumulative Environmental Management Association (CEMA). 2012. End Pit Lakes Guidance Document. CEMA, Fort McMurray, Alberta, Canada. Available from: https://www.cclmportal.ca/sites/default/files/2022-01/CEMA%20EPL%20Guide.pdf. Accessed May 12, 2024.

Cerato, A.B., and Lutenegger, A.J. 2007. Scale Effects of Shallow Foundation Bearing Capacity on Granular Material. Journal of Geotechnical and Geoenvironmental Engineering, **133**(10): 1192–1202. doi:10.1061/(ASCE)1090-0241(2007)133:10(1192).

Chalaturnyk, R.J., Don Scott, J., and Özüm, B. 2002. Management of oil sands tailings. Petroleum Science and Technology, **20**(9–10): 1025–1046. doi:10.1081/LFT-120003695.

Clark, K.A., and Pasternack, D.S. 1932. Hot Water Separation of Bitumen from Alberta Bituminous Sand. Industrial & Engineering Chemistry, **24**(12): 1410–1416. doi:10.1021/ie50276a016.

Claveau-Mallet, D., Duhaime, F., and Chapuis, R.P. 2010. Characterisation of Champlain saline clay from Lachenaie using the Swedish fall cone. *In* Proceedings of the 63rd Canadian Geotechnical Conference. Canadian Geotechnical Society, Calgary, Alberta, Canada. pp. 134–141.

Canada's Oil Sands Innovation Alliance (COSIA). 2012. Technical Guide for Fluid Tailings Management. COSIA and Oil Sands Tailings Consortium, Calgary, Alberta, Canada. Available from: https://pathwaysalliance.ca/research/technical-guide-for-fluid-f-ine-tailings-management/. Accessed May 30, 2022.

Canada's Oil Sands Innovation Alliance (COSIA). 2014a. Guidelines for Performance Management of Oil Sands Fluid Fine Tailings Deposits to Meet Closure Commitments. COSIA, Calgary, Alberta, Canada. Available from: https://pathwaysalliance.ca/research/guidelines-for-performance-management-of-oil-sands-fluid-fine-tailings-deposits-fo-meet-closure-commitments/. Accessed September 30, 2022.

Canada's Oil Sands Innovation Alliance (COSIA). 2014b. Unified Fines Method for minus 44 micron material and for Particle Size Distribution. COSIA, Calgary, Alberta, Canada.

Canada's Oil Sands Innovation Alliance (COSIA). 2015. Measuring Undrained Shear Strength of Oil Sands Tailings Deposits. COSIA Deposit Characterization Committee, Calgary, Alberta, Canada. Available from: https://pathwaysalliance.ca/research/measuring-undrained-shear-strength-of-oil-sands-tailings-deposits/. Accessed September 30, 2022.

Canada's Oil Sands Innovation Alliance (COSIA). 2022. Deep Deposit Design Guide for Oil Sands Tailings. COSIA, Calgary, Alberta, Canada. Available from: https://pathwaysalliance.ca/research/measuring-undrained-shear-strength-of-oil-sands-tailings-deposits/. Accessed July 7, 2022.

Cossey, H.L., Batycky, A.E., Kaminsky, H., and Ulrich, A.C. 2021. Geochemical Stability of Oil Sands Tailings in Mine Closure Landforms. Minerals, **11**(8): 830. doi:10.3390/min11080830.

Darbari, Z., Jaradat, K.A., and Abdelaziz, S.L. 2017. Heating–freezing effects on the pore size distribution of a kaolinite clay. Environmental Earth Sciences, **76**(20): 713. doi:10.1007/s12665-017-7069-8.

Edgar Minerals Inc. 2018. Safety Data Sheet (EPK Kaolin). Available from: https://www.theceramicshop.com/product/122/epk-kaolin/. Accessed February 7, 2024.

Elias, J.A. 2019. Measurement of Floc Size and the Influence of Size Distribution on Geotechnical Properties of Oil Sands Fluid Fine Tailings, MSc Thesis, University of Alberta, Edmonton, Alberta, Canada.

Feng, T.-W. 2001. A linear log d - log w model for the determination of consistency limits of soils. Canadian Geotechnical Journal, **38**(6): 1335–1342. doi:10.1139/t01-061.

Fredlund, D., Stone, J., Stianson, J., and Sedgwick, A. 2011. Obtaining unsaturated soil properties for high volume change oil sands material. *In* Proceedings of the 5th Asia Pacific Conference on Unsaturated Soils. Pattaya, Thailand. pp. 415–420.

Fredlund, D.G., Rahardjo, H., and Fredlund, M.D. 2012. Unsaturated Soil Mechanics in Engineering Practice. John Wiley & Sons, Inc., Hoboken, New Jersey, United States.

Fredlund, M. 1999. The role of unsaturated soil property functions in the practice of unsaturated soil mechanics. PhD Thesis, University of Saskatchewan, Saskatoon, Saskatchewan, Canada.

Fredlund, M., Pham, N., Donaldson, M., and Ansah-Sam, M. 2018. Preliminary study for sand capping of treated tailings. *In* Proceedings of the 6th International Oil Sands Tailings Conference. University of Alberta, Banff, Alberta, Canada.

Garcia Martinez, M.F., Tonni, L., Gottardi, G., and Rocchi, I. 2016. Influence of penetration rate on CPTU measurements in saturated silty soils. *In* Proceedings of the 5th International Conference on Geotechnical and Geophysical Site Characterisation. Australian Geomechanics Society, Gold Coast, Queensland. pp. 473–478.

Gidley, I., and Moore, T. 2013. Impact of Test Methodology on the Atterberg Limits of Mature Fine Tailings [slide deck]. *Presented at* CONRAD Oil Sands Clay Conference February 20-21, 2013. Edmonton, Alberta, Canada.

Government of Alberta. 2023. Oil sands facts and statistics [online]. Available from https://www.alberta.ca/oil-sands-facts-and-statistics.aspx. Accessed 12 November 12, 2023.

Hang, P.T., and Brindley, G.W. 1970. Methylene Blue Absorption by Clay Minerals. Determination of Surface Areas and Cation Exchange Capacities. Clays and Clay Minerals, **18**: 203–212.

Hansbo, S. 1957. A new approach to the determination of the shear strength of clay by the fall-cone test. Swedish Geotechnical Institute Proceedings, **14**: 5–47.

Innocent-Bernard, T. 2013. Evaporation, cracking, and salinity in a thickened oil sands tailings. MASc Thesis, Carleton University, Ottawa, Ontario, Canada.

Jakubick, A.T., and McKenna, G. 2001. Stabilisation of Soft Tailings: Practice and Experience. *In* Proceedings of the 8th International Conference on Radioactive Waste Management and Environmental Remediation. American Society of Mechanical Engineers, Bruges, Belgium. pp. 1465–1471.

Jakubick, A.T., McKenna, G., and Robertson, A.M. 2003. Stabilisation of tailings deposits: International experience. *In* Proceedings of Mining and the Environment, volume III. Sudbury, Ontario, Canada.

Jeeravipoolvarn, S. 2005. Compression behaviour of thixotropic oil sands tailings. MSc Thesis, University of Alberta, Edmonton, Alberta, Canada.

Jeeravipoolvarn, S. 2010. Geotechnical Behavior of In-Line Thickened Oil Sands Tailings. PhD Thesis, University of Alberta, Edmonton, Alberta, Canada.

Jeeravipoolvarn, S., Scott, J.D., Donahue, R., and Ozum, B. 2008. Characterization of oil sands thickened tailings. *In* Proceedings of the 1st International Oil Sands Tailings Conference. University of Alberta, Edmonton, Alberta, Canada. pp. 132–142.

Jeeravipoolvarn, S., Wu, E.J., Proskin, S.A., Junaid, A., and Freeman, G. 2020. Field water release and consolidation performance of XUR Treated Fluid Fine Tailings. *In* Proceedings of the 26th International Conference on Tailings and Mine Waste. Colorado State University, Virtual. pp. 103–112.

Kabwe, L., Wilson, G.W., Beier, N.A., and Barsi, D. 2021. Effect of sand and flyash on unsaturated soil properties and drying rate of oil sands tailings. *In* Proceedings of the 25th International Conference on Tailings and Mine Waste. University of Alberta, Edmonton, Alberta, Canada. pp. 892–903.

Kabwe, L., Wilson, G.W., and Donahue, R. 2013. Determination of geotechnical properties of in-line flocculated fine fluid tailings for oil sands reclamation. *In* Proceedings of the 17th International Conference on Tailings and Mine Waste. University of Alberta, Banff, Alberta, Canada.

Kabwe, L.K., Abdulnabi, A., Wilson, G.W., Beier, N.A., and Scott, J.D. 2019. Geotechnical and unsaturated properties of metal mines and oil sands tailings. *In* Proceedings of the 23rd International Conference on Tailings and Mine Waste. Edited by J. Goodwill, D. van Zyl, and M. Davies. University of British Columbia, Vancouver, British Columbia, Canada. pp. 1053–1066.

Kabwe, L., Wilson, G., Barsi, D., and Beier, N. 2023a. Consolidation and unsaturated properties of in-line flocculated fluid fine tailings and centrifuged tailings from oil sands mines. *In* In Proceedings of the 25th International Conference on Paste, Thickened, and Filtered Tailings. University of Alberta and Australian Centre for Geomechanics, Banff, Alberta, Canada. pp. 481–494.

Kabwe, L.K., Wilson, G.W., Beier, N.A., and Barsi, D. 2023b. Application of Tempe Cell to Measure Soil Water Characteristic Curve along with Geotechnical Properties of Oil Sands Tailings. Geosciences, **13**(2): 36. doi:10.3390/geosciences13020036.

Kaminsky, H. 2008. Characterization of an Athabasca oil sand ore and process streams. PhD Thesis, University of Alberta, Edmonton, Alberta, Canada.

Kaminsky, H. 2014. Demystifying the methylene blue index. *In* Proceedings of the 4th International Oil Sands Tailings Conference. University of Alberta, Lake Louise, Alberta, Canada.

Kaminsky, H., Etsell, T., Ivey, D.G., and Omotoso, O. 2006. Fundamental particle size of clay minerals in Athabasca oil sands tailings. Clay Science, **12**(Supplement 2): 217–222. doi:10.11362/jcssjclayscience1960.12.Supplement2_217.

Kaminsky, H., and Omotoso, O. 2016. Variability in Fluid Fine Tailings. *In* Proceedings of the 5th International Oil Sands Tailings Conference. University of Alberta, Lake Louise, Alberta, Canada. pp. 178-183.

Liu, Q.B., Lehane, B.M., and Tian, Y. 2020. Bearing Capacity and Stiffness of Embedded Circular Footings on Stiff-Over-Soft Clay. Journal of Geotechnical and Geoenvironmental Engineering, **146**(11): 06020020. doi:10.1061/(ASCE)GT.1943-5606.0002393.

Liu, T.K., and Thornburn, T.M. 1964. Study of the reproducibility of Atterberg Limits. Highway Research Board of the Division of the Division of Engineering and Industrial Research, Washington DC, United States. Available from: https://onlinepubs.trb.org/Onlinepubs/hrr/1964/63/63-003.pdf. Accessed April 8, 2023.

Locat, J., and Demers, D. 1988. Viscosity, yield stress, remolded strength, and liquidity index relationships for sensitive clays. Canadian Geotechnical Journal, **25**: 799–806. doi:10.1139/t88-088.

MatWeb. n.d. Imerys EPK Kaolin. Available from: https://www.matweb.com/search/DataSheet.aspx?MatGUID=ffb851eaeaad4a7dbba94037a46f4ecd. Accessed June 25, 2024.

Masliyah, J., Zhou, Z., Xu, Z., Czarnecki, J., and Hamza, H. 2004. Understanding Water-Based Bitumen Extraction from Athabasca Oil Sands. Canadian Journal of Chemical Engineering, **82**: 628–684.

McKenna, G., Mooder, B., Burton, B., and Jamieson, A. 2016. Shear strength and density of oil sands fine tailings for reclamation to a boreal forest landscape. *In* Proceedings of the 5th International Oil Sands Tailings Conference. University of Alberta, Lake Louise, Alberta, Canada.

Mikula, R. 2018. The role of clays. *In* Introduction to Oil Sands Clays. Edited by O. Omotoso and D. Hockley. The Clay Minerals Society. pp. 129–181

Mikula, R., and Omotoso, O. 2006. Role of Clays in Controlling Tailings Behaviour in Oil Sands Processing. Clay Science, **12**(2): 177–182. doi:10.11362/jcssjclayscience1960.12.Supplement2_177.

Miller, W.G., Scott, J.D., and Sego, D.C. 2009. Flume deposition modeling of caustic and noncaustic oil sand tailings. Canadian Geotechnical Journal, **46**(6): 679–693. doi:10.1139/T09-014.

Miller, W.G., Scott, J.D., and Sego, D.C. 2010. Influence of the extraction process on the characteristics of oil sands fine tailings. CIM Journal, **1**(2): 93–112.

Mitchell, J.K., and Soga, K. 2005. Fundamentals of Soil Behavior. 3rd ed. John Wiley & Sons, Inc., Hoboken, New Jersey, United States.

Mossop, G.D. 1980. Geology of the Athabasca Oil Sands. Science, **207**: 145–152. doi:10.1126/science.207.4427.145.

Park, H., Lee, S.R., and Jee, S.H. 2010. Bearing Capacity of Surface Footing on Soft Clay Underlying Stiff Nonhomogeneous Desiccated Crust. International Journal of Offshore and Polar Engineering, **20**(3): 224-232.

Pollock, G., Liu, X., McRoberts, E., Williams, K., Wells, P.S., and Fournier, J. 2010. *In* Proceedings of the 14th International Conference on Tailings and Mine Waste. Suncor oil sands tailings pond capping project. Colorado State University, Fort Collins, Colorado, USA. pp. 367–379.

Randolph, M. 2004. Characterisation of soft sediments for off-shore applications. *In* Proceedings of the 2nd International Conference of geotechnical and Geophysical Site Characterization. Millpress, Porto, Portugal. pp. 209–232.

Rozina, E. 2013. Bearing Capacity of Multilayer-deposited In-line Flocculated Oil Sands Tailings. MASc Thesis, Carleton University, Ottawa, Ontario, Canada.

Salam, M.A. 2020. Effects of Polymers on short-and long-term dewatering of oil sands tailings. PhD Thesis, Carleton University, Ottawa, Ontario, Canada.

Scott, J.D., Dusseault, M.B., and David Carrier, W. 1985. Behaviour of the clay/bitumen/water sludge system from oil sands extraction plants. Applied Clay Science, **1**(1–2): 207–218. doi:10.1016/0169-1317(85)90574-5.

Scott, J.D., Kabwe, L.K., Wilson, G.W., Sorta, A., and Jeeravipoolvarn, S. 2013. Properties which affect the consolidation behaviour of mature fine tailings. *In* Proceedings of the 17th International Conference on Tailings and Mine Waste. University of Alberta, Banff, Alberta, Canada.

Seed, H.B., Woodward, R.J., and Lundgren, R. 1964. Fundamental Aspects of the Atterberg Limits. Journal of the Soil Mechanics and Foundations Division, **90**(6): 75–106. doi:10.1061/JSFEAQ.0000685.

Sethi, A. 1995. Methylene Blue Test for Clay Activity Determination in Fine Tails. MRRT Procedures.

Sharma, B., and Bora, P.K. 2003. Plastic Limit, Liquid Limit and Undrained Shear Strength of Soil—Reappraisal. Journal of Geotechnical and Geoenvironmental Engineering, **129**(8): 774–777. doi:10.1061/(ASCE)1090-0241(2003)129:8(774).

Shimobe, S., and Spagnoli, G. 2020. Relationships between undrained shear strength, liquidity index, and water content ratio of clays. Bulletin of Engineering Geology and the Environment, **79**(9): 4817–4828. doi:10.1007/s10064-020-01844-5.

Skempton, A.W., and Northey, R.D. 1952. The Sensitivity of Clays. Géotechnique, **3**(1): 30–53. doi:10.1680/geot.1952.3.1.30.

Sobkowicz, J.C., and Morgenstern, N.R. 2009. A geotechnical perspective on oil sands tailings. *In* Proceedings of the 13th International Conference on Tailings and Mine Waste. University of Alberta, Banff, Alberta, Canada. pp. xvii–xli.

Sobkowicz, J.C., and Morgenstern, N.R. 2010. Reclamation and closure of an oil sand tailings facility. *In* Proceedings of the 2nd International Oil Sands Tailings Conference. University of Alberta, Edmonton, Alberta, Canada. pp. 269–276.

Sorta, A.R. 2015. Centrifugal modelling of oil sands tailings consolidation. PhD Thesis, University of Alberta, Edmonton, Alberta, Canada.

Tang, J. 1997. Fundamental behaviour of composite tailings. MSc Thesis, University of Alberta, Edmonton, Alberta, Canada.

Tate, M., Leikam, J., Fox, J., and Romaniuk. 2017. Use of calcium hydroxide as a coagulant to improve oil sands tailings treatment. *In* Proceedings of the 21st International Conference on Tailings and Mine Waste. University of Alberta, Banff, Alberta, Canada.

Terzaghi, K. 1925. Simplified soil tests for subgrades and their physical significance. Public Roads, October.

Terzaghi, K., Peck, R.B., and Gholamreza, M. 1996. Soil Mechanics in Engineering Practice. 3rd ed. John Wiley & Sons, Inc.

Vietti, A. 2018. Clay-water interactions. *In* Introduction to Oil Sands Clays. *Edited by* D. Hockley and O. Omotoso. The Clay Minerals Society. pp. 61–74.

Wang, C.X., and Carter, J.P. 2002. Deep Penetration of Strip and Circular Footings into Layered Clays. International Journal of Geomechanics, **2**(2): 205–232. doi:10.1061/(ASCE)1532-3641(2002)2:2(205).

Wells, P.S., Caldwell, J., and Fournier, J. 2010. Suncor Pond 5 coke cap – The story of its conception, testing and advance to full-scale construction. *In* Proceedings of the 14th Annual Conference on Tailings and Mine Waste. Colorado State University, Fort Collins, Colorado, USA.

Wells, P.S., and Kaminsky, H. 2015. Slurry to soil clay behaviour model - using methylene blue to cross the process/geotechnical engineering divide. *In* Proceedings of the 19th International Conference on Tailings and Mine Waste. University of British Columbia, Vancouver, British Columbia, Canada. pp. 481-489.

Wijermars, E.A.M. 2011. Sedimentation of Oil Sands Tailings. BSc Thesis, TU Delft, Delft, Netherlands.

Williams, D.J. 2015. Chapter 2: Placing Soil Covers on Soft Mine Tailings. *In* Compaction, Grouting, and Geosynthetics. Ground Improvement Case Histories. *Edited by* B. Indraratna, J. Chu, and C. Rujikiatkamjorn. Elsevier. pp. 51–81. doi: 10.1016/B978-0-08-100698-6.00002-7.

Wilson, G.W., Kabwe, L.K., Beier, N.A., and Scott, J.D. 2018. Effect of various treatments on consolidation of oil sands fluid fine tailings. Canadian Geotechnical Journal, **55**(8): 1059–1066. doi:10.1139/cgj-2017-0268.

Wroth, C.P., and Wood, D.M. 1978. The correlation of index properties with some basic engineering properties of soils. Canadian Geotechnical Journal, **15**(2): 137–145. doi:10.1139/t78-014.

Yao, Y. 2016. Dewatering Behaviour of Fine Oil Sands Tailings - An Experimental Study. PhD Thesis, TU Delft, Delft, Netherlands.

Ye, H., Chu, C., Xu, L., Guo, K., and Li, D. 2018. Experimental Studies on Drying-Wetting Cycle Characteristics of Expansive Soils Improved by Industrial Wastes. Advances in Civil Engineering, **2018**: 1–9. doi:10.1155/2018/2321361.

Zheng, T. 2023. Preliminary evaluation of Speswhite kaolin as a physical analogue material for unsaturated oil sands tailings [presentation]. *Presented at* COSIA IRC/IRCC Update Session. June 9, 2023.

Zheng, T., and Beier, N. 2023. Preliminary evaluation of Speswhite kaolin as a physical analogue material for unsaturated oil sands tailings. *In* Proceedings of the 76th Canadian Geotechnical Conference. Canadian Geotechnical Society, Saskatoon, Saskatchewan, Canada.

Appendix A Summary and sources of Atterberg limits and strength data from literature

Table A.1. Atterberg limits of oil sands tailings summary

Tailings type	w_L (%)	w_P (%)	I_p (%)	# of data points
Untreated FT	30-61	20-32	9-33	16
MFT	36-68	19-31	17-37	35
Flocculated tailings	47-82	23-46	20-47	16
Coagulated tailings	54-58	29-29	25-29	2
Flocculated and coagulated tailings	69-73	27-28	42-45	2
Thickened tailings	25-57	14-27	5-37	47
Centrifuged tailings	57-80	24-56	31-56	4
Cyclone overflow	42-44	18-19	23-25	3
In-line thickened tailings	37-82	18-28	18-58	41
Filtered tailings	38-34	32-36	6-48	9

Table A.2. Atterberg limits data sources

Tailings type	Data sources
Centrifuged tailings	Chigbo et al. (2021), Schafer (2018), Smith et al. (2018), Stienwand (2021)
MFT	Bajwa (2015), Banas (1991), Chappel and Blond (2013), Gholami (2014), Guo and Shang (2014), Jeeravipoolvarn (2005), Masala and Matthews (2010), Nik (2013), Pollock (1988), Rima (2022), Rozina (2013), Scott et al. (2013), Shobrook (2014), Sorta (2014), Tang (1997), Torghabeh (2013), Yao (2016), Yao et al. (2016), Zhang (2012)
Flocculated tailings	Amoako (2020), Bajwa (2015), Gholami (2014), Jeeravipoolvarn et al. (2020), Rozina (2013)
Coagulated tailings	Miller et al. (2010)
Flocculated and coagulated tailings	Elias (2019)
Thickened tailings	Innocent-Bernard (2013), Jeeravipoolvarn et al. (2008), Kabwe et al. (2019), Kabwe et al. (2021), Masala and Matthews (2010), Masala et al. (2014), Sorta (2014), Wijermars (2011), Wilson et al. (2018), Yao (2016), Yao et al. (2012), Yao et al. (2016), Yuan and Lahaie (2009)
Cyclone overflow	Jeeravipoolvarn (2010), Sorta (2014)
In-line thickened tailings	Jeeravipoolvarn (2010), Kabwe et al. (2013), Rima (2022)
Filtered tailings	Ansah-Sam et al. (2021)
Untreated FT	Amoako (2020), Contreras et al. (2015), Elias (2019), Jeeravipoolvarn et al. (2008), Kabwe et al. (2021), Miller et al. (2010), Salam (2020), Stienwand (2021), Suthaker (1995), Wilson et al. (2018)

Table A.3 Remoulded undrained shear strength - liquidity index data sources

Tailings type	Data sources
MFT	Banas (1991), Beier et al. (2013)
Flocculated tailings	Bajwa (2015), Beier et al. (2013), Jeeravipoolvarn et al. (2020)

Appendix B Characterization data

Particle Size Distribution : CC

PARTICLE SIZE DISTRIBUTION CALCULATION SHEET

SOP: AB SOP-00049
TEST CODE: SIZEDIST

Attachment: 2

Date: 5/15/2023
Analyst: RDL
Batch No: A961889

Sample ID #: CENTRIFUGE_CAKE_OILSAND_TAILINGS
Sub Contract Job #: C323163
Sub Contract Sample #: BOL250-01
Sample Mass (g) = 34.5

Time	R	Temp (°C)	C	Co	X (um)	t1/2	% P	Part. Size (mm)
R_s	5.0	21.4	N/A	N/A	N/A	N/A	100.0	2.0000
R30s	37.5	21.4	32.5	34.5	61.0	0.7071	94.2	0.0610
R1min	36.5	21.4	31.5	34.5	43.5	1.0000	91.3	0.0435
R3min	35.5	21.4	30.5	34.5	25.3	1.7320	88.4	0.0253
R10min	32.0	21.1	27.0	34.5	14.2	3.1623	78.3	0.0142
R30min	27.5	21.1	22.5	34.5	8.5	5.4772	65.2	0.0085
R90min	22.5	21.2	17.5	34.5	5.1	9.4858	50.7	0.0051
R270min	18.5	21.8	13.5	34.5	3.0	16.4317	39.1	0.0030
R1080min	16.0	21.4	11.0	34.5	1.5	32.8634	31.9	0.0015

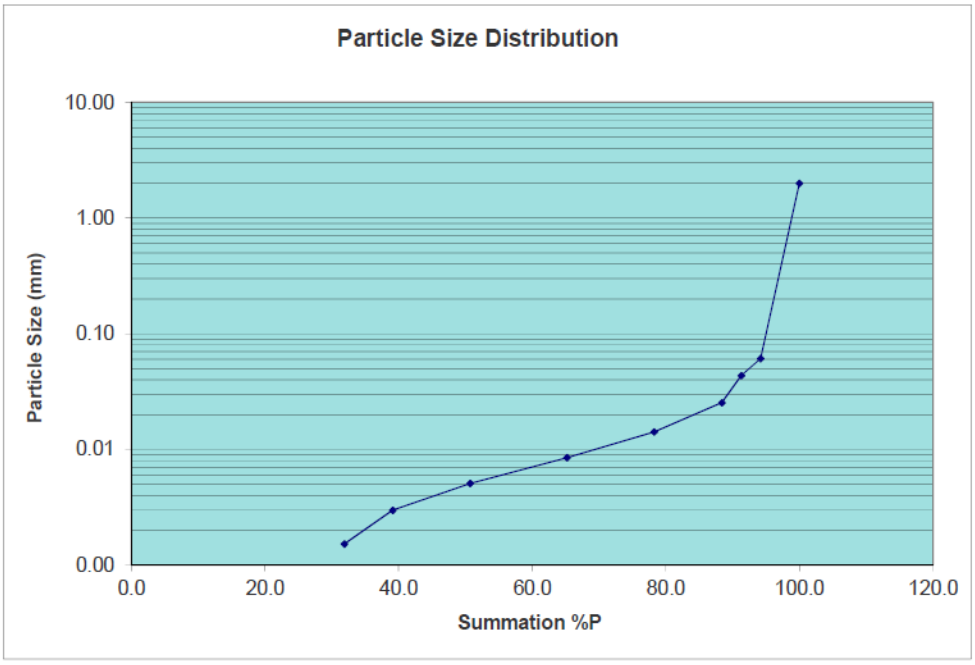

Particle Size Distribution: CC-DS

PARTICLE SIZE DISTRIBUTION CALCULATION SHEET

SOP: AB SOP-00049
TEST CODE: SIZEDIST

Attachment: 3

Date: 5/15/2023
Analyst: RDL
Batch No: A961889

Sample ID #: CENTRIFUGE_CAKE_DS_CLEANE
Sub Contract Job #: C323163
Sub Contract Sample #: BOR780-01
Sample Mass (g) = 40.88

Time	R	Temp (°C)	C	Co	X (um)	t1/2	% P	Part. Size (mm)
R_L	5.0	21.4	N/A	N/A	N/A	N/A	100.0	2.0000
R30s	36.5	21.4	31.5	40.9	61.5	0.7071	77.1	0.0615
R1min	35.5	21.4	30.5	40.9	43.8	1.0000	74.6	0.0438
R3min	34.0	21.4	29.0	40.9	25.5	1.7320	70.9	0.0255
R10min	26.0	21.1	21.0	40.9	14.8	3.1623	51.4	0.0148
R30min	20.5	21.1	15.5	40.9	8.9	5.4772	37.9	0.0089
R90min	16.0	21.2	11.0	40.9	5.3	9.4858	26.9	0.0053
R270min	13.0	21.8	8.0	40.9	3.1	16.4317	19.6	0.0031
R1080min	11.0	21.4	6.0	40.9	1.6	32.8634	14.7	0.0016

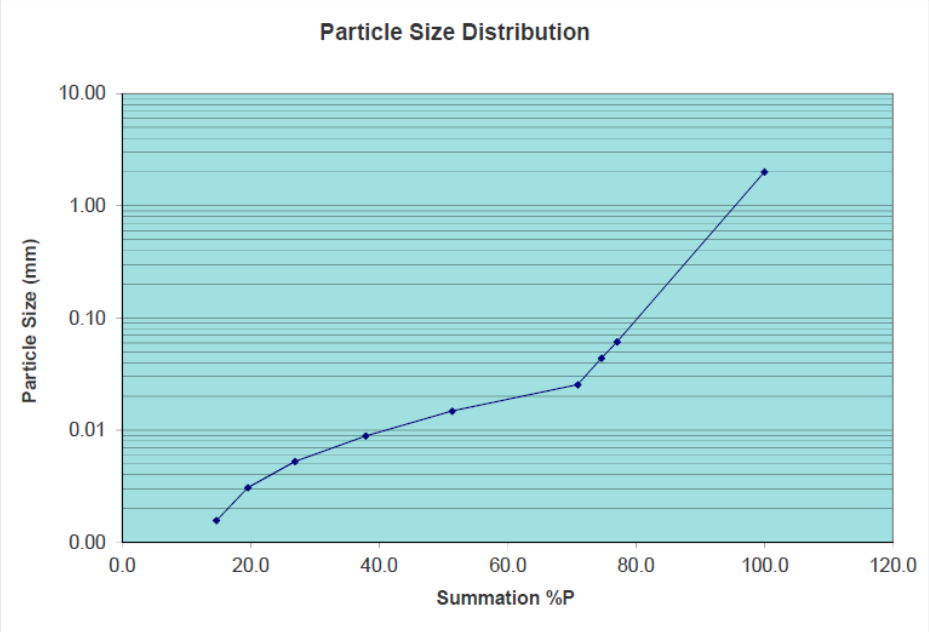

Particle Size Distribution: CC-CE

PARTICLE SIZE DISTRIBUTION CALCULATION SHEET

SOP: AB SOP-00049
TEST CODE: SIZEDIST

Attachment: 4

Date: 5/15/2023
Analyst: RDL
Batch No: A961889

Sample ID #: CENTRIFUGE_CAKE_COLD_EXTR
Sub Contract Job #: C323163
Sub Contract Sample #: BOR781-01
Sample Mass (g) = 43.609

Time	R	Temp (°C)	C	Co	X (um)	t1/2	% P	Part. Size (mm)
R_L	5.0	21.4	N/A	N/A	N/A	N/A	100.0	2.0000
R30s	47.0	21.4	42.0	43.6	59.6	0.7071	96.3	0.0596
R1min	46.0	21.4	41.0	43.6	42.1	1.0000	94.0	0.0421
R3min	45.0	21.4	40.0	43.6	24.3	1.7320	91.7	0.0243
R10min	42.5	21.1	37.5	43.6	13.3	3.1623	86.0	0.0133
R30min	38.0	21.1	33.0	43.6	7.8	5.4772	75.7	0.0078
R90min	32.5	21.2	27.5	43.6	4.7	9.4858	63.1	0.0047
R270min	28.0	21.8	23.0	43.6	2.8	16.4317	52.7	0.0028
R1080min	25.0	21.4	20.0	43.6	1.4	32.8634	45.9	0.0014

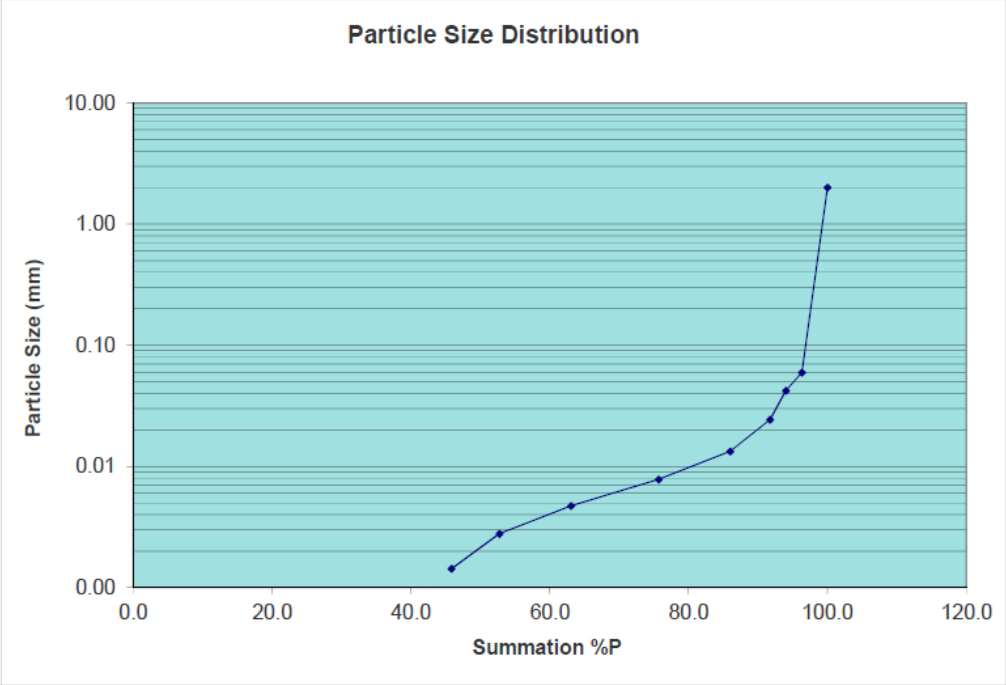

Particle Size Distribution: FT

PARTICLE SIZE DISTRIBUTION CALCULATION SHEET

SOP: PTC SOP-00022
TEST CODE: HYDPSD

Attachment: 2

Date: 10/16/2023
Analyst: SHK
Batch No: B154534

Sample ID #:
Sub Contract Job #: C381848
Sub Contract Sample #: CAR561
Sample Mass (g) = 42.6

Time	R	Temp (°C)	C	Co	X (um)	t1/2	% P	Part. Size (mm)
R_i	3.5	25.4	N/A	N/A	N/A	N/A	100.0	2.0000
R30s	40.0	25.4	36.5	42.6	56.7	0.7071	85.7	0.0567
R1min	38.0	25.4	34.5	42.6	40.7	1.0000	81.0	0.0407
R3min	36.0	25.4	32.5	42.6	23.9	1.7321	76.3	0.0239
R10min	34.0	24.2	30.5	42.6	13.5	3.1623	71.6	0.0135
R30min	29.5	24.3	26.0	42.6	8.1	5.4772	61.0	0.0081
R90min	25.0	24.5	21.5	42.6	4.8	9.4868	50.5	0.0048
R270min	20.0	25.4	16.5	42.6	2.8	16.4317	38.7	0.0028
R1080min	13.0	24.5	9.5	42.6	1.5	32.8634	22.3	0.0015

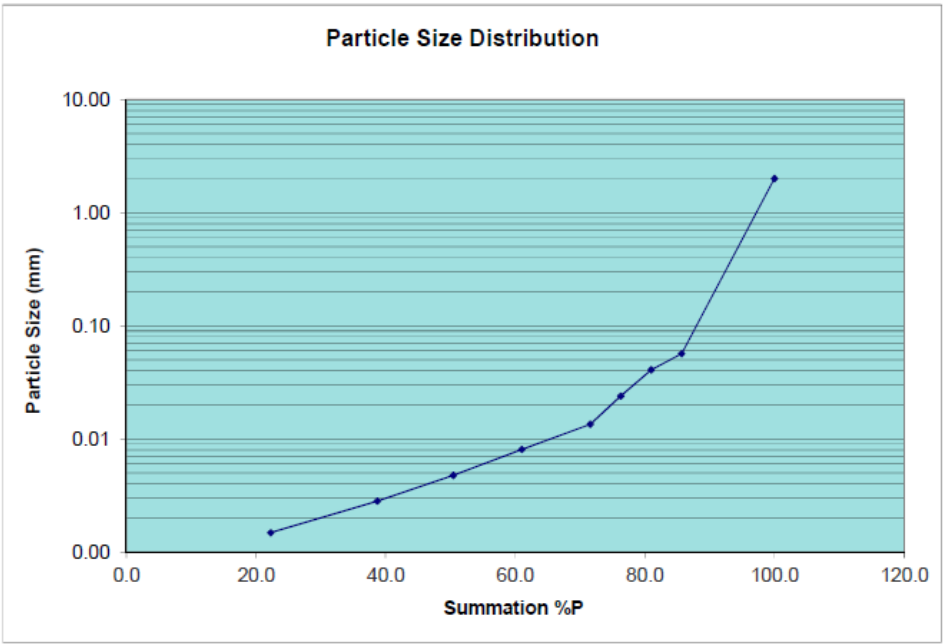

Particle Size Distribution: TT

Grain Size Analysis Report

Client Sample ID: THICKENED OIL SANDS TAILINGS
Maxxam Sample ID: BSE334-01
Maxxam Job #: C342363

Tot. Sample Wt (g)*: 11.08 Batch # (Sieve): B063499
> 2 mm Sample Wt (g)*: 0.00 Batch # (Hydro): B063450
* Dry mass based on Sieve Aliquot

Analysis Date (Sieve): 8/9/2023
Analysis Date (Hydro): 8/8/2023

	Description	Particle Size (mm)	Percent Passing
Sieve	Sieve 4	4.750	100.0
	Sieve 10	2.000	100.0
	Sieve 20	0.850	100.0
	Sieve 40	0.425	98.7
	Sieve 100	0.150	89.3
	Sieve 200	0.075	75.9
Hydrometer	R1min	0.0485	40.7
	R3min	0.0283	34.6
	R10min	0.0157	30.9
	R30min	0.0092	23.5
	R90min	0.0054	17.3
	R270min	0.0031	12.3
	R1080min	0.0016	4.9

Grain Size Proportion (%)**:

	Min (mm)	Max (mm)	Percentage
Sand	0.050	2.000	57.2
Silt	0.002	0.050	35.9
Clay	-	0.002	6.9

** Calculations based only on sub 2 mm fraction.
Compatible with USDA and Canadian Soil Triangles

Soil Classification***:

Based on the entire sample

Percentage (by mass) less than 0.075 mm = 75.9
Classification = **Fine Textured Soil**

Based on the < 2 mm fraction ****

Percentage (by mass) less than 0.075 mm = 75.9
Classification = **Fine Textured Soil**

**** Grain size analysis performed to classify the soil material according to the criteria prescribed in Section 42.2 of Ontario Regulation 153/04 as amended by Ontario Regulation 511/09, and conducted in accordance with test procedures outlined in ASTM D422.

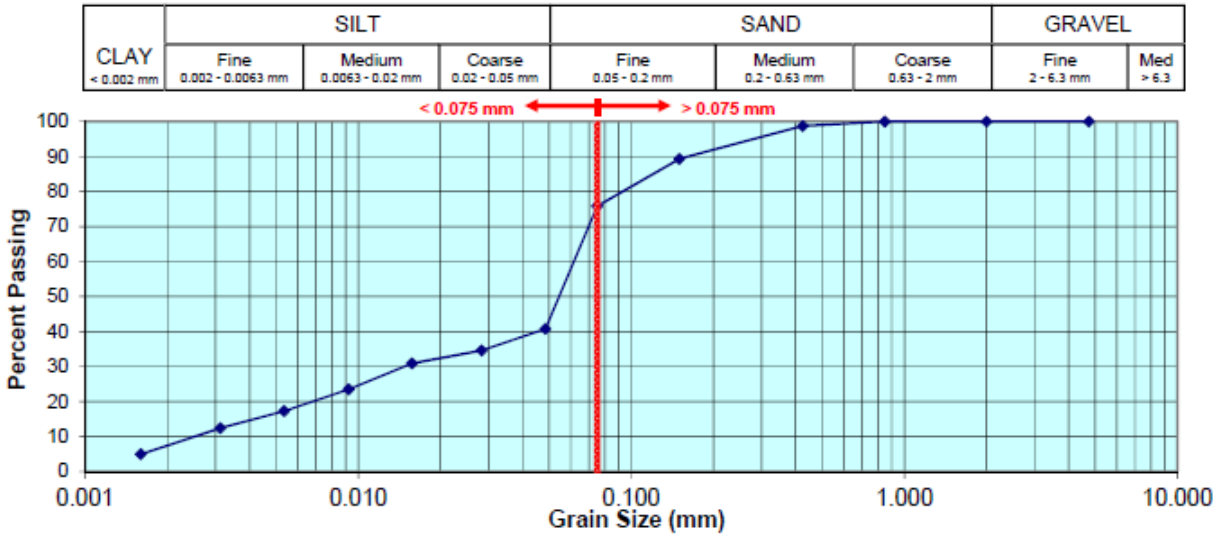

*** ON Regulation 153/04 requires coarse:fine determination on the < 2 mm fraction. Other jurisdictions may require the entire sample, thus both classifications are provided

Note: Clay/Silt/Sand/Gravel Graphic above Graph: Sand | Silt | Clay fractions in accordance with USDA and Canadian System of Soil Classification. Sub fractions in accordance with the British (BSI) system for information purposes.

Grain Size Analysis Report (QA-SRM)

Sieve Batch #: B063499
Hydrometer Batch #: B063450

Standard Reference Material

			Acceptance Limits	
	Fraction	% Recovery	Minimum	Maximum
Sieve	> 0.075 mm	100	75	125
	< 0.075 mm	100	75	125
Hydrometer	Sand	92	75	125
	Silt	124	75	125
	Clay	92	75	125

Dean Stark: CC

DEAN STARK

MaxxID	Client ID	Meter Number	C342363:BSE332-01 (Laboratory Number)
UNIVERSITY OF ALBERTA (Operator Name)		LSD	Well ID
CENTRIFUGED OIL SANDS TAILINGS (Well/Plant/Facility)		N/A (Initials of Sampler)	UNIVERSITY OF ALBERTA (Sampling Company)
Field or Area	Pool or Zone	CENTRIFUGED OIL SANDS TAILINGS (Sample Point)	PLASTIC BOTTLE (Container Identity) / Percent Full
Test Recovery			Sample Gathering Point / Solution Gas
Test Type / No. / Multiple Recovery	Interval From: To:	Elevations (m) KB / GRD	Well Fluid Status / Well Status Mode
Production Rates: Water m³/d / Oil m³/d / Gas 1000 m³/d	Gauge Pressures kPa: Source / As Received	Temperature °C: Source / As Received: 23.0	Well Status Type / Well Type
			Gas or Condensate Project / Licence No.
2023/06/09 (Date Sampled Start) / Date Sampled End	2023/06/12 (Date Received)	2023/08/10 (Date Reported) / Date Reissued	EZU (Analyst)

PARAMETER DESCRIPTION	RESULT	UNIT	METHOD	RDL
Dean Stark Analysis				
Mass Bitumen	8.5	g	OSRD Method 1.0	0.01
Mass Solids	273.66	g	OSRD Method 1.0	0.01
Mass Water	273.26	g	OSRD Method 1.0	0.01
Mass Total	557.1	g	OSRD Method 1.0	0.01
Mass % Bitumen	1.53	wt%	OSRD Method 1.0	0.01
Mass % Solids	49.12	wt%	OSRD Method 1.0	0.01
Mass % Water	49.05	wt%	OSRD Method 1.0	0.01
Mass % Recovery	99.7	wt%	OSRD Method 1.0	0.01

Results relate only to Items tested

Remarks:

Reference Method suffix "M" indicates test methods incorporate validated modifications from specific reference methods to improve performance.

Bureau Veritas Edmonton: 6744 - 50th Street T6B 3M9 Telephone (780) 378-8500 Fax (780) 378-8699

Dean Stark: FT

DEAN STARK

MaxxID | Client ID | Meter Number | C342363:BSE333-01 (Laboratory Number)

UNIVERSITY OF ALBERTA (Operator Name) | LSD | Well ID

FLUID FINE OIL SANDS TAILINGS (Well/Plant/Facility) | N/A (Initials of Sampler) | UNIVERSITY OF ALBERTA (Sampling Company)

Field or Area | Pool or Zone | FLUID FINE OIL SANDS TAILINGS (Sample Point) | 4L Pail (Container Identity) | Percent Full

Test Recovery | Sample Gathering Point | Solution Gas

Test Type | No. | Multiple Recovery | Interval From: To: | Elevations (m) KB GRD | Well Fluid Status | Well Status Mode

Production Rates: Water m^3/d | Oil m^3/d | Gas 1000 m^3/d | Gauge Pressures kPa: Source | As Received | Temperature °C: Source | 23.0 As Received | Well Status Type | Well Type

Gas or Condensate Project | Licence No.

2023/06/09 (Date Sampled Start) | Date Sampled End | 2023/06/12 (Date Received) | 2023/08/10 (Date Reported) | Date Reissued | EZU (Analyst)

PARAMETER DESCRIPTION	RESULT	UNIT	METHOD	RDL
Dean Stark Analysis				
Mass Bitumen	5.74	g	OSRD Method 1.0	0.01
Mass Solids	115.77	g	OSRD Method 1.0	0.01
Mass Water	355.27	g	OSRD Method 1.0	0.01
Mass Total	477.69	g	OSRD Method 1.0	0.01
Mass % Bitumen	1.2	wt%	OSRD Method 1.0	0.01
Mass % Solids	24.24	wt%	OSRD Method 1.0	0.01
Mass % Water	74.37	wt%	OSRD Method 1.0	0.01
Mass % Recovery	99.81	wt%	OSRD Method 1.0	0.01

Results relate only to Items tested

Remarks:

Reference Method suffix "M" indicates test methods incorporate validated modifications from specific reference methods to improve performance.

Bureau Veritas Edmonton: 6744 - 50th Street T6B 3M9 Telephone (780) 378-8500 Fax (780) 378-8699

MBI and Dean Stark: TT

DEAN STARK

MaxxID	Client ID	Meter Number	C342363:BSE334-01 (Laboratory Number)
UNIVERSITY OF ALBERTA (Operator Name)		LSD	Well ID
THICKENED OIL SANDS TAILINGS (Well/Plant/Facility)		N/A (Initials of Sampler)	UNIVERSITY OF ALBERTA (Sampling Company)
Field or Area	Pool or Zone	THICKENED OIL SANDS TAILINGS (Sample Point)	4L Pail (Container Identity)
Test Recovery			Sample Gathering Point / Solution Gas
Test Type / No. / Multiple Recovery	Interval From: To:	Elevations (m) KB / GRD	Well Fluid Status / Well Status Mode
Production Rates: Water m³/d / Oil m³/d / Gas 1000 m³/d	Gauge Pressures kPa: Source / As Received	Temperature °C: Source / As Received (23.0)	Well Status Type / Well Type
			Gas or Condensate Project / Licence No.
2023/06/09 (Date Sampled Start)	Date Sampled End	2023/06/12 (Date Received)	2023/08/10 (Date Reported) / Date Reissued / RM4,EZU,EBO,VSO,TL0,LZ0,SYF (Analyst)

PARAMETER DESCRIPTION	RESULT	UNIT	METHOD	RDL
Industrial				
See Attachment	ATTACHED	N/A	ASTM D7928-17 m	N/A
Titration				
Mass of Raw Slurry	2.1	g	CANMET Jan06, 2008	0.01
Mass of Sample Titrated	0.94	g	CANMET Jan06, 2008	0.01
Calculated Parameters				
pH Before MBI Titration	3.64	g	CANMET Jan06, 2008	N/A
Volume of Titrant	14.0	mL	CANMET Jan06, 2008	0.5
Methylene Blue Index	8.94	meq/100g	CANMET Jan06, 2008	0.05
Calculated % Clay	64.1	%	Calculation	0.64
Dean Stark Analysis				
Mass Bitumen	7.26	g	OSRD Method 1.0	0.01
Mass Solids	251.67	g	OSRD Method 1.0	0.01
Mass Water	301.32	g	OSRD Method 1.0	0.01
Mass Total	560.78	g	OSRD Method 1.0	0.01
Mass % Bitumen	1.29	wt%	OSRD Method 1.0	0.01
Mass % Solids	44.88	wt%	OSRD Method 1.0	0.01
Mass % Water	53.73	wt%	OSRD Method 1.0	0.01
Mass % Recovery	99.9	wt%	OSRD Method 1.0	0.01
Soluble Parameters				
Soluble Conductivity	1.5	dS/m	SM 23 2510 B m	0.020
Saturation %	48	%	Carter 2nd ed 15.2 m	N/A
Physical Properties				
Attachment	ATTACHED	%	ASTM D6913-17 m	N/A
Moisture	0.76	%	CCME PHC-CWS m	0.30

Results relate only to Items tested

Remarks:

Result indicates % of sample retained on the sieve.

Sample was analyzed past method specified hold time for Particle Size by Sieve (Dry). Exceedance of hold time increases the uncertainty of test results but does not necessarily imply that results are compromised. Sample was analyzed past method specified hold time for Grain Size Analysis Report. Sample was analyzed past method specified hold time for Conductivity @25C (Soluble).

Reference Method suffix "M" indicates test methods incorporate validated modifications from specific reference methods to improve performance.

Bureau Veritas Edmonton: 6744 - 50th Street T6B 3M9 Telephone (780) 378-8500 Fax (780) 378-8699

MBI and Conductivity: CC

DEAN STARK

MaxxID	CENTRIFUGE_CAKE_OILSAND_TAILINGS (Client ID)	Meter Number	C323163:BOL250-01 (Laboratory Number)
UNIVERSITY OF ALBERTA (Operator Name)		LSD	Well ID
CENTRIFUGE_CAKE_OILSAND_TAILINGS (Well/Plant/Facility)		NA (Initials of Sampler)	UNIVERSITY OF ALBERTA (Sampling Company)
Field or Area	Pool or Zone	CENTRIFUGE_CAKE_RAW (Sample Point)	4L Pail (Container Identity)
Test Recovery			Sample Gathering Point / Solution Gas
Test Type / No. / Multiple Recovery	Interval From: To:	Elevations (m) KB / GRD	Well Fluid Status / Well Status Mode
Production Rates: Water m³/d / Oil m³/d / Gas 1000 m³/d	Gauge Pressures kPa: Source / As Received	Temperature °C: Source / As Received (23.0)	Well Status Type / Well Type
			Gas or Condensate Project / Licence No.
Date Sampled Start / Date Sampled End	2023/04/04 (Date Received)	2023/05/16 (Date Reported)	Date Reissued / RM4,ABQ,EBO,EH2 (Analyst)

PARAMETER DESCRIPTION	RESULT	UNIT	METHOD	RDL
Industrial				
See Attachment	ATTACHED	N/A	ASTM D7928-17 m	N/A
Titration				
Mass of Raw Slurry	1.6	g	CANMET Jan06, 2008	0.01
Mass of Sample Titrated	0.77	g	CANMET Jan06, 2008	0.01
Calculated Parameters				
pH Before MBI Titration	3.72	g	CANMET Jan06, 2008	N/A
Volume of Titrant	17.5	mL	CANMET Jan06, 2008	0.5
Methylene Blue Index	13.6	meq/100g	CANMET Jan06, 2008	0.05
Calculated % Clay	97.7	%	Calculation	0.64
Dean Stark Analysis				
Mass % Solids	48.11	wt%	OSRD Method 1.0	0.01
Soluble Parameters				
Soluble Conductivity	2.1	dS/m	SM 23 2510 B m	0.020
Saturation %	120	%	Carter 2nd ed 15.2 m	N/A

Results relate only to items tested

Remarks:

Sample was analyzed past method specified hold time for Conductivity @25C (Soluble). Sample was analyzed past method specified hold time for Grain Size Analysis Report.

Reference Method suffix "M" indicates test methods incorporate validated modifications from specific reference methods to improve performance.

Bureau Veritas Edmonton: 6744 - 50th Street T6B 3M9 Telephone (780) 378-8500 Fax (780) 378-8699

MBI and Conductivity: CC-DS

DEAN STARK

MaxxID	Client ID	Meter Number	Laboratory Number
	CENTRIFUGE_CAKE_DS_CLEANED		C323163:BOR780-01

Operator Name	LSD	Well ID
UNIVERSITY OF ALBERTA		

Well/Plant/Facility	Initials of Sampler	Sampling Company
CENTRIFUGE_CAKE_DS_CLEANED	NA	UNIVERSITY OF ALBERTA

Field or Area	Pool or Zone	Sample Point	Container Identity	Percent Full
		CENTRIFUGE_CAKE_DS_CLEANED	4L Pail	

Test Recovery	Sample Gathering Point	Solution Gas

Test Type	No.	Multiple Recovery	Interval From:	Interval To:	Elevations (m) KB	Elevations (m) GRD	Well Fluid Status	Well Status Mode

Production Rates Water m³/d	Oil m³/d	Gas 1000 m³/d	Gauge Pressures kPa Source	Gauge Pressures kPa As Received	Temperature °C Source	Temperature °C As Received	Well Status Type	Well Type
						23.0		

Gas or Condensate Project	Licence No.

Date Sampled Start	Date Sampled End	Date Received	Date Reported	Date Reissued	Analyst
		2023/04/04	2023/05/16		RM4,ABQ,EBO,EH2

PARAMETER DESCRIPTION	RESULT	UNIT	METHOD	RDL
Industrial				
See Attachment	ATTACHED	N/A	ASTM D7928-17 m	N/A
Calculated Parameters				
pH Before MBI Titration	3.72	g	CANMET Jan06, 2008	N/A
Mass of Sample Titrated	1.33	g	CANMET Jan06, 2008	0.01
Volume of Titrant	25.5	mL	CANMET Jan06, 2008	0.5
Methylene Blue Index	11.5	meq/100g	ASTM C837	0.05
Calculated % Clay	82.4	%	Calculation	0.64
Dean Stark Analysis				
Mass Bitumen	5.86	g	OSRD Method 1.0	0.01
Mass Solids	171.29	g	OSRD Method 1.0	0.01
Mass Water	176.55	g	OSRD Method 1.0	0.01
Mass Total	356.07	g	OSRD Method 1.0	0.01
Mass % Bitumen	!! 1.65	wt%	OSRD Method 1.0	0.01
Mass % Solids	48.11	wt%	OSRD Method 1.0	0.01
Mass % Water	49.58	wt%	OSRD Method 1.0	0.01
Mass % Recovery	99.34	wt%	OSRD Method 1.0	0.01
Soluble Parameters				
Soluble Conductivity	1.4	dS/m	SM 23 2510 B m	0.020
Saturation %	79	%	Carter 2nd ed 15.2 m	N/A

Results relate only to items tested

Remarks:

Sample was analyzed past method specified hold time for Conductivity @25C (Soluble). Sample was analyzed past method specified hold time for Grain Size Analysis Report.

Reference Method suffix "M" indicates test methods incorporate validated modifications from specific reference methods to improve performance.

Bureau Veritas Edmonton: 6744 - 50th Street T6B 3M9 Telephone (780) 378-8500 Fax (780) 378-8699

MBI and Conductivity: CC-CE

DEAN STARK

MaxxID	Client ID: CENTRIFUGE_CAKE_COLD_EXTR	Meter Number	Laboratory Number: C323163:BOR781-01
Operator Name: UNIVERSITY OF ALBERTA		LSD	Well ID
Well/Plant/Facility: CENTRIFUGE_CAKE_COLD_EXTR		Initials of Sampler: NA	Sampling Company: UNIVERSITY OF ALBERTA
Field or Area	Pool or Zone	Sample Point: CENTRIFUGE_CAKE_COLD_EXTR	Container Identity: 4L Pail
Test Recovery		Sample Gathering Point	Solution Gas
Test Type / No. / Multiple Recovery	Interval From: To:	Elevations (m) KB / GRD	Well Fluid Status / Well Status Mode
Production Rates: Water m³/d / Oil m³/d / Gas 1000 m³/d	Gauge Pressures kPa: Source / As Received	Temperature °C: Source / As Received: 23.0	Well Status Type / Well Type
			Gas or Condensate Project / Licence No.
Date Sampled Start / Date Sampled End	Date Received: 2023/04/04	Date Reported: 2023/05/16	Date Reissued / Analyst: RM4,ABQ,EBO,EH2

PARAMETER DESCRIPTION	RESULT	UNIT	METHOD	RDL
Industrial				
See Attachment	ATTACHED	N/A	ASTM D7928-17 m	N/A
Calculated Parameters				
pH Before MBI Titration	3.64	g	CANMET Jan06, 2008	N/A
Mass of Sample Titrated	1.03	g	CANMET Jan06, 2008	0.01
Volume of Titrant	20.5	mL	CANMET Jan06, 2008	0.5
Methylene Blue Index	11.9	meq/100g	ASTM C837	0.05
Calculated % Clay	85.6	%	Calculation	0.64
Soluble Parameters				
Soluble Conductivity	1.4	dS/m	SM 23 2510 B m	0.020
Saturation %	84	%	Carter 2nd ed 15.2 m	N/A

Results relate only to items tested

Remarks:

Sample was analyzed past method specified hold time for Conductivity @25C (Soluble). Sample was analyzed past method specified hold time for Grain Size Analysis Report.

Reference Method suffix "M" indicates test methods incorporate validated modifications from specific reference methods to improve performance.

Bureau Veritas Edmonton: 6744 - 50th Street T6B 3M9 Telephone (780) 378-8500 Fax (780) 378-8699

MBI: FT

WATER ANALYSIS

C379055:CAR561-01
MaxxID | Client ID | Meter Number | Laboratory Number

UNIVERSITY OF ALBERTA
Operator Name | LSD | Well ID

OIL SANDS FLUID TAILINGS | N/A | UNIVERSITY OF ALBERTA
Well/Plant/Facility | Initials of Sampler | Sampling Company

Field or Area | Pool or Zone | OIL SANDS FLUID TAILINGS (Sample Point) | PLASTIC BOTTLE (Container Identity) | Percent Full

Test Recovery | Sample Gathering Point | Solution Gas

Test Type | No. | Multiple Recovery | Interval From: To: | Elevations (m) KB GRD | Well Fluid Status | Well Status Mode

Production Rates: Water m³/d | Oil m³/d | Gas 1000 m³/d
Gauge Pressures kPa: Source | As Received
Temperature °C: Source | As Received: 23.0
Well Status Type | Well Type | Gas or Condensate Project | Licence No.

Date Sampled Start | Date Sampled End | Date Received: 2023/10/02 | Date Reported: 2023/10/23 | Date Reissued | Analyst: RM4,EZU,YZH,YT2,SHK,ADI,YD0

PARAMETER DESCRIPTION	RESULT	UNIT	METHOD	RDL
Calculated Parameters				
pH Before MBI Titration	3.59	g	CANMET Jan06, 2008	N/A
Mass of Sample Titrated	1.05	g	CANMET Jan06, 2008	0.01
Volume of Titrant	14.5	mL	CANMET Jan06, 2008	0.5
Methylene Blue Index	8.29	meq/100g	ASTM C837	0.05
Calculated % Clay	59.5	%	Calculation	0.64
Dean Stark Analysis				
Mass Bitumen	11.1	g	OSRD Method 1.0	0.01
Mass Solids	219.96	g	OSRD Method 1.0	0.01
Mass Water	639.2	g	OSRD Method 1.0	0.01
Mass Total	872.39	g	OSRD Method 1.0	0.01
Mass % Bitumen	1.27	wt%	OSRD Method 1.0	0.01
Mass % Solids	25.21	wt%	OSRD Method 1.0	0.01
Mass % Water	73.27	wt%	OSRD Method 1.0	0.01
Mass % Recovery	99.75	wt%	OSRD Method 1.0	0.01
Physical Properties				
See Attachment	SEE ATTACH	N/A	ASTM D7928	N/A
Particle Size: RL	2.0	mm	ASTM D7928	N/A
Summation: RL	100	%	ASTM D7928	2
Particle Size: R30s	0.057	mm	ASTM D7928	N/A
Summation: R30s	86	%	ASTM D7928	2
Particle Size: R1min	0.041	mm	ASTM D7928	N/A
Summation: R1min	81	%	ASTM D7928	2
Particle Size: R3min	0.024	mm	ASTM D7928	N/A
Summation: R3min	76	%	ASTM D7928	2
Particle Size: R10min	0.014	mm	ASTM D7928	N/A
Summation: R10min	72	%	ASTM D7928	2
Particle Size: R30min	0.0081	mm	ASTM D7928	N/A
Summation: R30min	61	%	ASTM D7928	2
Particle Size: R90min	0.0048	mm	ASTM D7928	N/A
Summation: R90min	51	%	ASTM D7928	2
Particle Size: R270min	0.0028	mm	ASTM D7928	N/A
Summation: R270min	39	%	ASTM D7928	2
Particle Size: R1080min	0.0015	mm	ASTM D7928	N/A
Summation: R1080min	22	%	ASTM D7928	2

Results relate only to items tested

Remarks:
DATE SAMPLED HAS NOT BEEN RECORDED ON THE SAMPLING TAG.

Reference Method suffix "M" indicates test methods incorporate validated modifications from specific reference methods to improve performance.

Bureau Veritas Edmonton: 6744 - 50th Street T6B 3M9 Telephone (780) 378-8500 Fax (780) 378-8699

Water chemistry: CC

WATER ANALYSIS

C379055:CAR562-01 (Laboratory Number)

UNIVERSITY OF ALBERTA (Operator Name)

OIL SANDS CENTRIFUGED TAILINGS (Well/Plant/Facility)

N/A (Initials of Sampler)

UNIVERSITY OF ALBERTA (Well ID / Sampling Company)

OIL SANDS CENTRIFUGED TAILINGS (Sample Point)

PLASTIC BOTTLE (Container Identity)

23.0 (Temperature °C, As Received)

2023/10/02 (Date Received)

2023/10/23 (Date Reported)

YZH,YT2,YD0 (Analyst)

CATIONS

Ion	mg/L	meq/L
Na	388	16.9
K	30.5	0.781
Ca	90.6	4.52
Mg	48.4	3.97
Ba	0.21	0.0030
Sr	2.55	0.0582
Fe	0.04	0.0013

ANIONS

Ion	mg/L	meq/L
Cl	122.4	3.45
HCO_3	250	4.11
SO_4	705.7	14.7
CO_3	12	0.40
OH	<1.0	<0.03

Total Dissolved Solids (mg/L): 2080 Measured; 1500 Calculated

Relative Density: 1.001

Refractive Index: 1.333

Conductivity (µS/cm): 2390

Resistivity (Ω·m) @25°C: 4.18

Total Hardness as $CaCO_3$ (mg/L): 430

Total Alkalinity as $CaCO_3$ (mg/L): 230

Total Fe (mg/L):

Total Mn (mg/L):

Observed pH @ 22.1°C: 8.39

H_2S Spot Test: FALSE

Logarithmic Patterns of Dissolved Ions (meq/L)

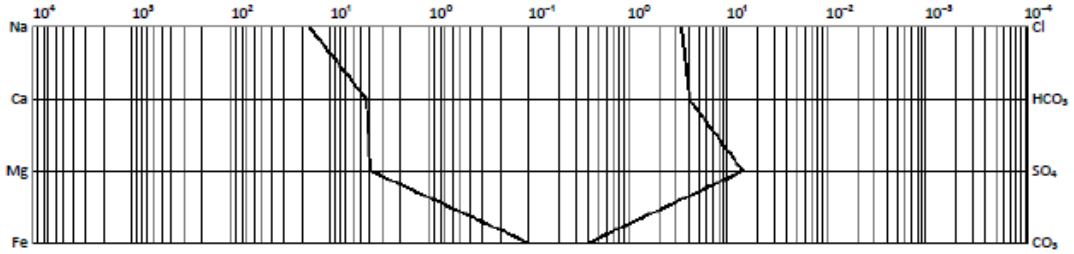

Results relate only to items tested

Remarks:

DATE SAMPLED HAS NOT BEEN RECORDED ON THE SAMPLING TAG.

Reference Method suffix "M" indicates test methods incorporate validated modifications from specific reference methods to improve performance.

2023/10/23 18:04 Page 1 of 1

Bureau Veritas Edmonton: 6744 - 50th Street T6B 3M9 Telephone (780) 378-8500 Fax (780) 378-8699

Water chemistry: FT

WATER ANALYSIS

C379055:CAR561-01 (Laboratory Number)

UNIVERSITY OF ALBERTA (Operator Name)

OIL SANDS FLUID TAILINGS (Well/Plant/Facility) | N/A (Initials of Sampler) | UNIVERSITY OF ALBERTA (Sampling Company)

OIL SANDS FLUID TAILINGS (Sample Point) | PLASTIC BOTTLE (Container Identity)

2023/10/02 (Date Received) | 2023/10/23 (Date Reported) | RM4,EZU,YZH,YT2,SHK,ADI,YDO (Analyst)

CATIONS

Ion	mg/L	meq/L
Na	321	14.0
K	20.0	0.511
Ca	31.6	1.58
Mg	23.4	1.92
Ba	0.14	0.0020
Sr	0.87	0.0198
Fe	0.02	0.0006

ANIONS

Ion	mg/L	meq/L
Cl	123.9	3.49
HCO_3	390	6.43
SO_4	279.1	5.82
CO_3	28	0.94
OH	<1.0	<0.03

Total Dissolved Solids (mg/L): 1310 Measured | 1000 Calculated

Relative Density: 1.000 | Refractive Index: 1.333

Conductivity (µS/cm): 1540 | Resistivity (Ω·m) @25°C: 6.50

Total Hardness as $CaCO_3$ (mg/L): 180 | Total Alkalinity as $CaCO_3$ (mg/L): 370

Total Fe (mg/L): | Total Mn (mg/L):

Observed pH @ 22.6°C: 8.56 | H_2S Spot Test: FALSE

Logarithmic Patterns of Dissolved Ions (meq/L)

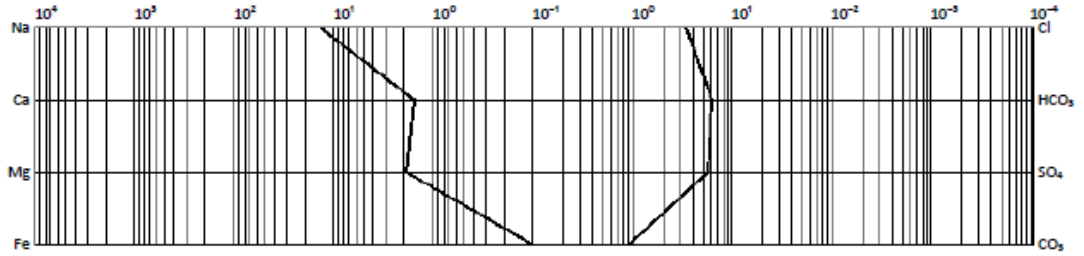

Results relate only to items tested

Remarks:

DATE SAMPLED HAS NOT BEEN RECORDED ON THE SAMPLING TAG.

Reference Method suffix "M" indicates test methods incorporate validated modifications from specific reference methods to improve performance.

2023/10/23 18:04 Page 1 of 2

Bureau Veritas Edmonton: 6744 - 50th Street T6B 3M9 Telephone (780) 378-8500 Fax (780) 378-8699

Water chemistry: TT

WATER ANALYSIS

C379055:CAR563-01 (Laboratory Number)

UNIVERSITY OF ALBERTA (Operator Name)

OIL SANDS THICKENED TAILINGS (Well/Plant/Facility) | N/A (Initials of Sampler) | UNIVERSITY OF ALBERTA (Sampling Company)

OIL SANDS THICKENED TAILINGS (Sample Point) | PLASTIC BOTTLE (Container Identity)

2023/10/02 (Date Received) | 2023/10/23 (Date Reported) | YZH,YT2,ADI,YD0 (Analyst)

CATIONS

Ion	mg/L	meq/L
Na	256	11.1
K	23.3	0.597
Ca	70.5	3.52
Mg	35.9	2.95
Ba	0.10	0.0014
Sr	1.62	0.0371
Fe	0.11	0.0039

ANIONS

Ion	mg/L	meq/L
Cl	12.4	0.349
HCO_3	300	4.84
SO_4	403.4	8.40
CO_3	33	1.09
OH	<1.0	<0.03

Total Dissolved Solids (mg/L): 1320 (Measured) | 980 (Calculated)

1.000 (Relative Density) | 1.333 (Refractive Index)

1520 (Conductivity (µS/cm)) | 6.56 (Resistivity (Ω·m) @25°C)

320 (Total Hardness as $CaCO_3$ (mg/L)) | 300 (Total Alkalinity as $CaCO_3$ (mg/L))

Total Fe (mg/L) | Total Mn (mg/L)

8.60 (Observed pH @ 21.9°C) | FALSE (H_2S Spot Test)

Logarithmic Patterns of Dissolved Ions (meq/L)

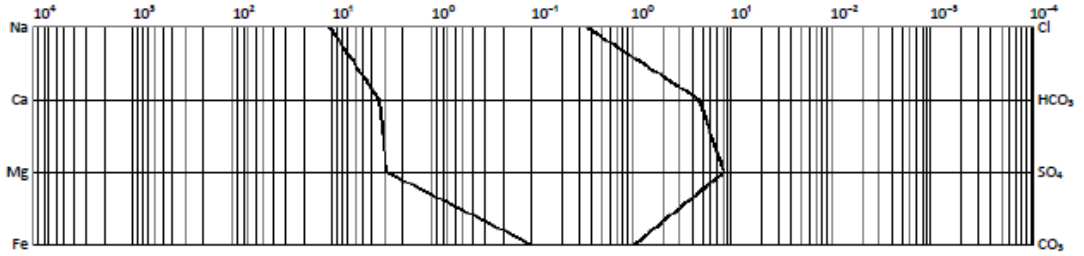

Results relate only to items tested

Remarks:

DATE SAMPLED HAS NOT BEEN RECORDED ON THE SAMPLING TAG.

Ionic imbalance, analysis for major ions was verified. The sample contains non-target dissolved anions.

Reference Method suffix "M" indicates test methods incorporate validated modifications from specific reference methods to improve performance.

Bureau Veritas Edmonton: 6744 - 50th Street T6B 3M9 Telephone (780) 378-8500 Fax (780) 378-8699

XRD: CC

WPF Report

Scan ID: CT-2_Bulk XRD.raw

Scan Parameters: 5.0°/64.986°/0.01998°/384(s), I(p)=11418/92, Co(35kV,40mA), March 13, 2024, 12:20 PM

☑ Zero Offset = 0.1272 (0.0008) ☐ Displacement = 0.0 ☐ Distance Slack = 0.0

☑ Kα2 Peaks Present ☐ Kα2/Kα1 Ratio = 0.5 ☐ X-Ray Polarization = 1.0

Geometry: Diffractometer Lp Fitted-Range: 5.0° - 65.0° BG-Model: Polynomial (5) λ: 1.78899Å (Co)

PSF: Pearson VII Broadening: Individual FWHM Curve Instrument: Constant FWHM = 0.1°

Phase ID (7)	Chemical Formula	PDF-#	Wt% (σ)	DD% (σ)	RIR	μ
Kaolinite-1A	Al2Si2O5(OH)4	04-013-3395	46.4 (1.6)	32.7 (1.6)	0.86	120.0
Microcline	K0.95Na0.05AlSi3O8	04-011-0524	6.5 (.5)	11.6 (.5)	0.75	186.1
Muscovite-2M1	K0.865Na0.135Mg0.04Ti0.01Fe0.09/	04-023-1597	13.6 (1.1)	17.1 (1.2)	1.00	190.6
Quartz	SiO2	98-000-0369	30.7 (0.8)	31.8 (0.6)	4.23	140.6
Siderite	Ca0.10Mg0.33Fe0.57(CO3)	04-009-7660	1.0 (0.4)	0.7 (0.3)	2.16	136.9
Muscovite-1M	KAl2Si3AlO10(OH)2	00-007-0025	0.9 (0.3)	4.4 (0.4)	(1.0)	181.3
Anatase	TiO2	04-007-0701	0.8 (?)	1.8 (?)	4.61	746.8

XRF(Wt%): Fe2O3=0.8%, TiO2=0.8%, CaO<0.1%, K2O=2.5%, SiO2=62.9%, Al2O3=26.0%, MgO=0.2%, Na2O=0.2%, CO2=0.4%

Refinement Halted (R/E=2.73), ♣ Round=4, Iter=6, P=35, R=12.73% (E=4.90%, EPS=0.5)

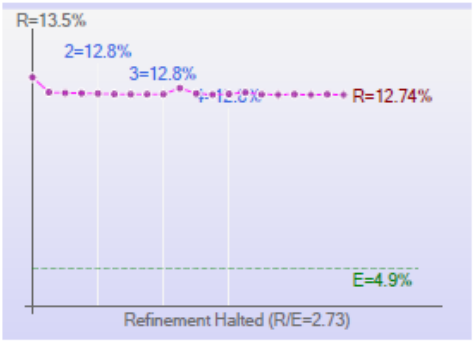

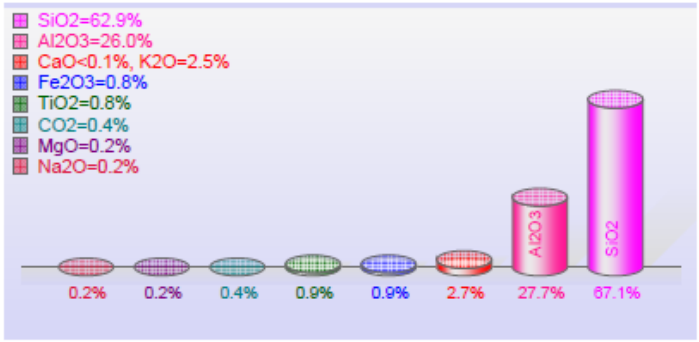

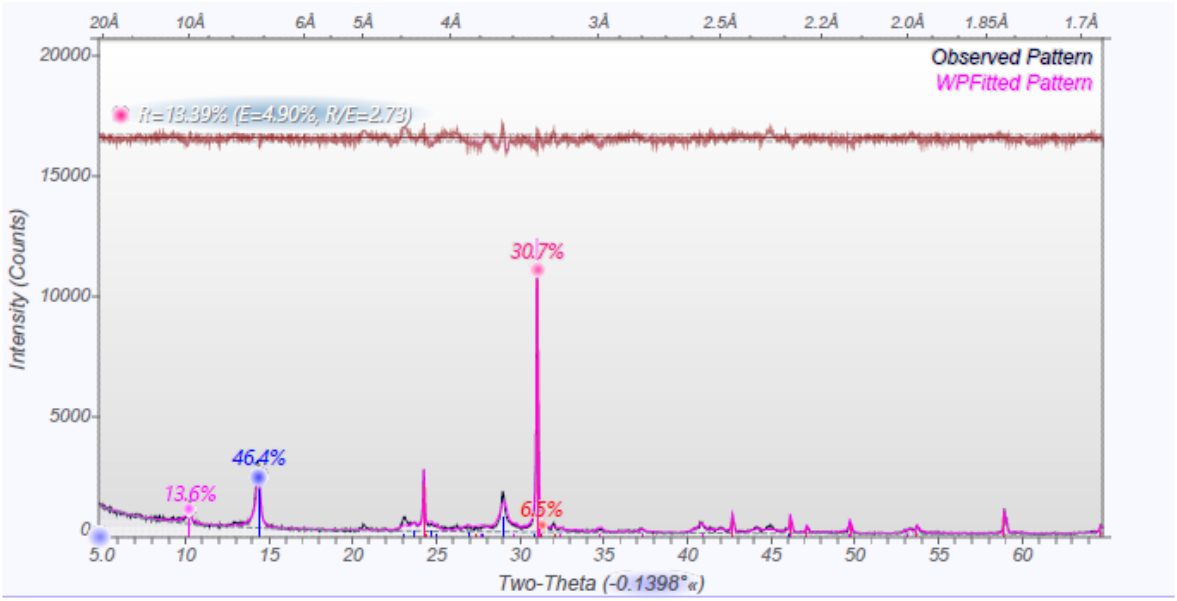

XRD: FT

WPF Report

Scan ID: ES4790_Bulk XRD-edited.mdi

Scan Parameters: 4.86°/64.847°/0.01998°/384(s), I(p)=10783/87, Co, April 2, 2024, 11:45 AM

Control File: C:\Users\MAKSUDAK\OneDrive - NAIT\XRDXRF_Projects\Quick Clay-2023\Jade\QuickClay_4789R_Bulk.wrk.xml

☑ Zero Offset = -0.0484 (0.0006) ☐ Displacement = 0.0 ☐ Distance Slack = 0.0

☑ Kα2 Peaks Present ☐ Kα2/Kα1 Ratio = 0.5 ☐ X-Ray Polarization = 1.0

Geometry: Diffractometer Lp **Fitted-Range:** 4.9° - 64.8° **BG-Model:** Polynomial (5) **λ:** 1.78899Å (Co)

PSF: Pearson VII **Broadening:** Individual FWHM Curve **Instrument:** Constant FWHM = 0.1°

Phase ID (6)	Chemical Formula	PDF-#	Wt% (σ)	DD% (σ)	RIR
Quartz	SiO2	98-000-0369	30.6 (0.7)	33.8 (0.6)	3.95
Kaolinite	Al4(OH)8(Si4O10)	98-000-0261	41.0 (1.2)	47.5 (1.2)	1.78
Muscovite-2M1	KAl3Si3O10(OH)2	04-017-9606	20.0 (1.0)	10.4 (1.1)	0.80
Potassium Aluminum Silicate	KAlSi3O8	04-023-9697	6.0 (0.9)	3.9 (0.9)	0.76
Siderite	Ca0.10Mg0.33Fe0.57(CO3)	04-009-7660	1.6 (0.3)	2.4 (0.3)	2.49
Rutile	TiO2	04-008-7847	0.7 (?)	2.0 (?)	3.16

XRF(Wt%): Fe2O3=0.7%, TiO2=0.7%, CaO<0.1%, K2O=3.4%, SiO2=62.7%, Al2O3=25.0%, MgO=0.2%, CO2=0.7%

Refinement Halted (R/E=2.2), ♣ Round=4, Iter=6, P=34, R=10.99% (E=5.00%, EPS=0.5)

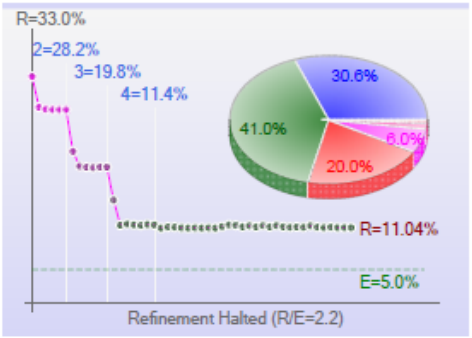

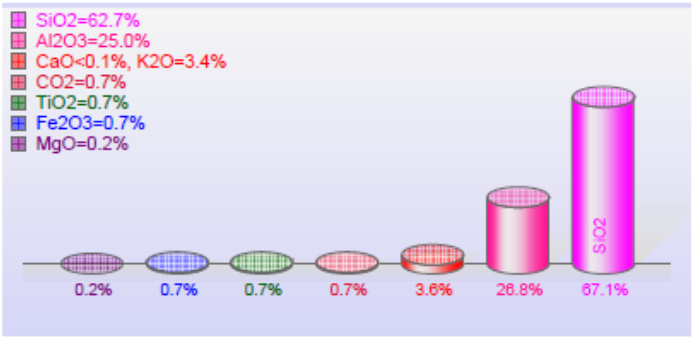

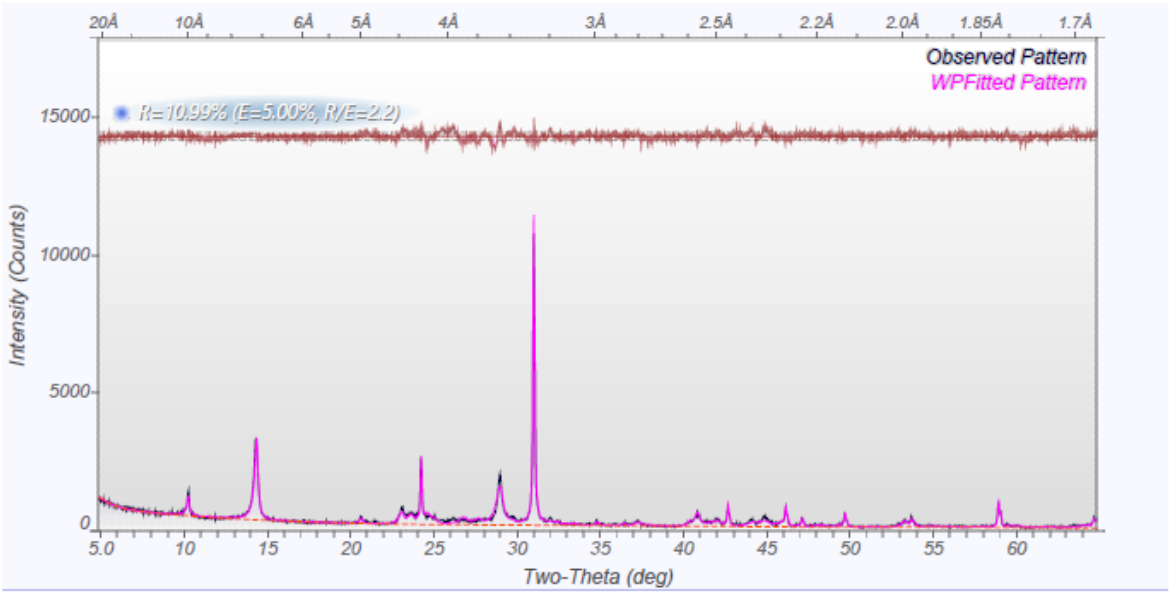

XRD:TT

WPF Report

Scan ID: TT-1_Bulk XRD_edited.mdi

Scan Parameters: 5.0°/64.986°/0.01998°/384(s), I(p)=11340/92, Co, March 15, 2024, 8:49 AM

☑ Zero Offset = 0.1092 (0.0005) ☐ Displacement = 0.0 ☐ Distance Slack = 0.0

☑ Kα2 Peaks Present ☐ Kα2/Kα1 Ratio = 0.5 ☐ X-Ray Polarization = 1.0

Geometry: Diffractometer Lp Fitted-Range: 5.0° - 65.0° BG-Model: Polynomial (5) λ: 1.78899Å (Co)

PSF: Pearson VII Broadening: Individual FWHM Curve Instrument: Constant FWHM = 0.1°

Phase ID (6)	Chemical Formula	PDF-#	Wt% (σ)	DD% (σ)	RIR	μ
Muscovite-2M1	K0.865Na0.135Mg0.04Ti0.01Fe0.09	04-023-1597	13.3 (1.2)	19.0 (1.2)	1.00	190.6
Quartz	SiO2	98-000-0369	37.9 (0.7)	34.9 (0.6)	4.23	140.6
Microcline | potassium tecto-alumotris	KAlSi3O8	04-008-1783	6.1 (0.9)	5.4 (0.9)	0.60	189.7
Kaolinite-1A	Al2Si2O5(OH)4	04-013-2830	40.7 (.9)	39.7 (9)	1.02	119.2
Anatase	TiO2	04-007-0701	0.8 (?)	0.4 (?)	4.61	746.8
Siderite	Ca0.10Mg0.33Fe0.57(CO3)	04-009-7660	1.2 (0.4)	0.7 (0.3)	2.17	136.9

XRF(Wt%): Fe2O3=0.8%, TiO2=0.8%, CaO<0.1%, K2O=2.3%, SiO2=66.5%, Al2O3=23.2%, MgO=0.2%, Na2O=0.1%, CO2=0.5%

Refinement Halted (R/E=2.3), ♣ Round=4, Iter=6, P=32, R=11.16% (E=4.96%, EPS=0.5)

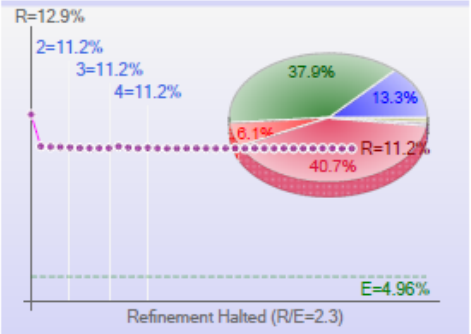

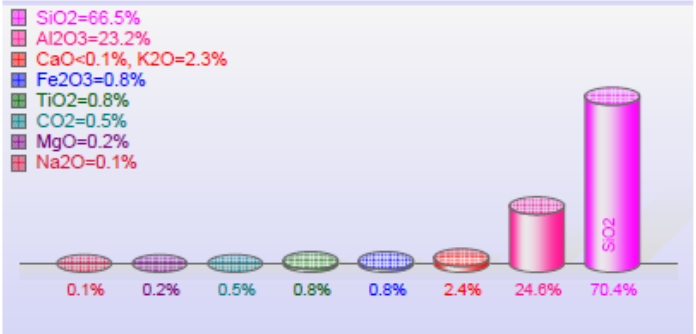

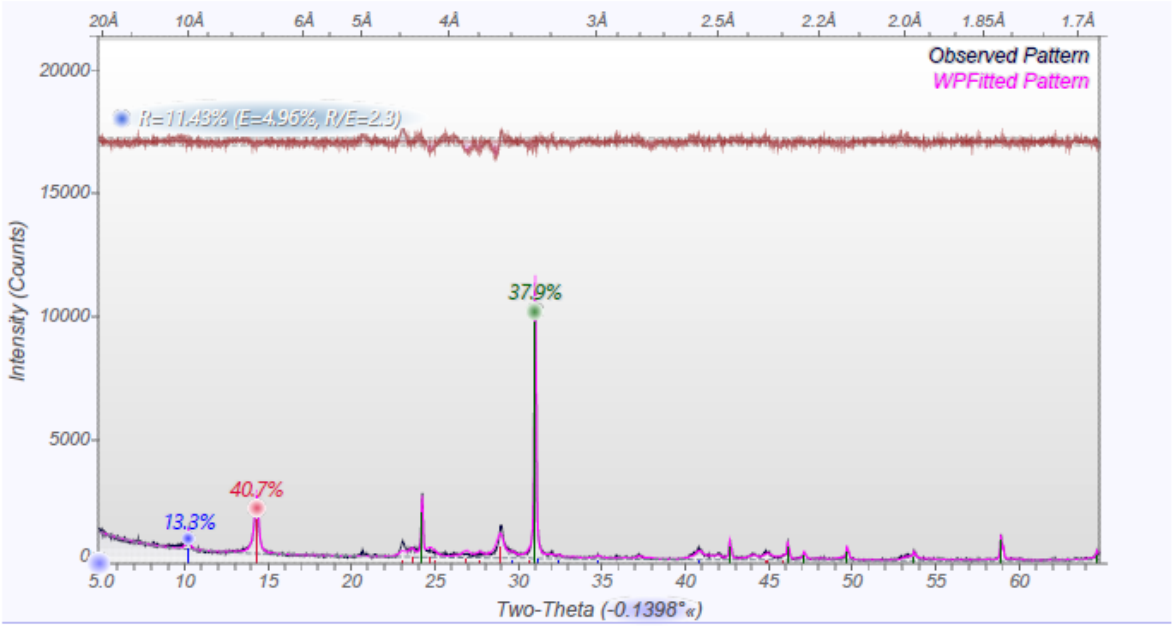

XRF (all)

	CC	FT	TT
Na_2O	0.254	0.26	0.264
MgO	0.905	0.761	0.906
Al_2O_3	24.584	25.193	24.207
SiO_2	67.436	67.38	67.421
P_2O_5	0.1043	0.0761	0.0949
K_2O	2.57	2.376	2.546
CaO	0.239	0.152	0.239
TiO_2	0.7916	0.6891	0.7932
V_2O_5	0.022	0.02	0.022
Cr_2O_4	0.0362	0.0355	0.0368
Fe_2O_3	3.224	2.99	3.211
ZnO	0.007	0.0075	0.0059
BaO	0.055	0.054	0.05
SrO	0.0212	0.0192	0.0205
ZrO_2	0.026	0.024	0.027
Mn_2O_3	0.069	0.083	0.08
LOI (%)	11.46	12.24	11.45